THE UNIVERSITY OF CHICAGO

# TAXOL-STABILIZED YEAST MICROTUBULES REVEAL THAT A SUBSET OF SPINDLE CHECKPOINT PROTEINS DELAY ANAPHASE ONSET IN RESPONSE TO LOW TENSION

A DISSERTATION SUBMITTED TO
THE FACULTY OF THE DIVISION OF THE BIOLOGICAL SCIENCES
AND THE PRITZKER SCHOOL OF MEDICINE
IN CANDIDACY FOR THE DEGREE OF
DOCTOR OF PHILOSOPHY

GRADUATE PROGRAM IN CELL AND MOLECULAR BIOLOGY

BY
KATHLEEN GRANT PROUDFOOT

CHICAGO, ILLINOIS
DECEMBER 2017

To my parents, brothers, and sister for all their support and inspiration.

# Table of Contents

## List of Figures

## List of Tables

## Abstract

To ensure genome stability during mitosis, the mitotic spindle must segregate sister chromosomes accurately. Multiple surveillance mechanisms, collectively referred to as the mitotic checkpoint, function to delay anaphase onset if sister chromosomes are not bound to microtubules from opposite spindle poles. Dominant signaling pathways within the mitotic checkpoint are the Spindle Assembly Checkpoint (SAC), which delays anaphase when kinetochores are not stably attached to microtubules, and the error correction mechanism, which induces detachment when microtubule-kinetochore attachments are not under tension. Together, these mechanisms promote stable, bipolar attachments in which dynamic microtubules can generate tension across sister kinetochores. However, the interdependency of kinetochore-microtubule attachment and tension has proved challenging to understanding whether this model fully explains how the mitotic checkpoint responds to the tension status at kinetochores. Unlike higher eukaryotes, budding yeast kinetochores bind only one microtubule, simplifying the relationship between attachment and tension. To address the role of tension in the mitotic checkpoint, we developed a Taxol-sensitive yeast model to reduce tension by stabilizing microtubules in fully assembled spindles. Our results show that reducing tension on bipolar, attached kinetochores delays anaphase onset. The tension-mediated delay is transient relative to the SAC delay imposed by unattached kinetochores. Furthermore, it requires the SAC proteins Bub1 and Bub3, but persists without Mad1, Mad2 and Mad3 (yeast BubR1). Together, our results demonstrate that reduced tension generates a ‘wait-anaphase’ signal during the mitotic checkpoint that is temporally and mechanistically distinct from that of unattached kinetochores.

# Chapter 1:

# Introduction

## 1.1 Overview

Critical to cell division is the accurate segregation of chromosomes. Chromosome missegregation in eukaryotes leads to aneuploidy, birth defects, and tumor progression (Siegel and Amon, 2012; Hassold and Hunt, 2001; Gordon et al., 2012). Faithful segregation requires that the kinetochores of sister chromosomes attach

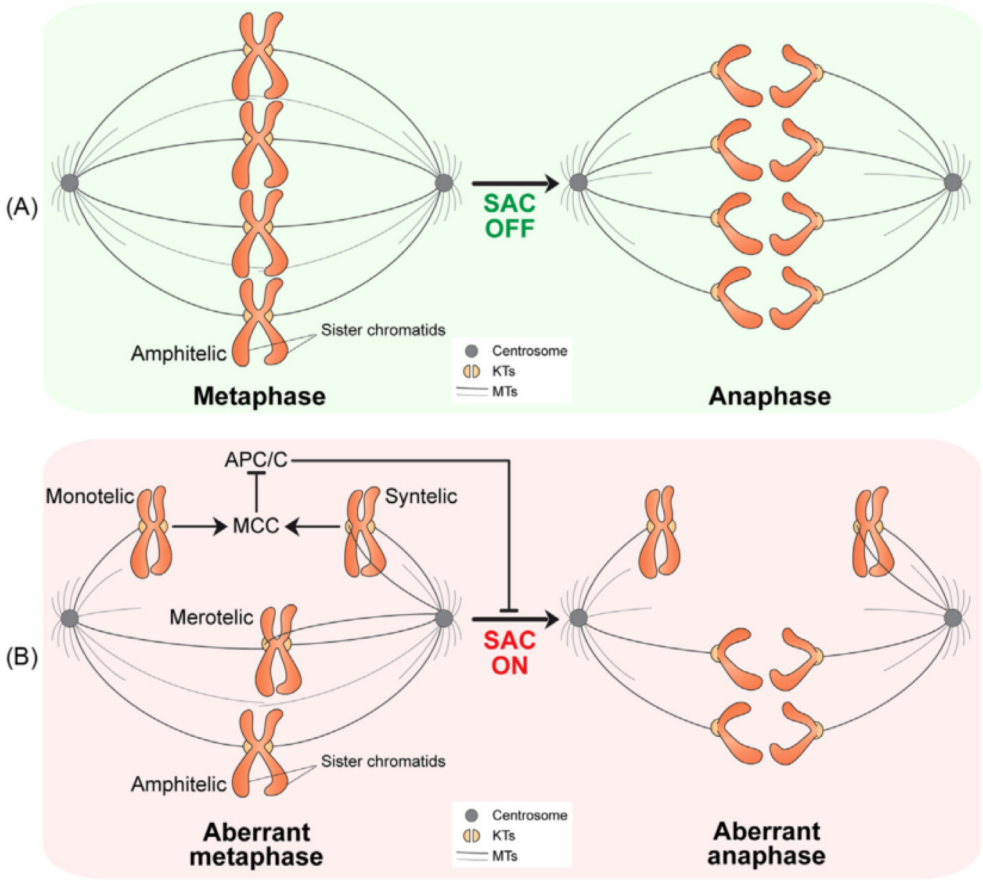


**Figure 1. Kinetochore orientations and anaphase onset** Source: Manic et al., 2017

**Figure 1, continued; Kinetochore orientations and anaphase onset.** (A) During normal mitosis, amphitelic, bioriented sister chromatids align at the metaphase plate prior to their partition into two daughter cells during anaphase. (B) During early mitosis or aberrant mitosis, monotelic and syntelic attachments (which are generated at relatively high frequencies) activate the spindle assembly checkpoint (SAC) by releasing from unattached or untensed kinetochore(s) the mitotic checkpoint complex (MCC), which inhibits the anaphase promoting complex (APC). This inhibits anaphase onset and thus prevents chromosome missegregation. In panel B, an amphitelic and a merotelic attachment, both of which are not sensed by the SAC, are also represented. KTs, kinetochores; MTs, microtubules.

to microtubules emanating from opposite spindle poles, a configuration also known as bipolar attachment or biorientation. Biorientation allows dynamic microtubules to generate tension across the sister kinetochores (Figure 1A and 2A), and only in this bipolar configuration will the sister chromatids segregate properly upon anaphase onset, one to each new daughter cell. On the other hand, chromatids whose kinetochores are unattached, or attached in monopolar or syntelic configurations (i.e. attached to a single spindle pole and therefore tensionless) will undergo an aberrant anaphase if not repaired (Figure 1B and 2B). Thus, these configurations activate the mitotic checkpoint to stall anaphase onset until the sister chromatids are attached in a bipolar fashion to the mitotic spindle.

Several surveillance mechanisms function to delay anaphase onset under conditions where either tension or attachment at kinetochores is lacking. The spindle assembly checkpoint (SAC) is recognized as the primary mechanism that arrests cells when spindles are not correctly assembled, but for many years it was unclear whether the SAC activated in response to kinetochore attachment status, tension status, or both signals (Figure 2). Currently, the prevailing thought is that the SAC activates in response to detached kinetochores to produce a prolonged metaphase arrest (Figure

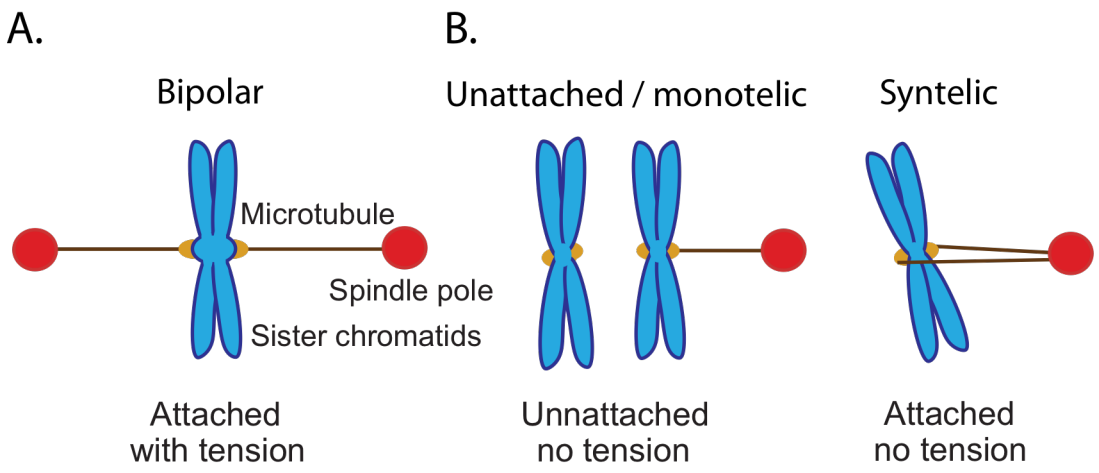


**Figure 2. Possible variations in kinetochore-microtubule attachment.** (A) When sister kinetochores attach to microtubules from opposite spindle poles, the dynamic microtubules can generate tension across the kinetochores. This bipolar configuration satisfies the requirements of the SAC. (B) Improper kinetochore-microtubule attachments: if one or both kinetochores are unattached (left), or both kinetochores are attached to microtubules emanating from the same spindle pole (right), microtubules cannot generate tension across the sister kinetochores. These configurations activate signaling that stalls anaphase onset until the spindle damage is repaired.

3A), only deactivating and allowing anaphase onset once all kinetochores have established stable bipolar connections to the spindle (Figure 2A) (For review: Joglekar, 2016; London and Biggins, 2014). Complimentary to the SAC, the error correction mechanism destabilizes syntelic sister kinetochores (Figure 2B) that are attached but under reduced tension, producing detached kinetochores. This subsequently activates the SAC, giving the cell a second chance to attach the newly unattached kinetochores in a bipolar configuration (For review: Sarangapani and Asbury, 2012; Krenn and Musacchio, 2015). Although on the surface, this canonical model involving SAC activation/error correction appears to provide a complete and elegant explanation of how cells assemble bipolar spindles; several mechanisms that do not fit within this

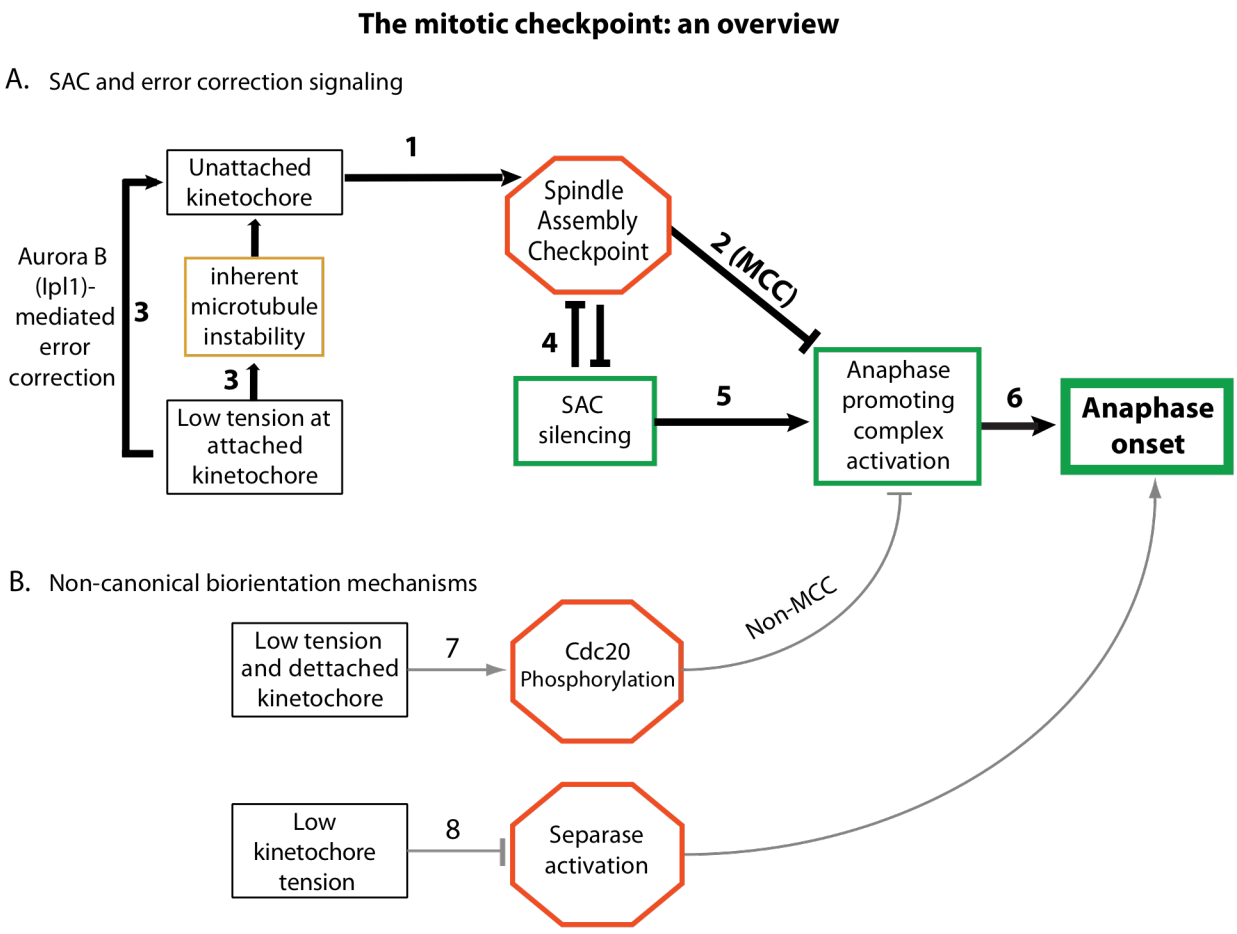


**Figure 3. The mitotic checkpoint is made up of many mechanisms that coordinate to promote accurate chromosome segregation.** (A) Bold arrows represent canonical mechanisms that activate in response to detached/tensionless kinetochores. (1) a detached kinetochore activates the spindle assembly checkpoint, which assembles (2) the mitotic checkpoint complex (MCC) to inhibit activation of the anaphase promoting complex. (3) Kinetochore attachments with insufficient tension are inherently unstable, and either come detached on their own or are actively destabilized via the Aurora B-mediated error correction pathway to activate the SAC as unattached kinetochores. (4) Signaling promoting SAC silencing and the spindle assembly checkpoint are in direct competition; however, when conditions favor SAC deactivation, i.e. when attachments come under tension, (5) SAC silencing rapidly promotes anaphase promoting complex activation and subsequent (6) anaphase onset. (B) Non-canonical mechanisms whose timing and purpose have not yet been fully incorporated into the traditional picture of the mitotic checkpoint further promote kinetochore biorientation. (7) low tension and kinetochore detachment both promote inhibitory phosphorylation of Cdc20 to inhibit the APC in a MCC-independent manner in HeLa cells. (8) Full tension at kinetochores signifies bipolar attachment and reversibly opposes an APC-independent mechanism that inhibits Separase and consequentially anaphase onset. Notably, the relative contributions of kinetochore tension status vs. attachment status remain unclear in both of these pathways.

canonical model have been described that are also reported to promote sister chromatid biorientation. However, because it is unclear how these pathways might function in conjunction with the canonical SAC/error correction model, these mechanisms remain incompletely understood. Among these additional signaling mechanisms are one that promotes SAC silencing (For review: Etemad and Kops, 2016) and processes that promote the preservation of sister chromatid cohesion and SAC- independent inhibition of the Anaphase Promoting Complex (APC) (Clift et al., 2009; Jia et al., 2016) (Figure 3B).

These mechanisms may act either in sequence or in parallel to the SAC and may be mediated by kinetochore attachment or tension; but overall, an understanding of these pathways is lacking, in large part due to experimental limitations in isolating these signaling cascades from one another. Ultimately, mitotic signaling is complex, and signaling crosstalk and overlap can obscure the boundaries of specific mechanisms. Regardless, cell cycle progression is governed by a group of interconnected signaling cascades that together promote accurate chromosome segregation, which we will collectively refer to within as “the mitotic checkpoint” (Figure 3).

### 1.2 Historical overview: discovery and challenges surrounding mitotic signaling

The timing of cell cycle progression is controlled by classes of protein teams called cyclins and cyclin dependent kinase (CDKs) (Pringle, 1978). CDKs are inactive without their cyclin partners, which are cyclically produced and destroyed at specific junctures throughout the cell cycle and serve to direct CDK activity to specific subsets of

target proteins (Evans et al., 1983). One purpose of these cyclin-CDK pairs is to promote a cell's transition to the next stage of the cell cycle, but their function can be countered during specific quality control checkpoints (Weinert and Hartwell, 1988; Hwang and Murray, 1997; For review Araujo et al., 2016; Malumbres, 2014). Cell cycle checkpoints activate phospho-signaling cascades during key junctures when essential aspects of cell cycle progression have not been carried out accurately. Checkpoint activation is typically associated with a cell cycle delay (Weinert and Hartwell, 1988), which gives cellular machinery time to repair the damage or overcome the deficiency that the checkpoint detected. The mitotic checkpoint, dominated by the SAC mechanism, is the phospho-signaling, quality control cascade that regulates the timing of anaphase onset in part by modulating destruction of Cyclin B (budding yeast Clb2), the coactivator of Cyclin Dependent Kinase 1 (CDK1, budding yeast Cdc28), as the cell builds the metaphase spindle (Holloway et al., 1993; Glotzer et al., 1991; Rudner et al., 2001; Jogelekar, 2016).

The initial observation that metazoan cells produce a 'wait anaphase' signal in response to chromosome misalignment was reported in classic studies (Bajer and Mole-Majer, 1955; Callan and Jacobs, 1957; Zirkle, 1970) in mantid spermatocytes. Subsequently, Bruce Nicklas investigated the process of chromosome alignment by performing micromanipulation of chromatids in grasshopper spermatocytes in meiosis I (Nicklas and Staehly, 1967; Nicklas and Koch,1969). By pushing and pulling on individual chromatids, Nicklas observed that kinetochore-microtubule attachments are more stable when under tension; this observation promoted the idea that both kinetochore-microtubule attachment and tension at kinetochores are important effectors

of SAC signaling. Moreover, Nicklas observed that cells never entered anaphase with detached or tensionless kinetochores.

With the knowledge that detached kinetochores arrested cells in metaphase, and that quality control checkpoints monitored advancement through the cell cycle (Pringle, 1978; Evans et al. 1983; Weinert and Hartwell, 1988), two screens were concurrently carried out searching for protein components of the mitotic checkpoint: the signaling responsible for arresting the cell cycle when chromosomes are not correctly assembled on the metaphase spindle. These screens independently uncovered the majority of central SAC proteins known today, but intriguingly they uncovered two, non-overlapping sets of proteins: the MADs (Mitotic Arrest Deficient) and the BUBs (Budding Uninhibited by Benzimidazole) (Li and Murray, 1991; Hoyt et al., 1991). Why these two screens uncovered two different sets of SAC proteins has not been clear; but one interesting possibility may be that these two related, yet fundamentally different, screening strategies selected for different aspects of mitotic checkpoint function. I will revisit this idea in Chapter 3.

With the discovery of many of the core SAC proteins, potential mechanisms behind SAC activation could be proposed. And as additional proteins essential to the process of chromosome alignment and checkpoint activation were discovered and their functions elucidated, the mechanism behind SAC activation began to take shape and build towards our current understanding of the SAC and accompanying signaling cascades. Laser ablation studies revealed that the SAC signal can originate from even a single unattached kinetochore (Rieder et al., 1995) and diffuse into the cytoplasm (Howell et al., 2000; Shah and Cleveland, 2000). Mps1 kinase was originally discovered

in a screen for genes essential to control spindle pole body duplication (Winey et al., 1991), but is now also largely thought to be at the apex of checkpoint signaling (Hiruma et al., 2015). Ipl1 kinase (Aurora B) was discovered in a colony sectoring-based screen that selected for mutants with increased chromosome missegregation (Chan and Botstein, 1993), and although initially it was unclear whether or not Ipl1 took part in the SAC proper, later studies revealed that it instead acts as a crucial player in the error correction mechanism (Biggins and Murray, 2001; Ditchfield et al., 2003; Pinsky et al., 2006).

One by one, the identity and/or function of additional mitotic checkpoint proteins were defined. Together, this information forms the basis of our current models of mitotic checkpoint signaling; however, despite this progress, our understanding is not complete. Specifically, in light of advances which have begun to uncover additional mechanisms of non-canonical mitotic signaling, it has become clear that there is still much more about the mitotic checkpoint left to uncover.

### 1.3 The current model of the mitotic checkpoint

Our understanding of mitotic checkpoint signaling has advanced significantly in recent years (For review see London and Biggins, 2014; Joglekar, 2016; Lampson and Grishchuk, 2017). Mechanistic insights have revealed important new facets of SAC signaling, several seemingly tension-mediated mechanisms have been proposed, and signaling surrounding Aurora B and error correction has crystalized. Here I will review

where the field currently stands in regards to the mechanistic understanding of mitotic checkpoint signaling.

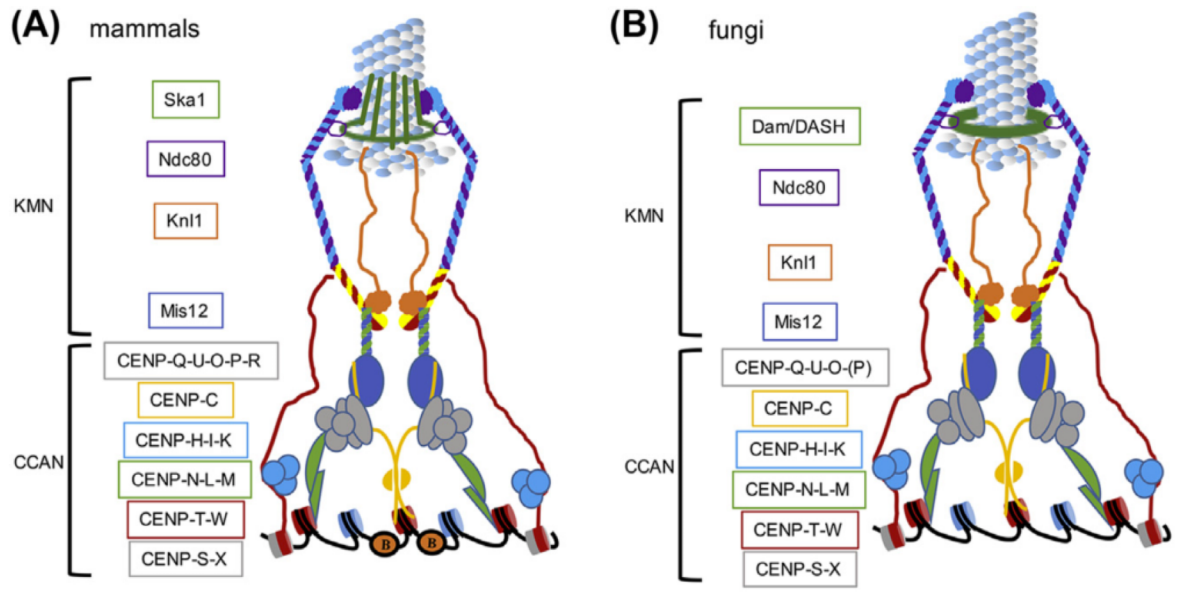


Source: Friedman and Freitag, 2017

**Figure 4. The kinetochore-microtubule binding interface.** Microtubule binding, outer kinetochore complexes within the KMN network (KNL1-MIS12-NDC80) localize to the constitutive centromere-associated network (CCAN, also known as the Ctf19 complex in *S. cerevisiae*), in which CENP-C plays a central role in promoting overall kinetochore assembly by bridging the inner centromere with the outer kinetochore and also contributing to the organization of the intermediate CCAN region. (A) Mammalian and (B) fungal kinetochores are generally functionally conserved, although there is some variation between proteins that serve a particular function. For instance, Ska1 in mammals and Dam/DASH in fungi perform similar microtubule binding functions.

### *1.3.1 The spindle assembly checkpoint*

Although the tension vs. attachment debate raged for many years (i.e. a debate as to whether reduced kinetochore tension or kinetochore detachment activated the SAC), recent studies have now lead to the current model in which the SAC is thought to

activate in response to detached kinetochores (For review: London and Biggins, 2014). Although the overall SAC signaling cascade is highly conserved from yeast to humans, there are slight differences that exist between yeast and higher model organisms due to both the components of the kinetochore-microtubule attachment (Figure 4A and B) and SAC signaling components themselves. The following will detail the SAC signaling pathway as it is known in yeast, but will also make note of how signaling varies in higher eukaryotes.

Microtubule binding and the SAC signaling assembly occurs at a kinetochore subcomplex called the KMN network (Knl1/Spc105/Blinkin, Mis12/mtw1, and Ndc80/Hec1) (Martin-Lluesma et al., 2002; McCleland et al., 2003; Cheeseman et al., 2006; Pagliuca et al., 2009). As a cell enters mitosis, Cdc28-Clb2 (yeast CDK1-CyclinB) begins phosphorylating Mps1 kinase, potentiating its ability to activate the SAC (Morin et al., 2012). Until spindle microtubules form end-on attachments with the outer kinetochore protein Ndc80's N-terminal region and Calponin Homology domains (Hec1 in vertebrate cells) (Deluca et al., 2002; Deluca et al., 2003), overlapping domains on Ndc80 recruit phosphorylated Mps1 (Ji et al., 2015; Hiruma et al., 2015). Additionally, in higher eukaryotes, in the absence of bipolar attachment, Mps1 recruitment to Ndc80 is enhanced by Ipl1-mediated (yeast Aurora B kinase) (Krenn and Musacchio, 2015) and Polo-like kinase 1 (Plk1)-mediated phosphorylation (Ikeda and Tanaka, 2017). Because pulling forces on the kinetochore are reduced in the absence of bipolar attachment, the flexible Ndc80 structure is thought to relax slightly, (Aravamudhan et al., 2015), enabling the initiation of SAC activation (Figure 5A). Ndc80-bound Mps1 then phosphorylates

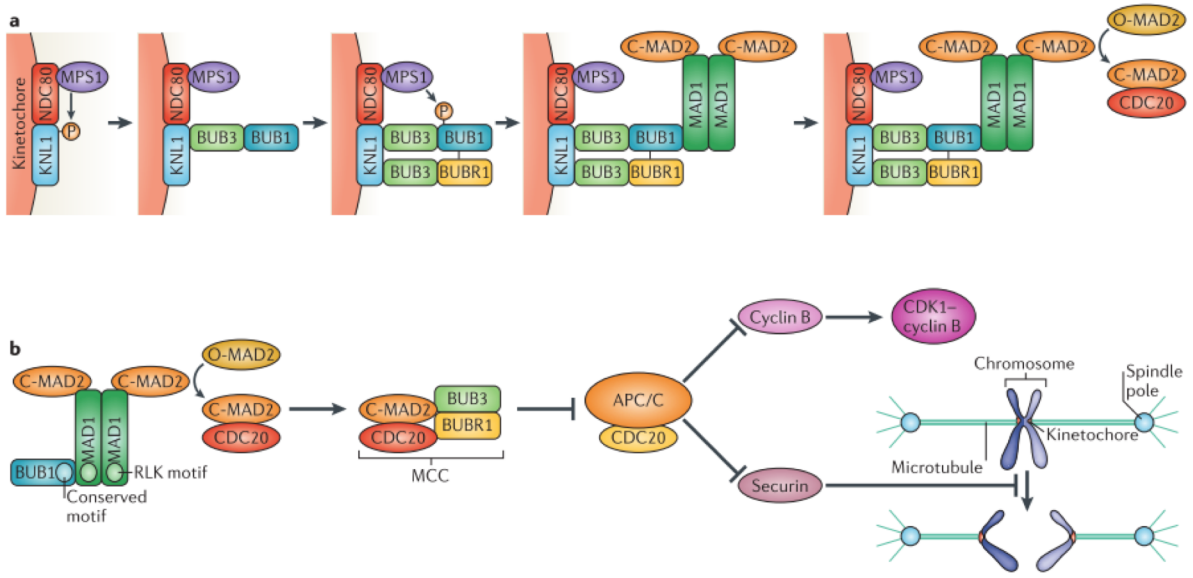


Source: London and Biggins, 2014b

**Figure 5. The kinetochore recruits SAC components in a hierarchical manner to achieve SAC activation.** (A) Hierarchical assembly of a functional checkpoint-signaling complex at kinetochores: Kinetochore null protein 1 (KNL1) and nuclear division cycle 80 (NDC80) are kinetochore proteins that form a scaffold for checkpoint protein recruitment. Budding uninhibited by benzimidazole 3 (BUB3) forms discrete complexes with BUB1 and BUB1‑related protein kinase (BUBR1; mitotic arrest-deficient 3 (Mad3) in yeast). Phosphorylation of Ndc80 and Knl1 by monopolar spindle 1 (MPS1) kinase recruits BUB1–BUB3, and BUB1 licenses localization of BUBR1. Next, a MAD1-BUB1 interaction recruits the MAD1–MAD2 heterotetramer. Kinetochore-bound MAD1–MAD2 facilitates checkpoint activation through catalytic conversion of soluble 'open' (O)-MAD2 to 'closed' (C)-MAD2. (B) Kinetochore recruitment of SAC proteins catalyzes the assembly of the mitotic checkpoint complex (MCC). Kinetochore-localized MAD1–C-MAD2 acts as a template to convert cytoplasmic O-MAD2 to C-Mad2, which then binds to cell division control protein 20 (CDC20), and MAD3–BUB3. The MCC inhibits the activity of the APC/C (anaphase-promoting complex, also known as the cyclosome)–CDC20 complex, and the crucial mitotic targets of the APC/C (cyclin B and securin) are thereby stabilized while the checkpoint is active, which prevents chromosome segregation. CDK1, cyclin-dependent kinase 1.

conserved Met-Glu-Lys-Thr-MELT) motif repeats of the outer kinetochore protein Spc105/KNL1 (London et al., 2012; Shepperd et al., 2012; Yamagishi et al., 2012; London and Biggins 2014a; Mora-Santos et al., 2016). Each phosphorylated MELT motif of Spc105/KNL1 can bind one Bub1-Bub3 heterodimer (Primorac et al., 2013), and once recruited, Bub1 is phosphorylated by Mps1, licensing Bub1 to recruit a Bub3-

Mad3 (yeast BubR1) heterodimer and Mad1. This Mad1 then recruits Mad2 to the unattached kinetochore in the 'closed' conformation (Jia et al., 2016; Mora-Santos et al., 2016; Di Fiore et al., 2015, London et al., 2014a). The metamorphic nature of Mad2, specifically its conversion between $Mad2^{open}$ and $Mad2^{closed}$ conformations, is key to the production of the inhibitory SAC signal.

At the unattached kinetochore, the Mad1- $Mad2^{closed}$ complex (Figure 5B) catalyzes the conversion of cytoplasmic, inactive $Mad2^{open}$ to the Cdc20-$Mad2^{closed}$ complex (De Antoni et al., 2005). The Cdc20-$Mad2^{closed}$ complex then binds with Bub3 and Mad3 to generate a stable structure known as the mitotic checkpoint complex (MCC). Once in complex, the MCC is free to diffuse through the cytoplasm and act as a powerful inhibitor of the anaphase promoting complex (APC). In addition to the copy of Cdc20 within the MCC, the MCC can bind a second copy of Cdc20 that has already bound to and activated the APC (Izawa and Pines, 2014) and promote Cdc20 autoubiquitination (Foster and Morgan, 2012). The fact that the MCC can bind a second copy of Cdc20 that is already in complex with the APC makes it especially powerful; when the MCC binds the APC-Cdc20 complex, autoubiquitination promotes Cdc20 degradation, lowering Cdc20 levels within the cell (Foster and Morgan 2012; Nilsson et al., 2008), and MCC binding partially deactivates the associated APC to prevent the ubiquitination of other APC substrates (Foster and Morgan 2012; Izawa and Pines, 2014). Thus the cell enhances its sensitivity to SAC activation by reducing the amount of APC activator that the SAC must counteract.

As each pair of sister chromatids is bioriented on the spindle, the SAC is silenced via mechanisms that both undo the phosphorylation events that activated it in the first

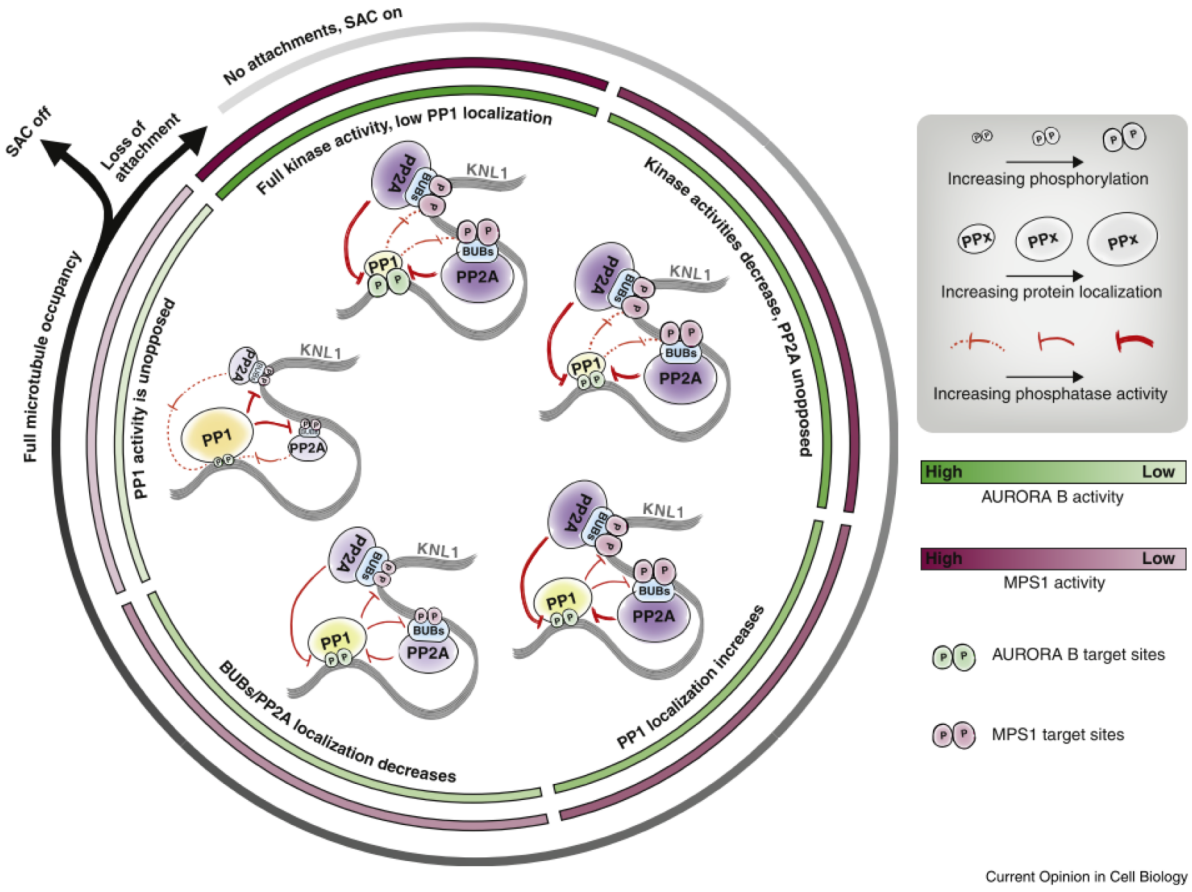


Source: Etemad et al., 2016

**Figure 6. SAC silencing promotes the timely but reversible inactivation of the SAC response.** PP2A recruits PP1 to participate in a negative feedback loop that reverses SAC activating phosphorylation events. KNL1 phosphorylation by Mps1 (repeat motifs shown in purple) and by Ipl1 (shown in green) are reversed, thereby indirectly opposing Mad3/PP2A and PP1 binding. When a kinetochore is unattached and the SAC is active, Mps1 and Ipl1 activity is high, opposing PP1 activity, but when Mps1 and Ipl1 activity is reduced, PP2A enacts dephosphorylation events that result in high PP1 activity. High PP1 activity inactivates the SAC response, but due to negative feedback that results in PP2A removal, any further loss of attachment will still remove PP1 and re-activate the SAC.

place and remove core SAC proteins from the kinetochore (Figure 6). At the kinetochore, microtubules generate pulling forces at the source of the signaling cascade that render its components out of reach of SAC-activating Mps1/Ipl1 phosphorylation. In turn, Protein Phosphatase 2A (PP2A) can recruit Protein Phosphatase 1 (PP1) to the

kinetochore. PP2A dephosphorylates KNL1 to disassemble the components necessary for catalytic production of the SAC signal (Espert et al., 2014). Similarly, PP1 removes Cdc28-mediated inhibitory phosphorylation of the APC activator, Cdc20 (Kim et al., 2017), and also contributes to dephosphorylating Spc105 MELT motifs, promoting the dissociation of Bub1-Bub3 (Rosenberg et al., 2011; London, 2012) and consequently all downstream SAC components. SAC scaffolding dissociation is further favored due to steric hindrance introduced by a proper kinetochore-microtubule binding event (Hiruma et al., 2015), while SAC proteins are also actively stripped from the kinetochore in metazoan cells by cytoplasmic dynein moving away from kinetochores along spindle microtubules (London and Biggins, 2014b). As the SAC signaling scaffold disassembles and MCC production decreases, APC activity targets several SAC proteins for ubiquitin-mediated degradation, thus preventing SAC re-activation (Qi and Yu, 2007; Palframan et al., 2006). Ultimately, however, the coordination of these events is incompletely understood, and SAC silencing is potentially a tension-dependent process that will be discussed in more detail below.

Finally, once the SAC ceases to inhibit the APC, the APC targets Pds1 (yeast Securin) and Clb2 for ubiquitin-mediated destruction (Sudakin et al., 1995; Holloway et al., 1993; Glotzer and Murray, 1991). With the destruction of its inhibitory chaperone Pds1, the enzyme Separase becomes free to cleave the Cohesin complex that holds sister chromatids together, promoting sister chromatid separation (Ciosk et al., 1998; Uhlmann et al., 2000). With the destruction of Clb2, Cdc28 activity decreases, and with it the origin of the SAC signal. As metaphase-specific signaling diminishes and sister chromatids separate, the cell both biochemically and physically transitions to anaphase.

### *1.3.2 The error correction mechanism*

Ipl1/Aurora B kinase was originally thought to function as an upstream regulator of the SAC, potentially functioning in a tension-mediated mechanism (Biggins et al., 1999). Although Ipl1 does have a role in SAC activation in that it promotes the recruitment of all downstream SAC proteins in higher eukaryotes (Saurin et al., 2011; Ditchfield et al., 2003)) and plays a number of other roles throughout the cell cycle (Krenn and Musacchio, 2015), it was later discovered to play a central role in a second mitotic signaling cascade: the error correction mechanism (Pinsky et al., 2006; for review: Sarangapani and Asbury, 2012). The error correction mechanism plays a vital role in promoting biorientation by detaching tensionless kinetochore microtubule attachments. These newly detached kinetochores initiate SAC signaling to arrest the cell in metaphase and give sister chromatids time to form new, bipolar attachments (For review: Krenn and Musacchio, 2015).

Ipl1 in complex with the Chromosomal Passenger Complex (CPC) is recruited to phosphorylated Histone H3 (Wang et al., 2010; Kelly et al., 2010) and the inner kinetochore complex CBF3 (Lau and Murray, 2012). Following recruitment, Ipl1 localizes at the kinetochore in two distinct pools at metaphase, one at the centromere and the other at the outer kinetochore (DeLuca et al., 2011); which pool of Ipl1 is primarily responsible for its function in chromosome alignment is currently a topic of debate. Ndc80 and Dam1 in yeast are outer kinetochore components that bind to microtubules and are both targets of Ipl1 phosphorylation (Cheeseman et al., 2002; Pinsky et al., 2006). Phosphorylation of Ndc80 and Dam1 destabilizes kinetochore

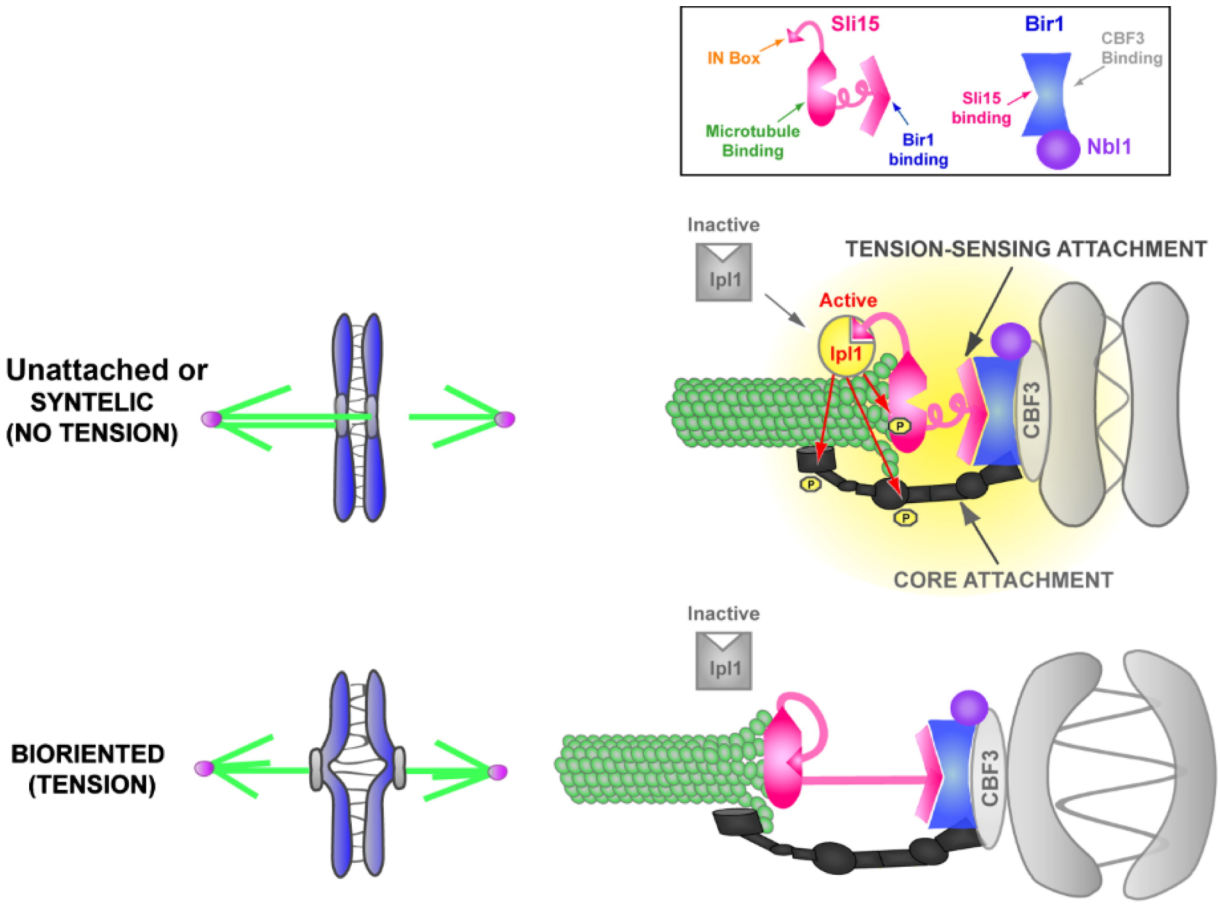


Adapted from: Sandall et al., 2006

**Figure 7. The tension-mediated model of the error correction mechanism.** The Chromosome passenger complex (CPC) is comprised of Sli15 (Yeast INCENP), Bir1 (yeast Survivin), Ipl1 (Yeast Aurora B), and Nbl1 (yeast Borealin). Bir1 in complex with Nbl1 is recruited to the kinetochore by the CBF3 complex and phosphorylated histone H3. Sli15 participates in microtubule binding and binds to and promotes the auto-phosphorylation of Ipl1, while Bir1 binding to Sli15 links it to the inner kinetochore via CBF3. When kinetochore-microtubule attachments are not attached/under tension, Ipl1 bound to Sli15 is active and able to phosphorylate both the core microtubule attachment (the KMN network and Dam1 complex, pictured here as a black rod), and the tensionless microtubule itself, together destabilizing any attachment. Conversely, when the kinetochore-microtubule attachment is under tension, Sli15 inactivates, thus ceasing to activate Ipl1. In this case kinetochore-microtubule attachments remain stable because Ipl1 is unable to enact the phosphorylation events that would otherwise inhibit them. (For review: Carmena et al., 2012b)

microtubule attachments; however, these microtubule binding sites are theorized to be out of reach of Ipl1 activity when kinetochores are attached in a bipolar fashion to the spindle (Figure 6) and there is tension between sister kinetochores (Biggins and Murray,

2001; Pinsky et al., 2006; Wang et al., 2008). It is only when kinetochores are not under tension (Figure 6) that this kinetochore architecture comes within reach of Ipl1 activity (Tanaka et al., 2002; Liu et al., 2009), i.e. when only one sister is attached or when both sister chromatids are attached to microtubules emanating from the same spindle pole. When Ipl1 phosphorylates Ndc80 and Dam1, it promotes detachment of these erroneous attachments, which will then activate canonical SAC signaling (Pinsky et al., 2006). With the initiation of SAC signaling, the cell arrests in metaphase until every pair of sister chromatids is bioriented on the spindle. When biorientation is finally achieved, coordinated efforts of phosphatases PP2A and PP1 counteract Ipl1 activity by dephosphorylating the KMN network. This dephosphorylation stabilizes attachments and generates tension, thus promoting timely achievement of end-on kinetochore-microtubule attachments.

In addition to this tension-mediated model, however, pools of Ipl1 exist beyond the inner kinetochore (Campbell and Desai, 2013), giving it constant, spatial access to each of these kinetochore components. And so, it is not clear that tension-dependent spatial separation of Ipl1 and its substrates is the only mechanism by which Ipl1 could be affecting cell cycle progression (Sarangapani and Asbury, 2012); for instance, it could be acting in other mechanisms that promote biorientation.

### *1.3.3 Non-canonical biorientation mechanisms*

Due to the interdependence between kinetochore tension and its attachment state, mechanisms by which the cell responds specifically to reduced kinetochore

tension are poorly understood compared to the mechanism of SAC activation. As additional components of the overall mitotic checkpoint come to light, however, it becomes increasingly clear that additional pathways promote sister kinetochore biorientation. These non-canonical pathways appear to affect the rate of events associated with anaphase onset and contribute significantly to accurate chromosome segregation in coordination with the canonical SAC. These pathways include, but are not limited to, SAC silencing, Cdc20 inhibition by Plk1-Bub1 in HeLa cells (Jia et al., 2016), and the Bub1/Sgo1/Cdc55 inhibition of Separase in budding yeast (Clift et al., 2009; Nerusheva et al., 2014). In the case of the latter two pathways, it remains unclear whether or not these are branches of SAC activation or function in parallel with it. Further study and elucidation of mitotic signaling is needed to determine how each signaling mechanism contributes to overall biorientation and whether each is evolutionarily conserved.

Entwined with protein recruitment and signaling to promote the SAC activation and error correction, outlined above, is the fact that the timing that dictates shifts in signaling appears to be tension dependent. Ipl1, in addition to Mps1, contributes to Bub1 kinase recruitment; Bub1 then goes on to phosphorylate Histone 2A (H2A) and recruit Sgo1 (Liu et al., 2015). Sgo1 regulates phosphorylation at kinetochores by recruiting Protein Phosphatase 2A (PP2A) and, in higher eukaryotes, Polo-like kinase 1 (Plk1) (Liu et al., 2013; Ikeda and Tanaka, 2017). Prior to bipolar attachment, kinase activity of Bub1 and Plk1 oppose PP2A dephosphorylation, but when biorientation is achieved, Bub1 dissociates from the kinetochore and PP2A dephosphorylation dominates. PP2A activity recruits PP1, and the two phosphatases go on to dismantle

mitotic checkpoint scaffolding and signaling. This dephosphorylation promotes stabilized end-on kinetochore-microtubule attachments (Carmena et al., 2012; Liu et al., 2010; Rosenberg and Cross, 2011), enabling the cell's transition into anaphase (For review: Manic et al., 2017).

Early on in mitotic checkpoint activation Bub1 recruits Sgo1 to govern sister chromatid cohesion. In particular, Sgo1 recruits the tripartite phosphatase PP2A and activates its regulatory subunit, Cdc55 (Clift et al., 2009). Activated Cdc55 inhibits Separase activity, protecting sister chromatid cohesion in a SAC-independent manner (Figure 3B). Again, recruitment of Bub1 is dependent on the tension-dependent phosphorylation of Spc105/Knl1, and therefore such signaling may be using reduced tension at kinetochores as a signal to inhibit Separase activity and delay the timing of sister chromatid separation and anaphase onset.

Bub1 is also known to form a complex with Plk1 in human cells, and together these kinases phosphorylate and inhibit Cdc20 in a MCC-independent manner (Jia et al., 2016). Bub1-Plk1 phosphorylation of Cdc20 acts in parallel to MCC inhibition of Cdc20 (Figure 3), and both pathways are necessary to sustain maximum APC inhibition (Jia et al., 2016). It remains to be seen whether these two mechanisms are connected, whether the Bub1-Plk1 mechanism acts purely in response to the tension status of kinetochores, or whether perhaps the Bub1-Plk1 mechanism acts in response to kinetochores that are tensionless because they are detached. One favored idea in HeLa cells, however, is that one or both of these potentially tension-mediated inhibitory mechanisms acts early on in M-phase as a supplement to inhibit the APC before Mps1 is fully in place to activate the canonical SAC (Masanori and Tanaka, 2017).

### *1.3.4 SAC silencing*

As described above, the timing of mitotic checkpoint activation and silencing is controlled by a balance of kinase and phosphatase activity (Figure 7). It is worth noting that several proteins involved in mitotic checkpoint signaling have multiple, seemingly contradictory roles in signaling activation and silencing. For instance, the sister chromatid cohesion protector, Sgo1, recruits PP2A; PP2A activity maintains Sgo1's kinetochore localization while checkpoint kinases counter its phosphatase activity. This promotes checkpoint signaling as the cell builds the spindle until it is time to proceed to anaphase, at which point PP2A recruits PP1 and the two phosphatases work to reverse the checkpoint-activating phosphorylation events carried out earlier in the cell cycle (Gallert et al., 2015). Similarly, while Plk1 kinase plays a prominent role in mitotic checkpoint activation in higher eukaryotes, as detailed above, Plk1 phosphorylation of Sgo1 causes Sgo1 dissociation, counteracting checkpoint signaling and sister chromatid cohesion (Tang et al., 2006; Jang et al., 2007). Thus, the many opposing roles of individual proteins at the kinetochore are intriguing, and a major challenge for the field will be to understand the functional significance of when various mechanisms come into play during mitosis in a chronological context. Although discussed to some degree above, here I will expand on studies of the mechanism of SAC silencing and anaphase onset.

Ultimately, as the cell prepares to transition to anaphase, the timing of SAC silencing is modulated by the tension status of kinetochores. In *Drosophila* S2 cells, intra-kinetochore stretch is correlated with the removal of SAC-activating

phosphorylation events, as determined by super-resolution light microscopy (Maresca and Salmon, 2009). Further, in HeLa cells suppression of intra-kinetochore stretch correlate with a delay in cyclin B degradation, suggesting reduced APC activation (Uchida et al., 2009). Together these studies implicate high intra-kinetochore stretch as a signal to silence the SAC.

However, this hypothesis has come under question in light of a study that revealed that the super-resolution approach to light microscopy that was used to measure intrakinetochore stretch can nonetheless be affected by variations in fixation techniques, visualization methods, and organizational changes in the kinetochore (Magidson et al., 2016). Such a revelation does not exclude the possibility that intrakinetochore stretch is a checkpoint silencing signal, but simply indicates that approaches and conclusions based on super-resolution imaging of intrakinetochore stretch must be viewed with increased caution. For instance, tension-mediated structural changes may be more or less visible based on particular differences in fixation or microscopy methods. In budding yeast, end-on kinetochore-microtubule attachment has been shown to physically separate Mps1 kinase from its KNL1 target Spc105 (Aravamudhan et al., 2015). It remains to be seen whether any other kinetochore proteins experience conformational changes that affect their ability to activate the SAC; this method of regulation appears to be a common theme because, as mentioned in regard to error correction, it is also used in CPC regulation. Thus, one barrier that the field must still overcome is to more completely define the tension-mediated structural changes that are read by checkpoint proteins at the kinetochore.

Ultimately, the precise physical deformations at sister chromatids' kinetochores that trigger SAC silencing remain to be determined. Contrary to several recent studies that will be discussed further below that suggest the SAC can be satisfied by microtubule attachment in the absence of tension (O'Connell et al., 2008; Tauchman et al., 2015; Etemad et al., 2015), a myriad of studies indicate that tension plays a role in overall mitotic checkpoint signaling. If one considers that bipolar attachment must be achieved prior to anaphase onset to ensure accurate chromosome segregation, it seems likely that kinetochores' tension status must regulate the timing of anaphase onset in some capacity, either in by activating the mitotic checkpoint to inhibit anaphase onset, by modulating the timing of SAC silencing, or by both processes.

Many SAC proteins play active roles in SAC silencing. Bub1/Bub3 promotes anaphase onset by promoting timely Separase activation under conditions where the spindle is assembled properly in *C. elegans*. This function of Bub1/Bub3 is beyond this complex's role in the SAC, but does require kinetochore localization and Bub1's kinase domain but not kinase activity (Kim et al., 2015; Yang et al., 2015). Subsequent research, also in *C. elegans*, indicates that the checkpoint silencing role of Bub1-Bub3 lies in its ability to recruit the APC activator Cdc20 to the kinetochore to experience one of two opposing fates. Bub1-Bub3 can either promote PP1-mediated dephosphorylation of Cdc20's inhibitory modifications so that it can go on to activate the APC, or bub1-Bub3 can inhibit Cdc20 by promoting its incorporation into the MCC. In this scenario, the fate of Cdc20 is decided by the attachment state of the kinetochore (Kim et al., 2017). Further, Plk1 is thought to modulate intrakinetochore stretch in human cells (Liu et al., 2012), and timely removal of Plk1 from the inner kinetochore also promotes SAC

silencing and an increase in microtubule dynamics to aid in the correction of kinetochore-microtubule attachment errors before anaphase onset (Liu et al., 2012). Broadly speaking, however, it is the contribution of two events that occur upon bipolar microtubule attachment that together lead to the dissociation of all SAC components. First, kinases become unable to phosphorylate Ndc80, allowing for the formation of stable KMT attachments; and second, microtubule binding displaces Mps1 from the microtubule binding site at Ndc80 (Ji et al., 2015; Hiruma et al., 2015), dismantling the original SAC signal and licensing anaphase onset.

### 1.4 Experimental intractability of separating attachment from tension in checkpoint signaling: notable methods to study checkpoint activation

Kinetochore attachment and tension at metaphase are interdependent. Kinetochores that are not attached to spindle microtubules are not under tension, and attached kinetochores that are not under tension quickly become detached, either actively via the error correction mechanism, or passively due to the inherent instability of tensionless kinetochore-microtubule attachments (Nicklas and Staehly, 1967; Akiyoshi et al., 2010; Krenn and Musacchio, 2015). Experiments using micromanipulation in insect spermatocytes (Nicklas and Staehly, 1967; Nicklas and Koch, 1969) or unpaired sister chromatids in yeast (Shonn et al., 2000; Stern and Murray, 2001) provide compelling evidence that reduced tension results in signaling to delay anaphase onset. However, these studies do not exclude the possibility of transient detachment or partial detachment in compound kinetochores of higher eukaryotes, which may activate the

canonical attachment mediated SAC to an unknown degree. Further, because these signaling cascades share the same relative mitotic timing and overlapping protein components, each signaling pathway becomes more difficult to define and distinguish from the others.

In all mitotic checkpoint signaling, the original activating signal (kinetochore tension/attachment) is not entirely defined. Interplay between kinetochore tension and attachment has the potential to affect the initiation or strength of each signaling cascade, and therefore the signals that moderate each branch of mitotic signaling (the SAC/error correction/biorientation) remain hazy. This is in part due to unavoidable limitations of past experimental systems that preclude complete isolation of kinetochore tension from kinetochore attachment (Table 1); importantly, because these techniques do not fully separate tension from attachment, our understanding of how tension at kinetochores affects mitotic progression remains limited.

| Method | Experimental objective | Confounding issue |
|---|---|---|
| Inhibit DNA replication | Reduce tension by producing unpaired chromatids | Can also stimulate detachment; disrupts inter-kinetochore structure |
| Inhibit cohesion between chromosomes | Reduce tension by separating sister chromatids | Can also stimulate detachment; disrupts inter-kinetochore structure |
| Kinetochore mutants | Promote unattached kinetochores | Also depletes tension; may disrupt kinetochore structure |
| Microtubule depolymerizing compounds | Promote unattached kinetochores | Also depletes tension |
| Microtubule stabilization with Taxol (higher eukaryotes only) | Reduce tension by inhibiting microtubule depolymerization | Inhibits kinetochore attachment |

**Table 1. Classic experimental methods to activate the spindle assembly checkpoint based on reducing tension and/or preventing kinetochore attachment.**

Classic techniques, particularly in budding yeast, were instrumental in elucidating the mechanisms of SAC activation and error correction. Microtubule destabilizers such as benomyl were critical in the discovery of key SAC proteins (Li and Murray, 1991; Hoyt et al., 1991), however because detached kinetochores are also tensionless, this method does not separate the two signals experimentally. Kinetochore mutants that inhibit microtubule attachment (Biggins et al., 2001; Lampson and Kapoor 2005; Pinsky et al., 2006) similarly do not separate the two signals, and further, mutant kinetochore architecture may affect signaling in unpredictable ways, for instance by affecting intrakinetochore stretch. By this logic, Cdc6 mutants, for which DNA replication is inhibited under specific conditions (Piatti et al., 1995; Stern and Murray, 2001), attach microtubules to single kinetochores incapable of being under tension; however, this occurs in cells whose spindle architecture is not bipolar and is therefore highly abnormal, potentially affecting signaling in unknown ways. In yeast, cohesin mutants relax or cleave cohesion of chromatids that are bioriented on the spindle, generating tensionless kinetochores (Biggins and Murray, 2001; Indejeian et al., 2005). However, this method again drastically alters spindle architecture by generating abnormally elongated metaphase spindles, potentially affecting checkpoint signaling in unknown ways. Perhaps the best illustration of this conundrum is the fact that when comparing systems in which DNA replication or cohesion is inhibited, systems which are supposed to reduce tension identically, the two sets of results indicate different protein requirements for tension-mediated signaling (Barnhart et al., 2011). Further, although many studies have examined the attachment status of kinetochores in these two systems and found them to remain attached to the spindle (Stern and Murray, 2001;

Indejeian et al., 2005), none of these studies unequivocally rules out transient detachment under conditions where tension is absent in yeast kinetochores.

In animal cells, the kinesin-5 inhibitor, Monastrol, (Kapoor et al., 2000; Lampson et al., 2004) produces monopolar spindles with tensionless sister chromatids, both attached to microtubules emanating from the single spindle pole. While this system simulates syntelic attachment remarkably well, it again reduces tension in cells with highly abnormal spindles that are not bipolar; however, this method remains a good model for the error correction mechanism (Lampson et al., 2004). Also in animal cells tension at kinetochores can be modulated through the use of microtubule stabilizing agents such as Taxol, Epothilone B, or low doses or microtubule destabilizing drugs such as nocodazole (Yang et al., 2009). These drugs reduce plus end microtubule dynamics at the kinetochore, reducing pulling forces on sister chromatids; however, kinetochores of higher eukaryotes have many microtubule binding sites per kinetochore, and it has been shown via electron microscopy in $PtK_1$ cells that one hour long Taxol treatment produces kinetochores with an abnormally variable number of microtubules bound to each, although the average number of microtubules bound remains constant in the presence/absence of Taxol (McEwen et al., 1997). Considering individual kinetochores in Taxol, however, it is difficult to predict how those with fewer microtubules bound than normal might activate tension or attachment-mediated signaling.

Several recent studies using various methods to reduce tension at kinetochores should be noted. In drosophila and HeLa cells, a microscopy technique measuring the distance between foci of inner and outer kinetochore components achieves super-

resolution measurements of intrakinetochore stretch. This 'super-resolution microscopy' was used to determine whether intrakinetochore stretch correlated with tension-mediated SAC satisfaction; however, these studies have produced conflicting results (Maresca and Salmon, 2009; Uchida et al., 2009; Wan et al., 2009; Tauchman et al., 2015; Etemad et al., 2015; Magidson et al., 2016). One group of studies reported that an increase in intrakinetochore stretch was associated with SAC satisfaction and timely anaphase onset (Maresca and Salmon, 2009; Uchida et al., 2009; Wan et al., 2009). Conversely, the other group of studies found that intrakinetochore stretch was not necessary for SAC satisfaction, and that only end-on kinetochore attachment was necessary to satisfy the SAC (Tauchman et al., 2015; Etemad et al., 2015). Moreover, it was also demonstrated that measurements of intra-kinetochore stretching obtained from super-resolution light microscopy are subject to variations due to altered kinetochore shape in response to tension, but also in response to additional factors such as changes in kinetochore organization, fixation techniques and methods of visualization (Magidson et al., 2016). Thus, measurements of intra-kinetochore tension must be viewed with caution in these studies.

However, the two studies which concluded that kinetochore end-on attachment is the only requirement for SAC silencing drew their conclusions from additional methods beyond super-resolution microscopy (Tauchman et al., 2015; Etemad et al., 2015). These studies used a novel technique to modulate tension at attached kinetochores in human cells: HEC1-9A mutants carry a non-phosphorylatable variant of the Ndc80 subunit, Hec1, that inhibits kinetochore-microtubule detachment, even in the absence of tension (Tauchman et al., 2015; Etemad et al., 2015) These studies concluded that,

because HEC1-9A cells still enter anaphase under these conditions, kinetochore attachment alone is sufficient to silence SAC activation even in the presence of spindle poisons that produce monopolar spindles, tensionless sister chromatids, and reduced microtubule dynamics. While brilliantly designed, semantics appear to be a point of contention when interpreting these assays, as with many others.

The experimental setup used by Tauchman et al. (Tauchman et al., 2015) treated cells with S-trityl-L-cysteine (STLC) to promote formation of monotelic and syntelic attachments. Cells expressing WT-HEC1 arrested in metaphase and retained Mad1 at kinetochores, indicating SAC activation and kinetochore detachment. On the other hand, cells expressing HEC1-9A formed stable syntelic attachments, did not retain Mad1 at kinetochores, and degraded Cyclin B shortly before entering anaphase. The fact that cells entered anaphase under these conditions indicated a lack of sustained SAC activation, along with the ability to silence any previous signaling (Tauchman et al., 2015). However, the fact that HEC1-9A cells containing syntelic attachments experience longer mitotic transit times was not explored in this study, and, while the SAC may be satisfied, it is only a subset of the signaling that makes up the mitotic checkpoint as a whole. Therefore, this study does not exclude the possibility that alternative tension-mediated checkpoint signaling, while not prohibitive to anaphase onset, does still play a role in the timing of anaphase onset.

Etemad et al. similarly employed the HEC1-9A mutant to interrogate the roles of kinetochore tension and attachment in HeLa cells (Etemad et al., 2015) and correlated the timing of Mad2 removal from kinetochores with the timing of anaphase onset. In this study HEC1-9A cells treated with STLC lost mad2 from virtually all kinetochores,

indicating stable, end-on syntelic attachments. Soon after the loss of Mad2 from all kinetochores, HEC1-9A cells exited mitosis. In contrast, cells expressing WT-HEC1 arrested in mitosis with high levels of Mad2 at kinetochores, indicating detachment. Both cell types were able to mount a full SAC response when detached kinetochores were present, as indicated by similar levels of SAC protein recruitment to detached kinetochores, and so HEC1-9A cells that entered anaphase with syntelic attachments were thought to have satisfied and silenced the SAC. The authors noted a delay in anaphase onset in STLC-treated HEC1-9A cells, but attributed it to steric hindrance slowing the formation of end-on syntelic attachments. Nonetheless, timing of Mad2 loss from all kinetochores always correlated well with the timing of anaphase onset, indicating SAC silencing. Once again, while the canonical SAC does appear to be convincingly silenced in this study, weaker, more transient signals in response to low kinetochore tension may have been undetectable or already extinguished by the time Mad2 had left kinetochores in this experimental setup. Altogether, the implication put forth by these two studies (Tauchman et al., 2015; Etemad et al., 2015), that end on attachment is the only thing necessary for SAC silencing and anaphase onset, risks overlooking possible transient hallmarks of the mitotic checkpoint that are a result of mechanisms outside of canonical SAC activation.

It further remains possible that tension-mediated events, while not required, enhance the speed of SAC silencing to promote timely anaphase onset and accurate chromosome segregation. For instance, bipolar attachment causes the tension-mediated physical separation of Mps1 kinase from Spc105, disrupting a crucial first step in SAC signaling (Aravamudhan et al., 2015). Thus, correct attachment generates

tension within the kinetochore that directly opposes mitotic checkpoint signaling. One common assumption is that small delays in anaphase onset are not the result of mitotic checkpoint signaling because they are temporarily distinct from canonical SAC signaling. However, this assumption may contribute to relatively shorter tension-mediated delays being largely overlooked in studies of mitotic checkpoint signaling.

### 1.5 Overview of thesis/Significance of my work

Mitotic checkpoint signaling is an evolutionarily conserved cellular process that promotes accurate segregation of chromosomes each time a cell divides. As it relates to human health, the mitotic checkpoint is also a major target for the widely used chemotherapeutic agents, taxanes. It is necessary to clearly separate the signals that both reduced tension and kinetochore detachment produce at metaphase in order to better understand the contribution each makes to mitotic checkpoint activation, and to implement this knowledge toward more effective or specific treatments such as chemotherapy.

Unattached kinetochores are inherently tensionless, and so kinetochore detachment cannot be studied in isolation. It is therefore necessary to create a system that reduces tension at attached kinetochores to extrapolate how tension and attachment individually contribute to mitotic checkpoint signaling and accurate spindle assembly. We have developed a novel system in budding yeast that draws on the strengths of several previous advances to reduce tension at attached kinetochores in otherwise normal, bipolar spindles. Through our work, we have demonstrated that Taxol

sensitive budding yeast can mount a tension mediated metaphase delay independent of kinetochore detachment, and that this delay is genetically and temporally distinct from canonical SAC activation.

### 1.6 Development of the Taxol sensitive yeast system

Budding yeast is an ideal system to study cell signaling for many reasons, not least of which is its genetic tractability and simplicity. Key to the unambiguous study of kinetochore tension and attachment is the fact that each budding yeast kinetochore binds only a single microtubule (Winey et al., 1995). Thus, sister chromatids can either be fully attached and can experience tension or completely unattached and unable to come under tension. Importantly, budding yeast cannot experience partial attachment and ambiguous signaling activation in the way that higher eukaryotes, whose kinetochores have many microtubule binding sites, can.

Because the mitotic checkpoint may respond to either inter- or intra-kinetochore changes, it highly advantageous to study tension-mediated signaling using an approach which does not introduce confounding alterations to the kinetochore or spindle architecture (such as kinetochore mutants, or mutants in which cohesion or DNA replication have been manipulated to reduce kinetochore tension). When examining tension-mediated signaling, experimental approaches that reduce kinetochore tension by dramatically altering spindle structure/kinetochore architecture risk inadvertently interfering with signaling within the pathway they wish to examine. In contrast, a major strength of higher eukaryotic model systems is the use of microtubule stabilizing drugs,

namely Taxol, to reduce tension at otherwise unperturbed kinetochores. Thus, we wanted to perform our study of tension-mediated signaling in a model system which combines the experimental tractability and advantageous single microtubule per kinetochore arrangement of budding yeast, with the microtubule stabilizing activity of Taxol, to reduce tension at otherwise unperturbed kinetochores. However, this was not immediately possible because budding yeast are not naturally sensitive to Taxol.

In two previous studies, budding yeast were rendered sensitive to Taxol through a series of targeted mutations (Gupta et al., 2003; Foland et al., 2005). Yeast β-tubulin does not bind to Taxol, whereas mammalian β-tubulin does. Based on sequence differences between yeast and mammalian β-tubulin, Gupta et al. introduced five amino acid substitutions into yeast β-tubulin (*A19K-T23V-G26D-N227H-Y270F*), which produced active Taxol-binding by yeast tubulin . *In vitro,* Taxol-sensitive tubulin polymerizes into microtubules that are readily stabilized by Taxol (Figure 8A), but yeast

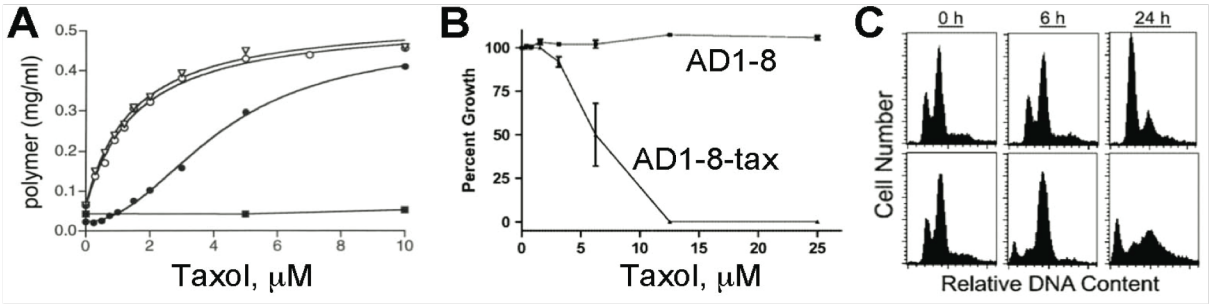


Source: Gupta et al., 2003; Foland et al., 2005

**Figure 8. Novel yeast model system is Taxol-sensitive.** (A) Taxol-stimulated assembly of wild-type yeast (■), mutated yeast (○), or bovine (●) tubulin. (B) Taxol-sensitivity of yeast cells containing wild-type (AD1-8) and mutated (AD1-8-tax) tubulin. (C) FACS analysis of cultures containing wild-type (top) and mutated (bottom) tubulin incubated with 25 μM Taxol for the indicated time.

cells expressing Taxol sensitive tubulin are not naturally sensitive to Taxol *in vivo* because drug resistance mechanisms that function to prevent harmful molecules from accumulating in the cell efficiently export the drug. Therefore, to create the first Taxol sensitive strain of budding yeast, AD1-8-tax, seven genes for ABC transporters and one ABC transporter transcription factor were inactivated in a strain expressing Taxol sensitive yeast β-tubulin (Foland et al., 2005). This strain fails to grow on agar plates containing high concentrations of Taxol. When grown in liquid media containing Taxol, the culture accumulates cells in metaphase (Figure8B and C).

Our current Taxol sensitive yeast strain has been modified from the original strain to make it more experimentally tractable while still retaining robust Taxol sensitivity. Our strain carries four of the five original β-tubulin amino acid substitutions (*A19K-T23V-G26D-Y270F*), and three genetic mutations that render it drug sensitive *pdr1Δ, pdr3Δ, and erg6Δ*. Leveraging this system, I show here that Taxol reduces tension at attached kinetochores in otherwise bipolar spindles. For the first time, I show that reduced tension at fully attached kinetochores delays anaphase onset by inducing signaling that is dependent on the SAC components Bub1 and Bub3, yet is independent of kinetochore detachment.

Importantly in this system, spindle architecture and dynamics remain comparable to that of wildtype cells, allowing us to assess kinetochore-microtubule attachment pre- and post-anaphase. Moreover, because our system utilizes yeast with typical bipolar spindles, we are also able to perform assays that directly visualize key hallmarks of anaphase onset, such as spindle elongation and chromosome separation, giving us

unprecedented time resolution when measuring the tension-mediated delay in anaphase onset.

Two caveats are central to synthesizing information about tension-mediated checkpoint signaling. First: in general, the Mitotic checkpoint mechanism is evolutionarily conserved; however, elements of mitotic checkpoint signaling are not conserved across all organisms. Therefore, conservation of tension-mediated signaling is also not guaranteed, and mechanisms described for one organism may not hold true for another. Second: various modifications to kinetochore tension may result in different tension-mediated mitotic checkpoint signaling. For instance, tensionless kinetochores that area result of microtubule detachment may produce a specific type of signaling, or no signaling (Deluca et al., 2011), whereas attached kinetochores under reduced tension may activate distinct signals, including error correction. Either of these possibilities may contribute to the number of conflicting conclusions various studies have reached over the years regarding tension as a checkpoint-activating signal.

In light of these incongruencies, we must consider that any artificial means to reduce tension at kinetochores may initiate different kinds of tension mediated responses depending on how it affects the kinetochore-microtubule attachment, and in particular, kinetochore architecture (For review: Sarangapani and Asbury, 2012). My research proceeds with this in mind and strives to serve as an example for future work. Although the evidence I present here indicates that reduced tension, independent of kinetochore microtubule detachment, produces a delay in anaphase onset that requires a specific subset of SAC proteins, Bub1 and Bub3, it will be important in future work not only to identify the other protein components of this mechanism, but also to determine

how our experimental system affects kinetochore microtubule architecture and to compare these results to those in other model systems, to establish to what degree this signaling is evolutionarily conserved. By categorizing which studies produce changes at the kinetochore that activate the same signaling pathways, it will become possible to assemble bodies of work from independent labs to build a better understanding of tension mediated mitotic checkpoint signaling.

# Chapter 2:

# Taxol sensitive yeast microtubules reveal a tension mediated delay that requires a subset of SAC proteins

## 2.1 Abstract

To ensure genome stability in mitosis, the spindle assembly checkpoint (SAC) delays anaphase if sister chromosomes are not bound to microtubules from opposite spindle poles. In this configuration, dynamic microtubules produce tension across sister kinetochores. The interdependency of kinetochore-microtubule attachment and tension has proved challenging to understanding SAC mechanisms. Thus, whether the SAC responds simply to kinetochore attachment status, or also to tension status remains obscure. Unlike higher eukaryotes, budding yeast kinetochores bind only one microtubule, simplifying the relationship between attachment and tension. To address the role of tension in the SAC, we developed a Taxol-sensitive yeast model that allows tension to be reduced by microtubule stabilization in fully assembled spindles. Our results show that reducing tension on bipolar attached kinetochores delays anaphase onset. The tension-mediated delay is transient relative to that imposed by unattached kinetochores. Furthermore, it requires the SAC proteins Bub1 and Bub3, but persists without Mad1, Mad2 and Mad3 (yeast BubR1). Together our results demonstrate that reduced tension generates a 'wait-anaphase' signal that is temporally and mechanistically distinct from that characterized for unattached kinetochores.

## 2.2 Introduction

Accurate chromosome segregation is critical to cell division. Missegregation leads to aneuploidy (Siegel and Amon, 2012), birth defects (Hassold and Hunt, 2001), and tumor progression (Gordon et al., 2012). In eukaryotes, faithful segregation requires that the kinetochores of sister chromosomes attach to microtubules emanating from opposite spindle poles. Only in this bipolar configuration can dynamic microtubules generate tension across the sister kinetochores (Figure 1A). To ensure segregation, a surveillance mechanism, termed the spindle assembly checkpoint (SAC), is active and delays anaphase onset under conditions where either attachment or tension is lacking (Figures 1B and 2B). A longstanding challenge has been to understand how the lack of tension contributes to SAC activation. It is widely accepted that unattached kinetochores activate the SAC (Li and Murray, 1991; Hoyt et al., 1991; London and Biggins, 2014b). Studies addressing the role of tension have produced contradictory evidence (Shannon et al., 2002; Rieder et al., 1994; O'Connell et al., 2008; Pinsky et al., 2006; Li and Nicklas, 1995; Nicklas et al., 1995; Stern and Murray, 2001; Biggins and Murray, 2001; Uchida et al., 2009; Wan et al., 2009; Maresca and Salmon, 2009; Skoufias et al., 2001; Waters et al., 1998; Tauchman et al., 2015; Rieder et al., 1995; King et al., 2007), and a consensus has not been obtained (Centromere tension: a divisive issue., 2010; Nezi et al., 2009; Pinsky and Biggins, 2005; Maresca and Salmon, 2010; Murray, 2011). Experiments using micro-manipulation in praying mantid spermatocytes (Li and Nicklas, 1995), or unpaired chromosomes in yeast (Shonn et al., 2000; Stern and Murray, 2001) provide compelling evidence that reduced tension results in SAC activation. However,

interpretation of these experiments has been confounded by the error correction mechanism; tensionless microtubule-kinetochore attachments are selectively destabilized by the activity of Aurora B kinase (Tanaka et al., 2002; Biggins and Murray, 2001; Pinsky et al., 2006; Krenn and Musacchio, 2015). Generally, this central caveat has prevented the exclusion of unattached kinetochores as a SAC signal under conditions of reduced tension. Notably, unattached kinetochores themselves are not under tension. Thus, whether a lack of tension contributes directly to SAC activation, independent of inducing kinetochore detachment, remains obscure (Figure 3).

In higher eukaryotes, the microtubule stabilizer Taxol reduces tension at kinetochore attachments and activates the SAC (Maresca and Salmon, 2009; Waters et al., 1998). Kinetochores in higher eukaryotes typically bind dozens of microtubules, and decreased tension is correlated with reduced binding occupancy (King and Nicklas, 2000; Nicklas and Ward, 1994; Nicklas et al., 2001). Although one hour Taxol treatment in mammalian $PtK_1$ cells does not reduce the average, it increases the variation in the number of microtubules bound to each kinetochore (McEwen et al., 1997). It is not known to what extent the unoccupied microtubule binding sites resulting from this altered microtubule occupancy are recognized as an unattached kinetochore. Also, evidence indicates that prolonged mitotic arrest in Taxol is associated with unattached kinetochores (Magidson et al., 2016; Waters et al., 1998). Thus, unoccupied binding sites, rather than a lack of tension, cannot be excluded as a SAC signal. Unlike higher eukaryotes, the budding yeast *S. cerevisiae* kinetochore binds just one microtubule (Winey et al., 1995). This simplifies the relationship between tension and attachment because budding yeast kinetochores are either unattached or fully attached; there is no

reduced microtubule occupancy. To date, microtubule stabilizers have not been used to study the SAC in yeast because Taxol does not stabilize wild-type yeast microtubules (Barnes et al., 1992; Bode et al., 2002).

To address the role of tension in the SAC, we utilized a Taxol-sensitive budding yeast model harboring an engineered β-tubulin that allows Taxol stabilization of yeast microtubules (Gupta et al., 2003; Foland et al., 2005). Unlike approaches that rely on unreplicated sister chromosomes or disrupted cohesion, which severely disrupt bipolar spindle organization (Piatti et al., 1995; Stern and Murray, 2001; Uhlmann et al., 2000), Taxol treatment did not similarly perturb preformed spindles. Using this system, we find that reduced tension on bipolar attached yeast kinetochores delays anaphase onset. This delay is transient relative to that imposed by unattached kinetochores. It requires the SAC proteins Bub1 and Bub3, but persists in the absence of Mad1, Mad2, and Mad3 (yeast BubR1), which are required for the response to unattached kinetochores. Thus, the tension mediated delay is temporally and genetically distinct from the canonical SAC response to unattached kinetochores.

## 2.3 Results

Yeast cells are not normally sensitive to Taxol because the drug does not bind to yeast tubulin. By modifying five amino acids, we previously created an active binding site in yeast β-tubulin that allows Taxol to robustly stabilize yeast microtubules in vitro. Yet, Taxol does not inhibit growth of cells harboring this tubulin because yeast efficiently export the drug. However, placing this tubulin in a strain deficient for the pleiotropic drug

response (ABC transmembrane transporters) renders cells susceptible to Taxol (Figure 9). This modified tubulin does not significantly perturb microtubule dynamics in the absence of Taxol. Yet, cellular microtubules become resistant to cold-induced depolymerization upon Taxol treatment, indicating they are stabilized by the drug. Moreover, Taxol treatment increases the percentage of large budded cells in cycling cultures over 2-fold, indicating a delay in mitotic progression. Thus, as in higher eukaryotes, Taxol stabilizes microtubules and induces mitotic delay in Taxol sensitive budding yeast.

Table 2. Parameters of dynamic instability for cytoplasmic microtubules in preanaphase cells.

| | Control | Taxol |
|---|---|---|
| Polymerization Rate (μm/min) | 1.42 ± 0.62 (36) | 0.83 ± 0.69 (2) |
| Depolymerization Rate (μm/min) | 2.10 ± 0.79 (33) | 1.27 ± 0.13 (2) |
| Catastrophe Frequency ($min^{-1}$) | 0.81 (28) | 0.03 (2) |
| Rescue Frequency (per $min^{-1}$) | 0.65 (12) | 1.3 (2) |
| Time spent polymerizing, % | 45.8 | 2.1 |
| Time spent depolymerizing, % | 34.7 | 1.0 |
| Time spent attenuated, % | 19.5 | 96.9 |
| Average polymerization duration, s | 40.7 ± 18 (36) | 21.0 ± 4 (02)* |
| Average depolymerization duration, s | 33.6 ± 17 (33) | 45.0 ± 30 (02) |
| Average attenuation duration, s | 29.6 ± 11 (21) | 105.1 ± 70 (39)* |
| Dynamicity, tubulin/sec | 38.9 | 0.85 |
| Total microtubule observed | 37 | 39 |
| Total time observed, s | 3196 | 4230 |

Sample number shown in parenthesis; Error = SD; *p < 0.05 versus control by unpaired, two-tailed t-test.

To examine the effect of microtubule stabilization on mitotic progression, we sensitized the commonly used s288c background to Taxol. Similar to previous results (Foland et al., 2005), Taxol does not inhibit growth of ‘drug sensitive’ yeast that have

been sensitized to exogenous compounds (*pdr1*Δ *pdr3*Δ *erg6*Δ). However, growth of drug sensitive yeast harboring the Taxol sensitive tubulin is inhibited by increasing concentrations of Taxol (Figure 9A). Further, upon closer examination of individual microtubules in live preanaphase cells expressing GFP-labeled tubulin (GFP-Tub1), the overall dynamicity of cytoplasmic microtubules is reduced by approximately 98% in cells treated with Taxol, indicating that Taxol significantly stabilizes microtubules in Taxol-sensitive yeast cells (Table 2).

### *2.3.1 Taxol treatment during spindle assembly delays anaphase onset with unattached and low tension kinetochores present*

In higher eukaryotes, Taxol inhibits spindle assembly and produces a SAC-dependent delay in anaphase onset (Long and Fairchild, 1994; Schiff and Horwitz, 1980; De Brabander et al., 1981; Jordan et al., 1993; Fuchs and Johnson, 1978; Waters et al., 1998). To monitor the timing of anaphase onset in Taxol treated yeast we utilized a G1 release assay (Figure 9B). We released G1-synchronized cells into the cell cycle, split them into sister cultures either with or without Taxol, and monitored cell cycle progression by following cell morphology and chromosome separation. All assays were scored blinded with respect to cell genotype and Taxol treatment (as described in methods). Cells budded with identical kinetics in both cultures, indicating that Taxol does not affect the timing of cell cycle initiation (Figure 9C and D). However, Taxol treatment produced an approximately hour-long delay in anaphase onset (Figure 9E).

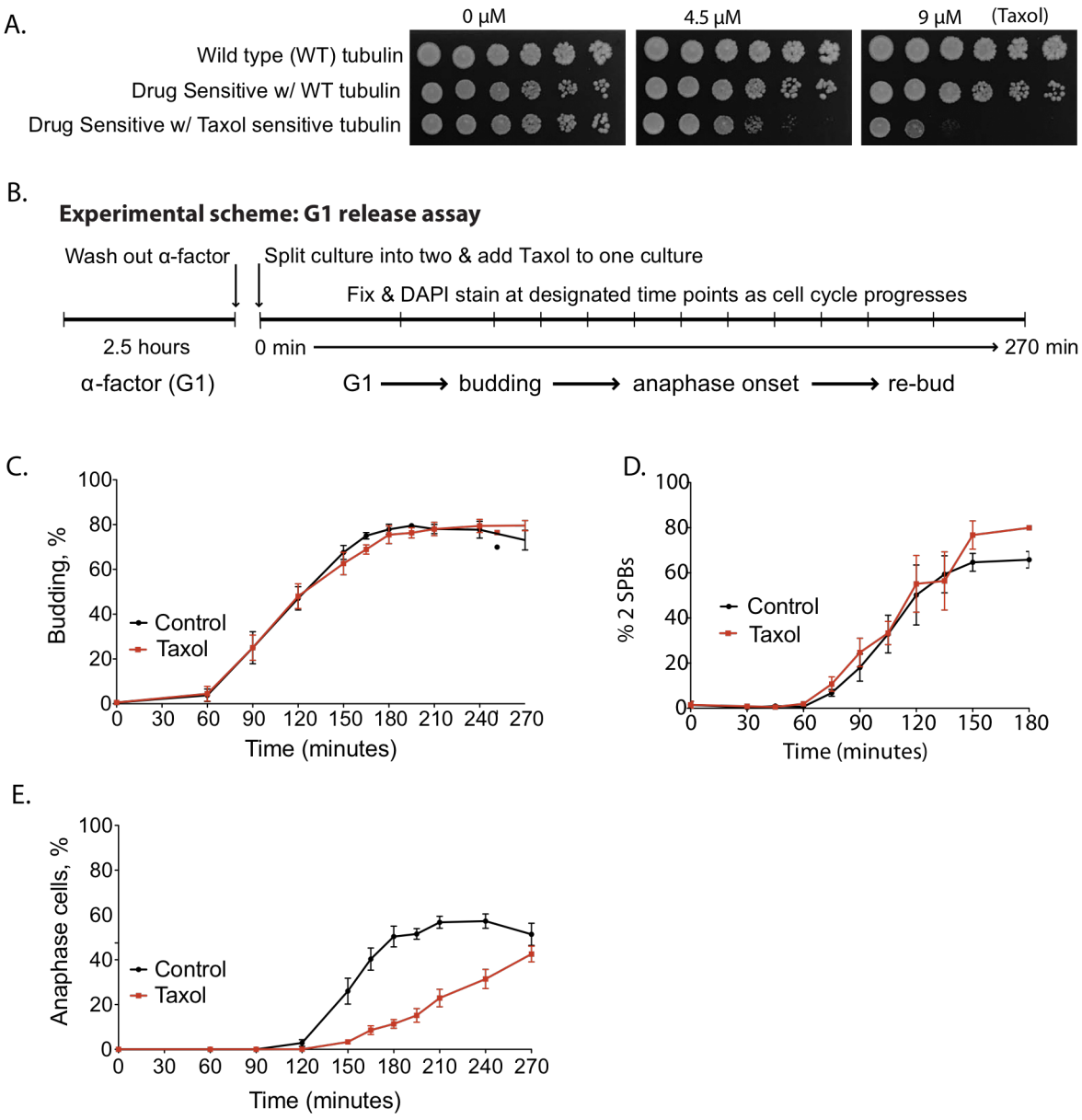


**Figure 9. Taxol treatment during spindle assembly delays anaphase onset without disrupting bud emergence or spindle pole body duplication.** (A) Serial dilutions of control cells with wild type tubulin, drug sensitive cells with wild type tubulin, and drug sensitive cells with Taxol sensitive tubulin (Taxol sensitive cells) were spotted on agar plates with the indicated Taxol concentration. (B) Experimental scheme of the G1 release assay. (C-E) Timing of bud emergence (C) timing of spindle pole body (SPB) duplication (D) timing of anaphase onset in Taxol sensitive cells monitored by the G1 release assay (± 30µM Taxol). For bud emergence (D) and anaphase onset (E) values represent mean ± SEM of 11 experiments, with n = 100-200 cells scored per time point and drug condition for each experiment. Some time points were not included in 4 of the 11 replicates. For SPB duplication values represent the mean ± SEM of 3 experiments, with n = 100-200 cells scored per time point and drug condition for each experiment.

To examine the effect of Taxol on spindle assembly, we labeled spindle poles (Spc29-mRFP) and monitored the position of sister centromeres by marking *CEN1* with GFP (*CEN1*-tetO/tetR-GFP). Centromere alignment on the spindle axis between the poles is indicative of kinetochore attachment (He et al., 2000; Goshima and Yanagida, 2000; Tanaka et al., 2002). Imaging of attached centromeres in live cells revealed that they typically lie up to ~300 nm off the central pole-to-pole axis (Haase et al., 2012). Therefore, we scored centromeres, and their associated kinetochores, as attached to the spindle if they were within a square created by extending lines from each pole at 45˚ angles to the spindle axis (Figure 10A). Conversely, they were scored as detached if they were outside this square (Figure 10A). We treated cycling cells with or without

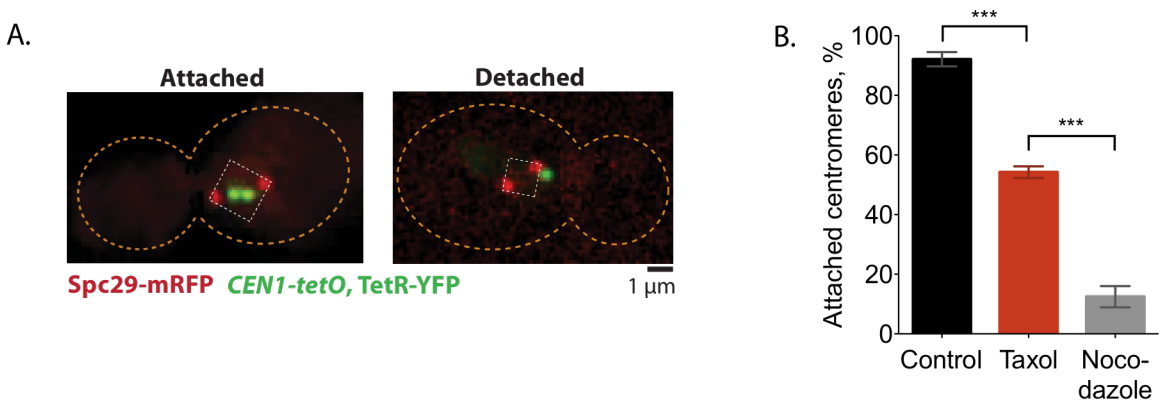


**Figure 10. Taxol treatment during spindle assembly delays anaphase onset with both unattached and low tension kinetochores present.** (A) Fluorescence micrographs of metaphase cells. Cell outline is indicated by an orange hashed line; spindle poles are red (outer spots); a single centromere (*CEN1*), or pair during mitosis, is green (inner spots); a box (white, hashed) was generated by right angles emanating from each spindle pole. Centromeres were considered attached if both centromere spots were within this box, and detached if centromere spots were outside this box. (B) Percent cells with attached centromeres when Taxol or nocodazole is present during spindle assembly. Log phase cultures of Taxol sensitive cells were incubated at 30˚C for 2 hours in the absence (control) or presence of either Taxol or nocodazole. Cells were fixed and centromere attachment (via associated kinetochores) was scored as described in (A). Bars represent mean ± SEM from 3 independent experiments; n = 114, 81, 108 for control, 107, 118, 106 for Taxol and 130, 113, 125 for nocodazole treated cells; $p$ = 0.0003 and 0.0005 for Taxol compared to control and nocodazole treated cells, respectively.

Taxol and examined pre-anaphase cells with separated spindle poles. In these cells, Taxol treatment reduced centromere attachment by nearly 50% (Figure 10B). As a control, treating cells with the microtubule destabilizer nocodazole reduced centromere attachment by 90% (Figure 10B). Microtubules cannot generate tension on unattached kinetochores. Thus, Taxol treatment during spindle assembly results in kinetochores that are both unattached and under low tension, and either condition could contribute to the observed delay in anaphase onset.

### *2.3.2 Taxol reduces tension at attached kinetochores in preformed yeast spindles*

We sought to exploit the tractability of yeast, and the fact that budding yeast kinetochores bind only one microtubule, to control the tension status of attached kinetochores. Cdc20 activates the Anaphase Promoting Complex (APC) to drive cells from metaphase to anaphase. Cells depleted for Cdc20 are unable to enter anaphase even though spindle assembly is complete and the SAC is satisfied (Lim et al., 1998). We released G1-synchronized cells into methionine-containing media to repress *CDC20* expression (*pMET3-CDC20*). After 60 min, the vast majority of cells displayed metaphase spindles with *CEN1* properly attached. To ensure sufficient time to complete assembly, we allowed an additional 15 min. We then split the culture and treated one half with Taxol and the other without (Figure 11A). After 15 min cells were fixed and imaged. Spindle length is unchanged in control and Taxol treated cells, suggesting Taxol does not significantly disrupt the architecture of preformed spindles (Figure 11B). Notably, centromere attachment to preformed spindles remains similar in control and

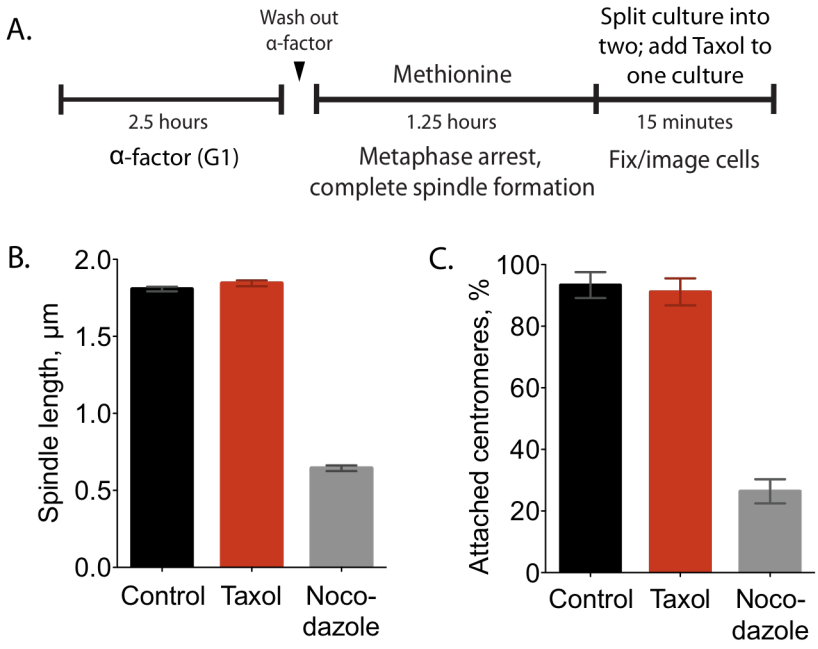


**Figure 11. Taxol does not detach kinetochores in preformed spindles.** (A) Schematic of Taxol treatment of preformed metaphase spindles. Cells synchronized in G1 (alpha-factor) were released into media containing methionine to hold cells in metaphase with fully formed spindles (Cdc20 depletion). Cultures were split, treated with DMSO ± 30µM Taxol or 15 µg/ml nocodazole for 15 minutes, and imaged fixed (B) Spindle length measured from outer edges of Spc29-mRFP marked spindle pole bodies. Mean ± SEM; n = 469, 429, and 258 for control, Taxol, and nocodazole treated. (C) Percent cells with attached centromeres when Taxol or nocodazole is added to preformed spindles. Attachment was measured as in Figure 10A. Mean ± SEM from 3 independent experiments; n = 111, 110, 155 for control, 148, 100, 178 for Taxol and 100, 58, 100 for nocodazole treated cells.

Taxol treated cells (Figure 11C). In contrast, nocodazole treatment of preformed spindles reduces length by 70% and dramatically induces centromere detachment (Figure 11B-C). Thus, under these conditions Taxol treatment does not cause significant kinetochore detachment from preformed yeast spindles.

We next examined the tension status of kinetochores in preformed spindles treated with Taxol. In diverse organisms, when sister chromosomes are attached to the spindle in bipolar configuration, dynamic microtubules generate tension that increases the distance between their centromeres/kinetochores (Kelling et al., 2003; Waters et al.,

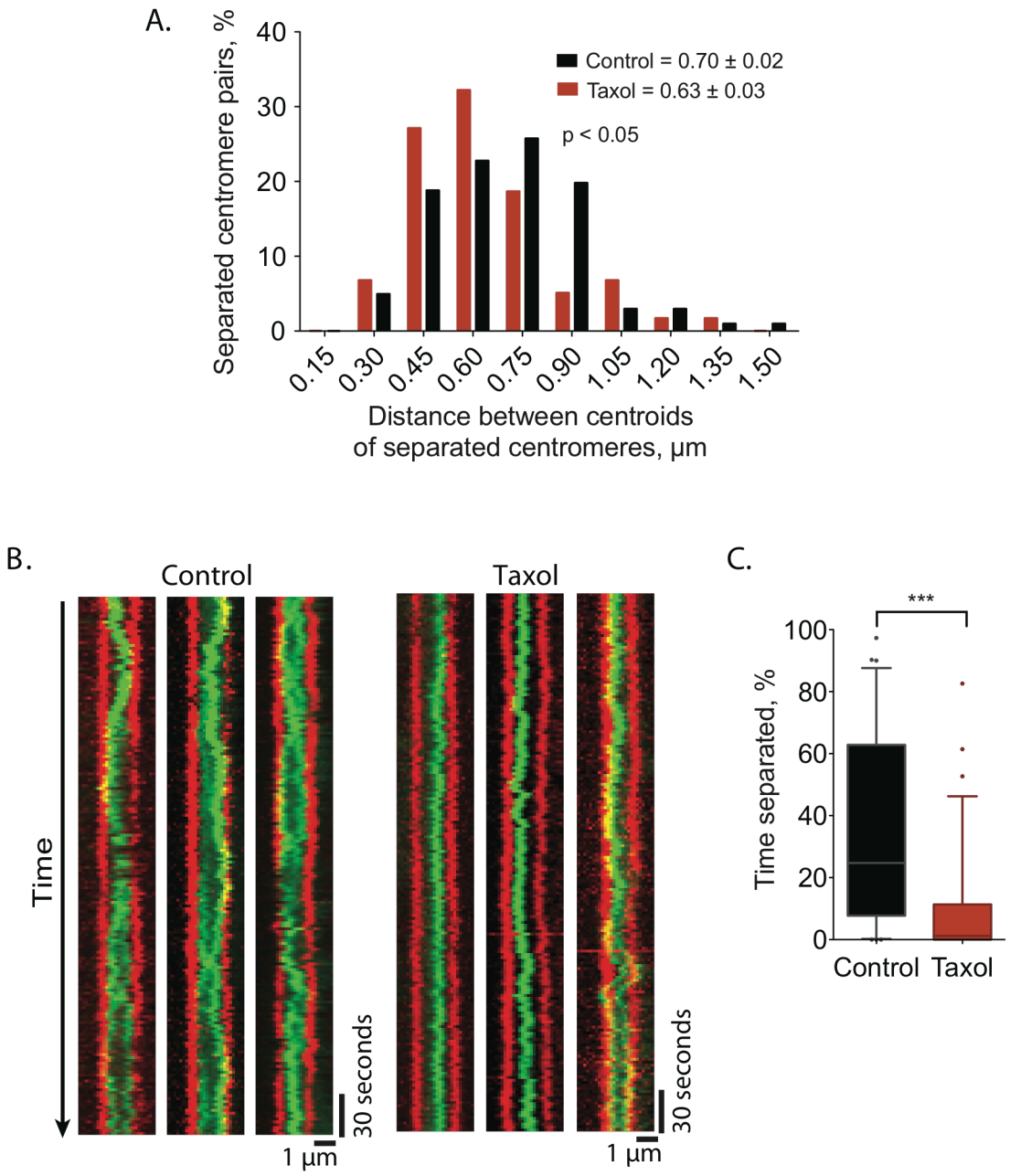


**Figure 12. Taxol treatment reduces distance between centromeres centromere breathing dynamics in live cells.** Cells with preformed metaphase spindles were treated with DMSO ± 30µM Taxol as in Figure 11A and imaged either fixed (A) or live (B and C). (A) Distance between *CEN1*-GFP centroids of sister centromeres in cells with separated centromeres. Inset reports mean ± SEM, n = 101 for control and 59 for Taxol treated cells, $p < 0.047$. (B) Kymographs of metaphase spindles in mock (DMSO) and Taxol (30µM in DMSO) treated cells. Spindle pole marked with Spc42-mRFP (red); *CEN1* marked with GFP (green). (C) Percent time sister centromeres are visibly separated on metaphase spindles in mock (DMSO) and Taxol (30µM in DMSO) treated cells. Data points represent time separated in individual cells. Center line is median, boxes encompass center quartiles, whiskers encompass 5$^{th}$ to 95$^{th}$ percentiles, n=31 cells for both, $p = 0.0007$.

1998; Goshima and Yanagida, 2000; He et al., 2000; Maresca and Salmon, 2009; Uchida et al., 2009; Wan et al., 2009). In budding yeast, bipolar attached sister centromeres oscillate between states of increased and decreased separation, in which the tetO/tetR-marked centromeres appear as two or one distinct foci, respectively (Goshima and Yanagida, 2000; Tanaka et al., 2000; He et al., 2000; Indjeian and Murray, 2007).

First, we measured the distance between the centroids of the two foci when centromeres are in the separated state. Centromeres in control cells are pulled significantly further apart then those in Taxol treated cells (Figure 12A). Consistent with previous reports, kymographs from time-lapse imaging reveal that GFP-tagged centromeres in control spindles oscillate between separated and unseparated foci (Figure 12B). In contrast, centromeres in Taxol treated spindles appear less motile (Figure 12B). When observed by time-lapse imaging of individual cells, Taxol dramatically reduces the time centromeres spend in the separated state (Figure 12C; median = 24.7 and 1.2% for control and Taxol treated cells, respectively). Additionally, the frequency of transition between the separated and unseparated states is reduced by Taxol (Figure 13A). Similarly, in populations of fixed cells, Taxol reduces the percentage of cells with separated centromere foci by 36%, along with the average distance between sister centromeres (Figure 13B-C). As a control, nocodazole, which induces kinetochore detachment, reduces the proportion of separated centromeres and the distance between them significantly more than Taxol treatment (Figure 13B-C). Overall these data reveal that Taxol treatment reduces both the time during which bipolar attached sister centromeres are pulled apart, as well as the distance to which they are

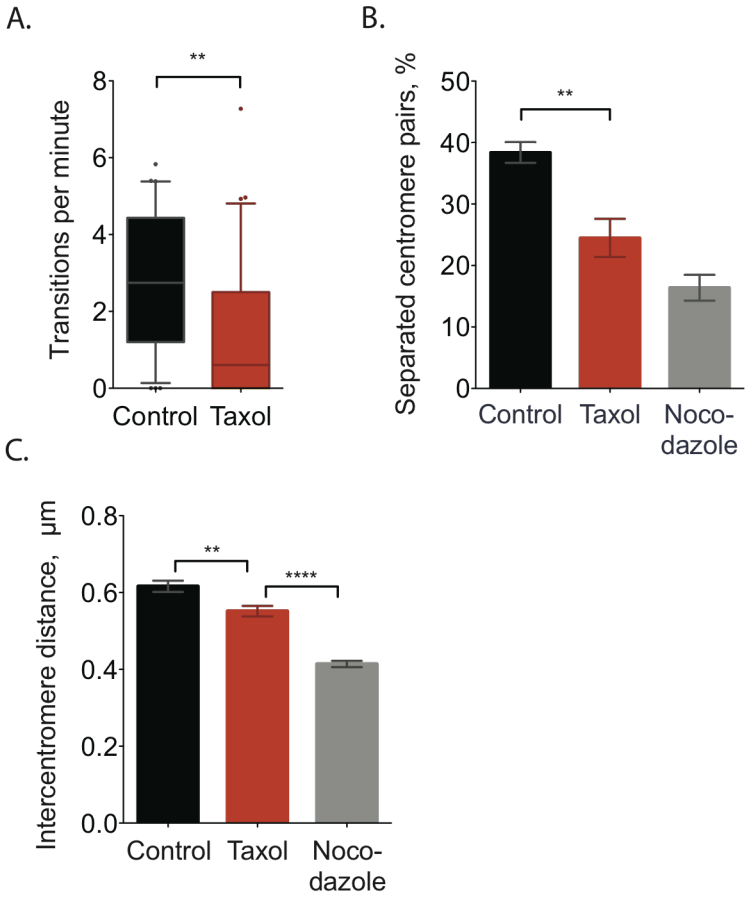


**Figure 13. Taxol treatment reduces tension at attached kinetochores in fixed cells.** Taxol sensitive cells were released from G1 synchronization (alpha-factor) into methionine-containing media to hold cells in metaphase with fully formed spindles (Cdc20 depletion). Cultures were split, treated with DMSO ± 30µM Taxol or 15 µg/ml nocodazole for 15 min, and imaged either live (A) or fixed (B-C). Experimental scheme described in Figure 11A. Sister centromeres were localized by *CEN1*-tetO/tetR-GFP imaging. (A) Boxplot depicting the frequency of transition between either one or two visible *CEN1*-GFP foci. Data points represent individual cells. Center line is median, boxes encompass center quartiles, whiskers encompass 5$^{th}$ to 95$^{th}$ percentiles, n = 31 cells for both, $p$ = 0.0058. Median = 2.7 and 0.6, mean ± SEM = 2.8 ± 0.3 and 1.4 ± 0.3 for control and Taxol treated cells, respectively. (B) Percent metaphase cells in which sister *CEN1*-GFP are visible as separate foci (separated). Mean ± SEM from 3 independent experiments; n = 111, 110, 155 for control, 148, 100, 178 for Taxol treated, and 100, 58, 100 for nocodazole treated cells. $p < 0.008$ for control versus Taxol treated cells. (C) Distance between the outer edges of *CEN1*-GFP foci (both separated and unseparated). Mean ± SEM from 4, 4 and 3 experiments for control (n = 178, 156, 145, 169), Taxol (n = 179, 178, 153, 98), and nocodazole (n = 86, 84, 100) treated cells, respectively. $p$ = 0.0015 for control versus Taxol, and $p < 0.0001$ for Taxol versus nocodazole treated cells. Statistical significance was determined by unpaired, two-tailed *t*-test.

pulled apart. Thus, Taxol reduces the microtubule-generated tension at sister centromeres/kinetochores.

Our results demonstrate that, in preformed spindles, Taxol treatment reduces microtubule-generated tension across the population of cells. Yet there is no significant increase in unattached kinetochores. Budding yeast kinetochores bind just one microtubule, and thus cannot experience partial microtubule occupancy (Winey et al., 1995). Taken together, we have established conditions to reduce tension at otherwise fully attached kinetochores.

### *2.3.3 Reduced tension at attached kinetochores produces a delay in anaphase onset*

To test the role of reduced kinetochore tension in delaying anaphase onset we developed a 'Cdc20 release assay'. We synchronized cells with preformed spindles, then released them into anaphase in the presence or absence of Taxol (Figure 14A). This approach allowed us to score the timing of anaphase onset in individual cells. As expected, cells in untreated cultures progress synchronously into anaphase. By comparison, cells in Taxol treated cultures display a transient, but reproducible delay in anaphase onset (Figure 14B). In addition to monitoring chromosome segregation by DAPI staining, we observed similar results observing spindle elongation in Spc29-mRFP cells (not shown). Additionally, Taxol does not delay anaphase onset in drug sensitive yeast cells harboring wildtype tubulin (Figure 15A). This shows the delay is due to microtubule stabilization and not any secondary effect of Taxol in the cell. We

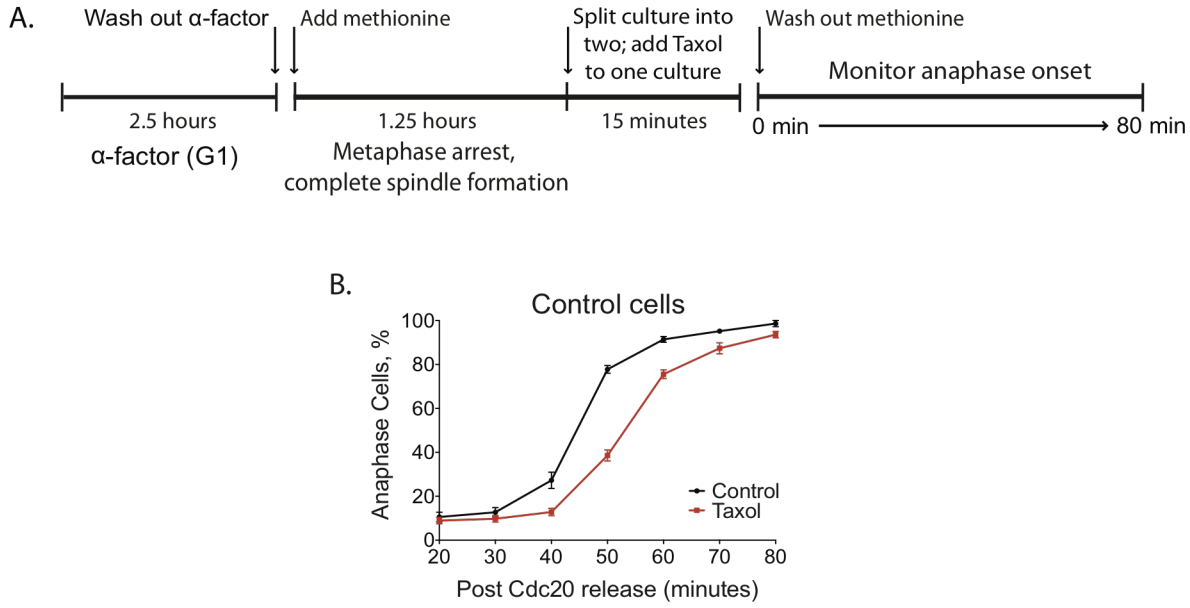


**Figure 14. Reduced tension at attached kinetochores produces a delay in anaphase onset.** (A) Experimental scheme of the Cdc20 release assay. (B) Timing of anaphase onset in Taxol sensitive control cells monitored by the Cdc20 release assay (± 30μM Taxol). Time points along curves represent average ± SEM from 17 experiments, with n = 100-200 cells scored per time point and drug condition for each experiment.

considered the possibility that a decrease in spindle elongation rate may slow chromosome separation. While not statistically significant, Taxol reduced elongation rate ~15% in the Cdc20 release assay (Figure 15B). This reduction could account for only ~1 min delay in a spindle reaching 6 μm in length, at which point telomere segregation is readily apparent (Straight et al., 1997). Thus, the observed delay is not due to decreased spindle elongation rate.

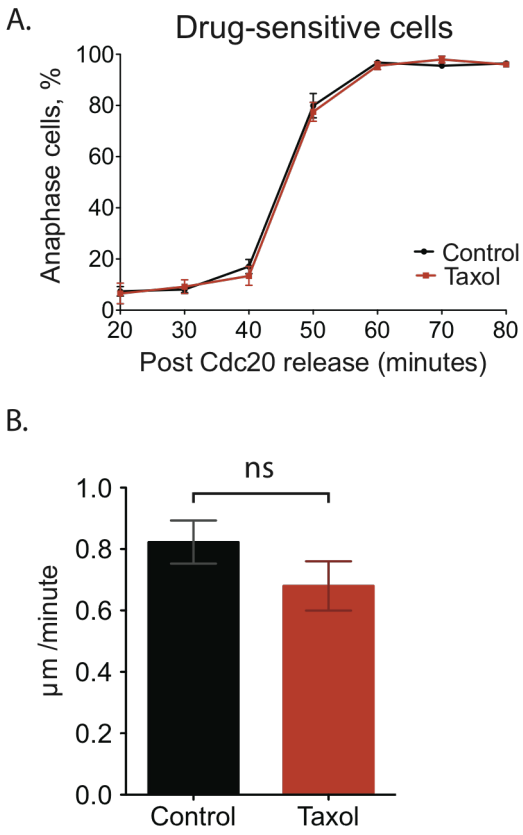


**Figure 15. The Taxol-induced metaphase delay is dependent on Taxol-tubulin binding, although Taxol does not reduce anaphase spindle elongation rates.** (A) Timing of anaphase onset in drug sensitive cells with wild type yeast tubulin monitored by the Cdc20 release assay (± 30µM Taxol). Cells synchronized in G1 (alpha-factor) were released into media containing methionine to hold cells in metaphase with fully formed spindles (Cdc20 depletion). Cultures were split, treated with DMSO ± 30µM Taxol and released from metaphase. Experimental scheme of the Cdc20 release assay described in Figure 14A. Values represent mean ± SEM from 3 experiments, with n = 100-200 cells scored per time point and drug condition for each experiment. (B) Anaphase spindle elongation rate in Taxol sensitive cells following release from Cdc20 depletion (± 30µM Taxol treatment). Cells carrying GFP-Tub1 (α-Tubulin) were imaged at 2 min intervals. Spindle elongation rate during the initial rapid phase was determined by measuring spindle length over time. Mean ± SEM from 19 control and 20 Taxol treated cells, $p = 0.19$, ns = not statistically significant.

Multiple lines of evidence indicate the Taxol-mediated delay in anaphase onset is not due to detached kinetochores. First, detached kinetochores produce a lengthy delay in anaphase onset (Hoyt et al., 1991; Li and Murray, 1991). Second, the delay is observed in the entire population of cells. Thus, if the delay were due to detached kinetochores, every cell would possess at least one. Yet, our attachment assay revealed that Taxol does not significantly increase kinetochore detachment (Figure 11C). Third, detached kinetochores are predicted to increase chromosome missegregation. However, missegregation is not increased when cells with preformed spindles are treated with Taxol (Figure 16A and B). Fourth, we monitored chromosome missegregation in cells lacking Mad3, which cannot delay anaphase onset in response

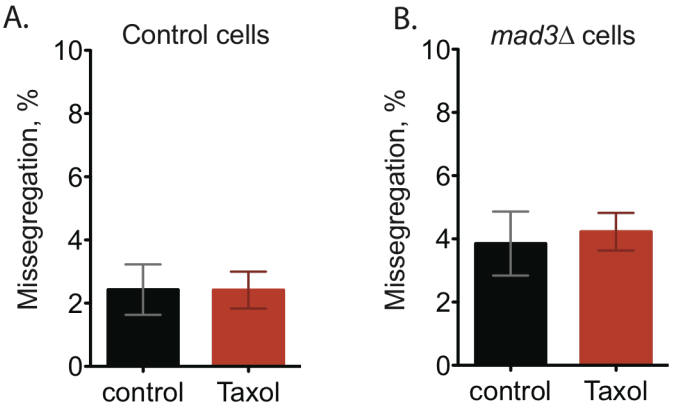


**Figure 16: Reduced tension at attached kinetochores does not induce chromosome missegregation whether or not cells can sense kinetochore detachment.** (A and B) Percent missegregation of *CEN1*-GFP marked chromosomes in control (A) and *mad3*Δ (B) cells following anaphase onset in the Cdc20 release assay. Mean ± SEM from 8 control and 4 *mad3*Δ experiments. For control cells n = 113, 124, 133, 127, 98, 149, 110, 117 for untreated and 109, 133, 128, 151, 109, 127, 113, 139 for Taxol treated cells. For *mad3*Δ cells n = 131, 147, 134, 91 for untreated and 147, 137, 116, 111 for Taxol treated cells. For both control cells with intact checkpoint (A) and *mad3*Δ cells (B) the difference between control and Taxol treatment is not significant by unpaired two-tailed *t*-test.

to kinetochore detachment (Hardwick et al., 2000; Li and Murray, 1991; Alexandru et al., 1999; London and Biggins, 2014b). If kinetochores become detached, they should missegregate at a high frequency in *mad3*Δ cells. Yet, missegregation rates remain the same in control and Taxol treated *mad3*Δ cells (Figure 16B). Thus, although Taxol produces a delay across the population of cells, evidence demonstrates the majority of cells do not possess unattached kinetochores. Together, these results support the conclusion that reduced tension at attached kinetochores induces a delay in anaphase onset, independent of kinetochore detachment.

*2.3.4 The tension-mediated delay in anaphase onset requires Bub1 but not Mad3*

Next, we sought to determine if the SAC mediates the tension-responsive delay in anaphase onset. The SAC components Bub1 and Mad3 are both required for the SAC response to detached kinetochores (London and Biggins, 2014b; Li and Murray, 1991; Hoyt et al., 1991). Therefore, we tested whether they were needed for the tension-mediated delay revealed by the Cdc20 release assay. In contrast to control *BUB1* cells, the Taxol-mediated delay is essentially lost in *bub1*Δ cells (Figure 17B). Thus, the tension-mediated delay requires Bub1. Strikingly, the tension-mediated delay is unaffected by loss of Mad3 (Figure 17A).

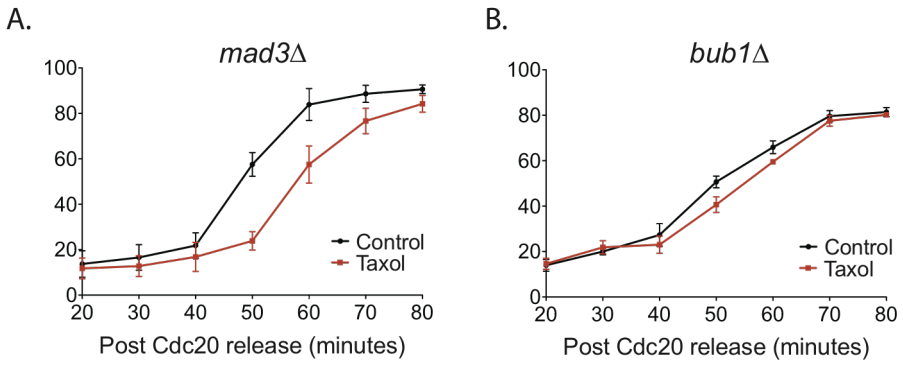


**Figure 17. the tension mediated delay requires SAC Bub1 but not Mad3.** Timing of anaphase onset in Taxol sensitive (A) *mad3*Δ, and (B) *bub1*Δ cells monitored by the Cdc20 release assay (± 30μM Taxol). Time points along curves represent average ± SEM from 5 *bub1*Δ, and 4 *mad3*Δ experiments, with n = 100-200 cells scored per time point and drug condition for each experiment.

The fact that Mad3 is not needed provides additional evidence that the Taxol-mediated delay results from reduced tension. If the delay were due to detached kinetochores, it should be abolished in *mad3*Δ cells (Li and Murray, 1991; London and Biggins, 2014b). Additionally, chromosome missegregation is not increased in *mad3*Δ

cells treated with Taxol, indicating kinetochores remain attached during the Cdc20 release assay (Figure 16B). Yet, anaphase onset is delayed in these cells (Figure 17A). Taken together, these results reveal that reduced tension at attached kinetochores induces a delay in anaphase onset that is mediated by some, but not all, of the core SAC components.

### *2.3.5 SAC components mediate distinct responses to the attachment and/or tension status at kinetochores*

In the Cdc20 release assay, reduced tension at kinetochores generates a delay that is significantly shorter than that reported for unattached kinetochores (Jacobs et al., 1988; Li and Murray, 1991; Hoyt et al., 1991; Biggins and Murray, 2001). Indeed, in the G1 release assay, with unattached kinetochores present, anaphase onset is delayed approximately one hour (Fig. 1G). In the Cdc20 release assay, *CDC20* is expressed from the inducible *pMET3* promoter. Overexpression of *CDC20* overrides the SAC and promotes premature anaphase onset (Hwang et al., 1998). Thus, in the Cdc20 release assay the duration of the tension-mediated delay may be shortened due to altered kinetics of *CDC20* expression. To address this possibility, we sought to determine the length of the tension-mediated delay with *CDC20* expression under endogenous regulation.

In control cells, when Taxol is present during spindle assembly in the G1 release assay, anaphase onset is delayed with both unattached and low tension kinetochores present (Figure 18A). Bub1 is required for the SAC-mediated delay in response to

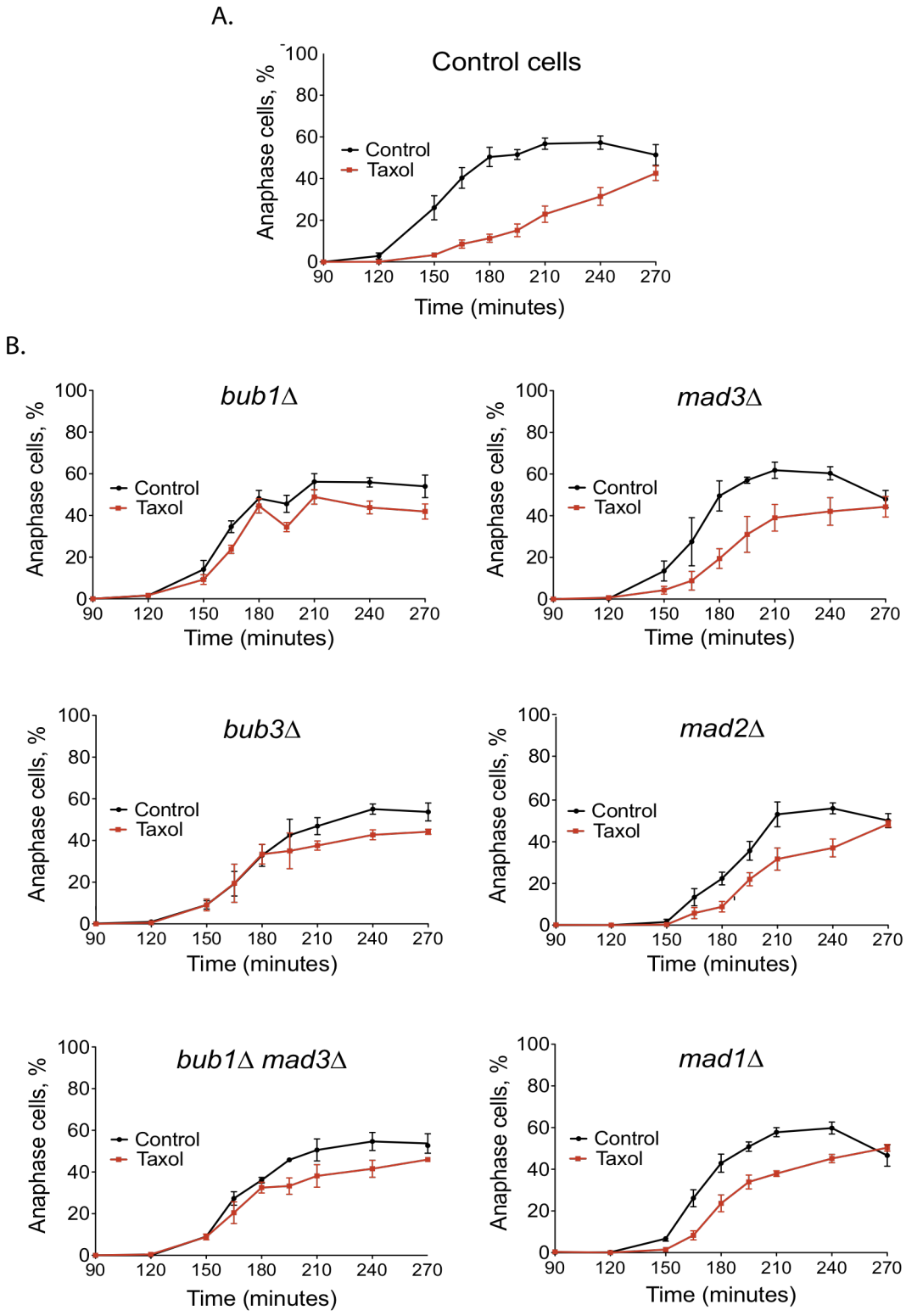


**Figure 18. Components of the Spindle Assembly Checkpoint mediate distinct responses to the attachment and/or tension status at kinetochores.**

**Figure 18 Continued. Components of the Spindle Assembly Checkpoint mediate distinct responses to the attachment and/or tension status at kinetochores.** (A) Timing of anaphase onset in Taxol sensitive control cells monitored by the G1 release assay (± 30μM Taxol). Control cells delay anaphase onset for approximately one hour during Taxol treatment, which produces both unattached and low tension kinetochores. Data for control cells (A) is also represented in Figure 1G. (B) Timing of anaphase onset in Taxol sensitive control cells of the indicated genotype monitored by the G1 release assay (± 30μM Taxol). *bub1*Δ cells, which do not display a tension-mediated delay in anaphase onset in the Cdc20 release assay (Fig. 3B), fail to significantly delay anaphase onset during Taxol treatment in the G1 release assay. *mad3*Δ cells, which do display a tension-mediated delay in the Cdc20 release assay (Fig. 3B) also delay anaphase onset during Taxol treatment in the G1 release assay. Similar to *bub1*Δ cells, *bub3*Δ cells fail to delay anaphase onset, whereas *mad1*Δ and *mad2*Δ cells delay anaphase onset during Taxol treatment. *bub1*Δ *mad3*Δ cells do not delay anaphase onset during Taxol treatment. Plotted values in (B) represent the mean ± SEM from >3 experiments, with n = 100-200 cells scored per time point and drug condition for each experiment.

unattached kinetochores (Hoyt et al., 1991; London and Biggins, 2014b). Our results with preformed spindles in the Cdc20 release assay reveal that Bub1 is also required to delay anaphase onset due to reduced tension (Figure 17B). Thus, in the G1 release assay, *bub1*Δ cells should fail to respond to either the unattached or low tension status of kinetochores. Consistent with this prediction, the Taxol-induced hour-long delay observed in control cells is abolished in *bub1*Δ cells (Figure 18B).

Because Mad3 is required for the SAC response to unattached kinetochores (Li and Murray, 1991; London and Biggins, 2014b), *mad3*Δ cells should not delay due to the unattached kinetochore status in the G1 release assay. However, results from the Cdc20 release assay, where Taxol is added after spindle assembly, demonstrate that Mad3 is not required for the tension-mediated delay in anaphase onset (Figure 17A). Thus, although *mad3*Δ cells cannot respond to unattached kinetochores, they should retain the ability to delay anaphase onset due to the low-tension status in the G1 release assay. Indeed, in this assay *mad3*Δ cells delay anaphase onset approximately 30 min during Taxol treatment (Figure 18B). As with control cells, Taxol does not affect the timing of cell cycle initiation in *bub1*Δ or *mad3*Δ cells (Figure 19). Additionally, in

*bub1*Δ *mad3*Δ cells, Taxol treatment does not induce a delay in anaphase onset (Figure 18B). This indicates the delay observed in *mad3*Δ cells is mediated through Bub1, and is not a secondary effect of *MAD3* deletion. Therefore, Taxol treatment following G1 release induces a mitotic delay that is distinct from the canonical SAC response to unattached kinetochores, and recapitulates the tension-mediated delay observed with preformed spindles (Fig. 14). Together, these data demonstrate that reduced microtubule-generated tension delays anaphase onset, and that this delay is dependent on Bub1, but not Mad3.

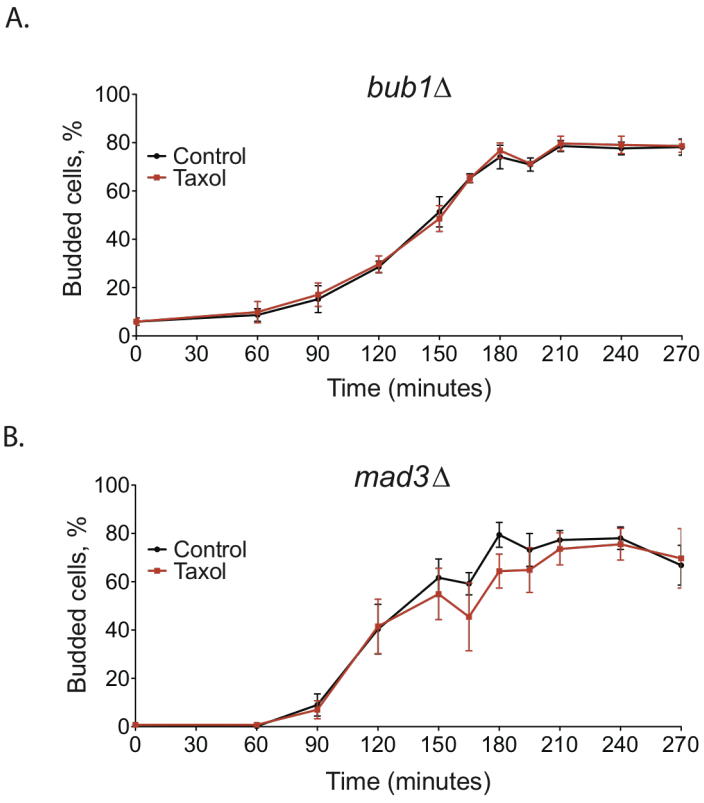


**Figure 19. Budding index in (A) *bub1*Δ and (B) *mad3*Δ cells monitored in the G1 release assay.** Taxol sensitive cells synchronized in G1 (alpha-factor) were released into the cell cycle and split into sister cultures either with or without 30μM Taxol. During the ensuing cell cycle anaphase onset was monitored by cell morphology and chromosome separation. Experimental scheme of the G1 release assay described in Figure 1E. Plotted values represent the mean ± SEM from 7 experiments for *bub1*Δ and 6 experiments for *mad3*Δ cells, with n = 100-200 cells scored per time point and drug condition for each experiment.

We next tested the role of additional SAC components using the G1 release assay. Similar to Bub1 and Mad3, the proteins Bub3, Mad1 and Mad2 are required for

the canonical SAC response to unattached kinetochores (Li and Murray, 1991; Hoyt et al., 1991; London and Biggins, 2014b). As with *bub1*Δ cells, the Taxol-mediated delay is abolished in *bub3*Δ cells (Figure 18B). Thus, in addition to the response to unattached kinetochores, Bub3 is also required for the delay induced by low tension. In contrast, a Taxol-mediated delay, similar to that seen in *mad3*Δ cells, persists in both *mad1*Δ and *mad2*Δ cells (Figure 18B). These results indicate that the tension-mediated delay does not strictly require Mad1 and Mad2. Overall the data segregate these core SAC proteins into two classes. The first class, Bub1 and Bub3, function in both the attachment and tension mediated responses, while the second class, Mad1, Mad2 and Mad3, are not required to delay anaphase onset in the presence of tensionless kinetochores.

### *2.3.6 Yeast cells lacking spindle assembly checkpoint components display differential sensitivity to Taxol*

Our results predict that the SAC mutants should have different sensitivities to Taxol. At very low Taxol concentrations, bipolar kinetochore attachments will likely be assembled in a timely manner, and yeast cells will not be dependent on the SAC for viability. We reasoned, however, that at moderately low concentrations, the establishment of proper microtubule-kinetochore attachments will become slightly delayed. At these concentrations, although cells lacking Mad1, Mad2 or Mad3 cannot respond to unattached kinetochores, they will still be provided the time needed to achieve proper attachments by the tension mediated mechanism. However, because cells lacking Bub1 or Bub3 respond to neither unattached nor tensionless kinetochores,

they are not granted time to complete the bipolar attachment process and lose viability at these concentrations. At higher Taxol concentrations microtubules become increasingly stabilized, and more time is required for spindle assembly than the tension mediated mechanism can provide. At this point, the longer delay induced by unattached kinetochores, which is absent in cells lacking Mad1, Mad2 or Mad3, becomes essential for viability.

To test this prediction, we monitored the growth of Taxol sensitive cells lacking SAC components on medium containing the drug (Figure 20). Relative to control cells with an intact SAC, *mad1*Δ, *mad2*Δ, and *mad3*Δ cells display increased Taxol sensitivity (Figure 20). As predicted, both *bub1*Δ and *bub3*Δ cells are even more sensitive than the *mad* mutants (Figure 20). This indicates that Bub1 and Bub3 do not function only in a

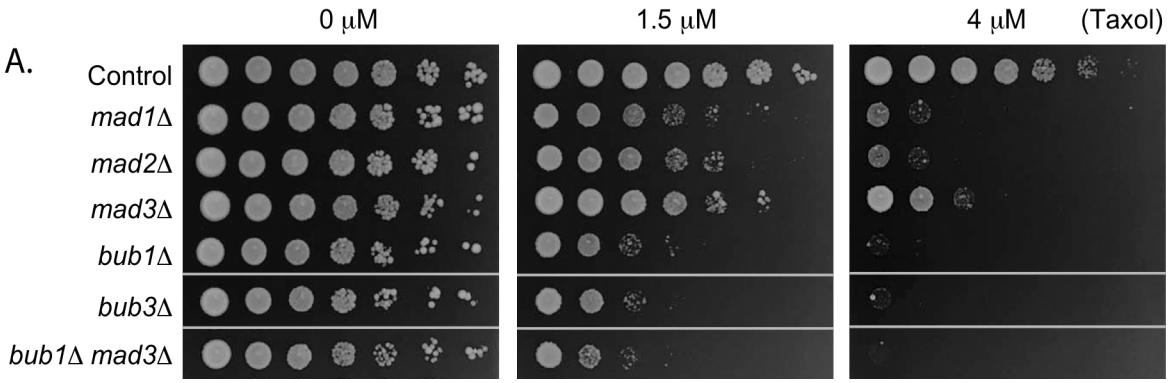


**Figure 20. Cells lacking spindle assembly checkpoint components display differential sensitivity to Taxol.** Taxol sensitive cells of the indicated genotype were serially diluted and equal volumes were spotted onto agar plates containing the indicated concentration of Taxol. All strains were grown on the same plate; gray lines denote where additional lanes were cropped.

single linear pathway with the Mad proteins in response to Taxol treatment. Rather than an additive effect, the Taxol sensitivity of *bub1*Δ *mad3*Δ cells is similar to that of *bub1*Δ cells (Figure 20). This is consistent with the idea that all five checkpoint proteins share a

common function, but that Bub1 and Bub3 play an additional role required to protect cells from the effects of Taxol treatment. Overall our results support the conclusion that while Bub1, Bub3, Mad1, Mad2 and Mad3 all function in response to unattached kinetochores, Bub1 and Bub3 also function separately in response to low microtubule-generated tension.

### *2.3.7 Using Taxol sensitive yeast to search for a new tension sensing protein*

All of the proteins we initially tested in our G1 release assay are required for attachment mediated SAC signaling, but we found that only a subset are required for the tension mediated delay. We therefore questioned whether additional proteins exist that are required for tension mediated signaling, but are dispensible for attachment mediated signaling. We returned to the original screen (Hoyt et al., 1991) in which Bub1 and Bub3 were discovered alongside a third protein, Bub2. Since the discovery of Bub2, studies have described its fundamental role in the spindle positioning checkpoint (Fraschini et al., 1999a) and as an inhibitor of the mitotic exit network (Baro et al., 2013); however, it is not known to play a role in canonical SAC signaling.

We hypothesized that along with Bub1 and Bub3, Bub2 may have a novel role in the tension mediated delay we observe in Taxol treated cells. If true, cells lacking bub2 should have no tension mediated delay, but would still be able to mount an attachment mediated arrest. We noted that previous studies of *bub2*$\Delta$ mutants report an abbrieviated attachment mediated arrest (Fraschini et al., 1999b; Krishnan et al., 2000); therefore, the attachment mediated portion of the arrest observed in G1 release in the

presence of Taxol may be shorter than in control cells and diffeicult to interpret. However, in cells lacking both Bub2 and Mad1, or in cells lacking both Bub2 and Mad3, cells should not delay in response to unattached kinetochores, and only the tension mediated delay will remain. In these scenarios, if Bub2 is required for the tension mediated delay, then these cells should not delay at all in Taxol. To test this prediction, we performed the G1 release assay on a *bub2*Δ mutant, a *bub2*Δ *mad1*Δ mutant, and a *bub2*Δ *mad3*Δ mutant. In this assay, *bub2*Δ and *bub2*Δ*/mad1*Δ mutants appear to delay 30 minutes in Taxol relative to the control, while a *bub2*Δ*/mad3*Δ mutant initiated anaphase onset at the same time in control and Taxol-treated cultures.

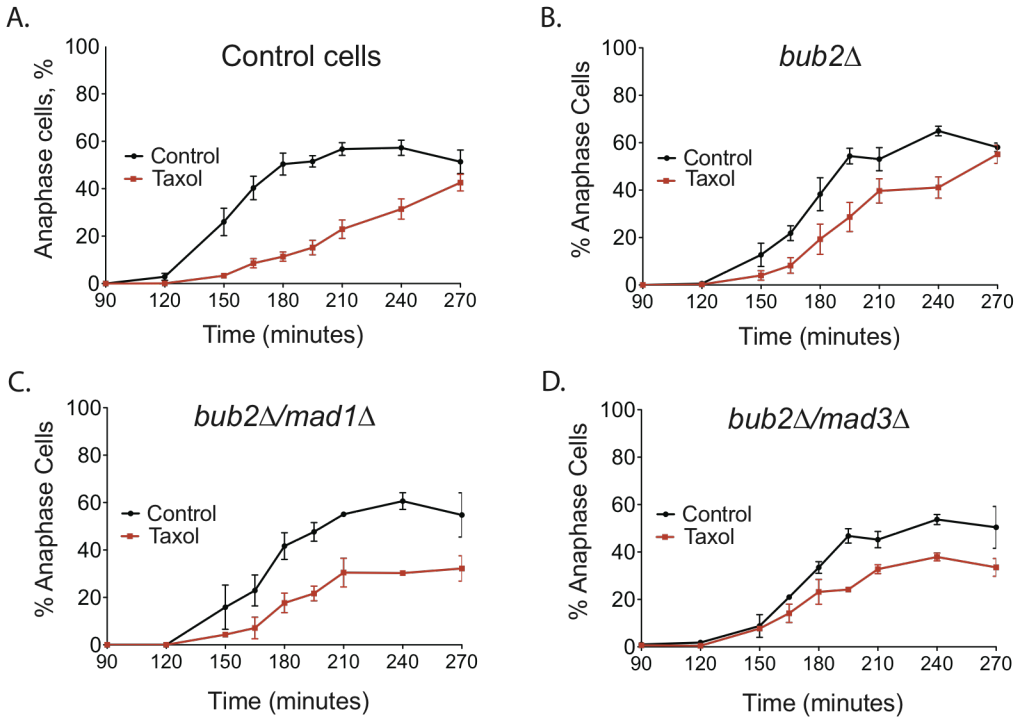


**Figure 21. Applying the G1 release assay to determine if Bub2 is required for tension sensing.** Budding index in (A) control (B) *bub2*Δ (C) *bub2*Δ/*mad1*Δ and (C) *bub2*Δ/*mad3*Δ cells monitored in the G1 release assay. Taxol sensitive cells synchronized in G1 (alpha-factor) were released into the cell cycle and split into sister cultures either with or without 30μM Taxol as in Figure 18. During the ensuing cell cycle anaphase onset was monitored by cell morphology and chromosome separation. Experimental scheme of the G1 release assay described in Figure 9B. Plotted values represent the mean ± SEM from 3 experiments for *bub1*Δ and 6 experiments for *mad3*Δ cells, with n = 100-200 cells scored per time point and drug condition for each experiment.

However, we acknowledged that we could not truly define a strain's phenotype in Taxol based solely on tracking its rate of anaphase onset over time; the delay profiles of these mutants were difficult to assess qualitatively, in part because the maximum percent anaphase onset reached varied significantly between the strains. Therefore, we utilized an unbiased approach to measuring each mutant's delay in anaphase onset. We used a non-linear regression model fitting our experimental data for each strain in our G1 release assay to a sigmoidal curve to determine the time it took for each strain

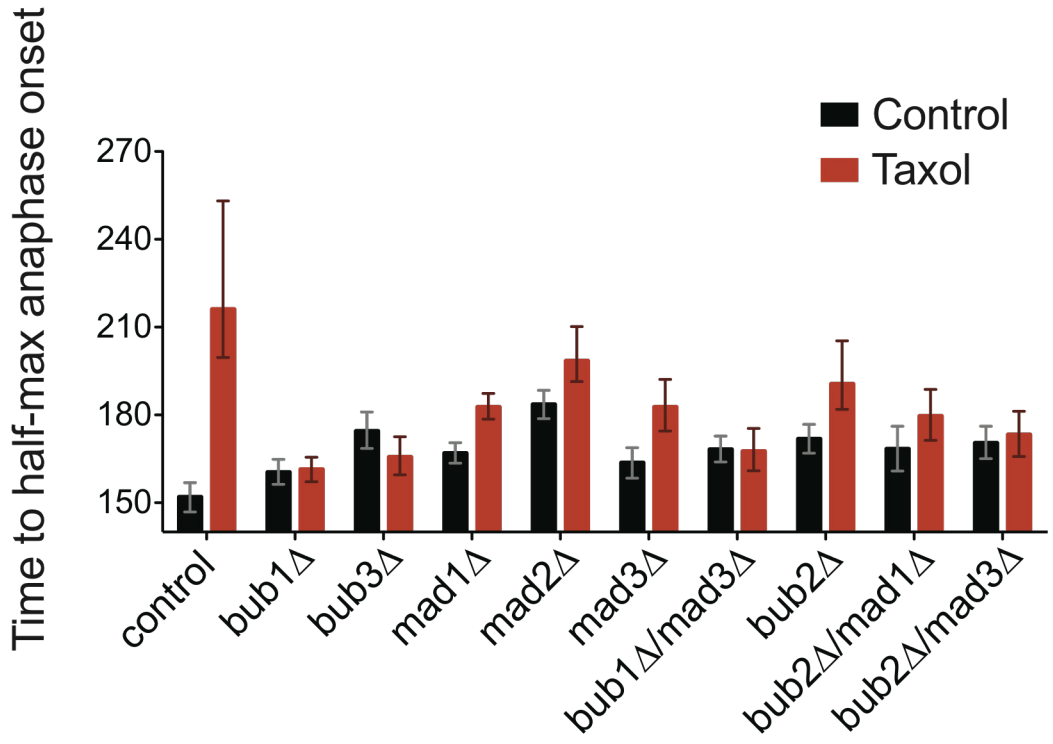


**Figure 22. The true delay for each strain is measured by determining the time to half-max anaphase onset +/- Taxol.** A non-linear regression model was used to generate best-fit sigmoidal curves according to the G1 release data for each strain. Bars represent average time to half-max anaphase for control (●) and Taxol-treated (■) cells; error bars represent ± the 95% confidence interval of that value based on how well the experimental data fit to its best-fit curve.

to reach half-maximum anaphase onset. Comparing time to half max ± Taxol signifies an accurate value of each strain's delay because it disregards the cells that were sickly and died during the experiment or weren't synchronized, and therefore did not experience a mitotic checkpoint-mediated delay.

We used this unbiased method to reassess G1 release data for all ten strains (Figure 22). Estimated delays based on the data regarding the control and our original SAC mutants (Figure 18) matched well with the time to half-max delay calculated using this method (Figure22), corroborating our conclusions that Bub1 and Bub3 are required in both tension and attachment sensing, and Mad1, Mad2, and Mad3 only in attachment sensing. Importantly, fitting Bub2 mutant G1 release data to curves provided vital quantitative insight (Figure 22). Cells lacking Bub2 do indeed experience a shorter delay compared to control cells. On the other hand, when the *bub2*Δ is combined with a mutation that inactivates the attachment mediated SAC, cells no longer show a statistically significant delay in Taxol.

That *bub2*Δ*/mad1*Δ and *bub2*Δ*/mad3*Δ mutants do not show a statistically significant delay in Taxol during the G1 release assay raises several possibilities. One possibility is that, like *bub1*Δ*/mad3*Δ mutants whose attachment and tension sensing pathways are both inactivated, *bub2*Δ*/mad1*Δ and *bub2*Δ*/mad3*Δ mutants are also now unable to mount both the attachment-mediated SAC arrest and the tension mediated delay (i.e. the short delay we see in the *mad* mutants) (Figure 22). Alternatively, the lack of a delay could signify Bub2's role in a different SAC-independent process that affects the timing of mitotic progression, such as inhibition of the mitotic exit network. In this scenario, mitotic exit network inhibition by Bub2 could be required to see the

longest tension delay at metaphase. These two possibilities could be addressed in budding yeast by performing our Cdc20 and G1 release assays in cells ± Bub2 that have the mitotic exit network inactivated. Thus, if Bub2 promotes the tension delay at metaphase independently of its role in mitotic exit network inhibition, it would suggest that Bub2 participates directly in biorientation and spindle assembly, likely in the tension sensing mechanism in coordination with Bub1 and Bub3. On the other hand, if the delay in Bub2 mutants is dependent on an otherwise intact mitotic exit network, the Bub2-dependent delay we observe during Taxol treatment may represent, in part, a general function of the mitotic exit network in preventing mitotic slippage. In sum, further targeted genetic experiments may reveal whether Bub2 functions to delay anaphase onset in response to low tension at kinetochores in addition to its other roles in mitotsis.

More broadly, this method can be applied to any protein to interrogate its involvement in mitotic checkpoint signaling. The protein in question may be inactivated alone or in combination with known checkpoint proteins. Quantitative analysis of G1 release assay with these mutants will reveal the delay profile, indicating which proteins work in a single pathway and which work in parallel. Although, as demonstrated with Bub2, this method does not always clearly define which pathway or pathways a given protein functions in; yet it does highlight the complex cross-talk occuring between mitotic signaling pathways. Understanding which proteins play a role in more than one process is the first step to constructing more detailed experimentatal approaches designed to distinguish between each role.

## 2.4 Discussion: microtubule generated tension and the SAC

How tensionless microtubule-kinetochore attachments delay mitotic progression has been a longstanding question. Experimental approaches to reduce tension in higher eukaryotes can be confounded by variable microtubule occupancy (King and Nicklas, 2000; Nicklas and Ward, 1994; Nicklas et al., 2001; Waters et al., 1998; McEwen et al., 1997) and perturb spindle organization (O'Connell et al., 2008; Tauchman et al., 2015; Etemad et al., 2015). Similarly, approaches in budding yeast disrupt spindle organization, leaving it difficult to exclude kinetochore detachment in SAC activation (Stern and Murray, 2001). Using a unique Taxol-sensitive yeast model, we show that reduced tension at attached kinetochores directly delays anaphase onset. Furthermore, this delay is dependent on the core SAC protein Bub1. Unlike experiments with unpaired chromosomes, Taxol treatment of preformed spindles does not significantly perturb bipolar spindle organization or anaphase elongation. This allows assessment of kinetochore attachment pre- and post-anaphase, which is not altered by Taxol treatment of preformed spindles. It is unclear why Ipl1-mediated error correction does not detach kinetochores in the preformed spindles treated with Taxol. Because Taxol does not reduce tension completely in our system, sufficient tension may remain to avoid error correction. Alternatively, Taxol-mediated microtubule stabilization may directly oppose kinetochore-microtubule detachment. However, chromosome missegregation is not increased in *mad3*Δ cells, which fail to respond to unattached kinetochores (Li and Murray, 1991; London and Biggins, 2014a), indicating that kinetochores maintain bipolar attachments. Although we did not mutate kinetochore proteins or perturb inter-

centromeric structure to reduce tension, we cannot rule out the possibility that Taxol-mediated microtubule stabilization alters the nature of end-on kinetochore attachments. However, experiments in cells harboring wild-type tubulin confirm the delay results from microtubule stabilization. Together our results demonstrate that reduced tension at kinetochores functions via core SAC components to delay anaphase onset, independent of kinetochore detachment.

Whether microtubule generated tension actively silences the SAC is currently under debate. Studies using super-resolution light microscopy of kinetochore components in Drosophila and HeLa cells revealed that an increase in stretch within the kinetochore is correlated with SAC satisfaction (Maresca and Salmon, 2009; Uchida et al., 2009; Wan et al., 2009). In HeLa cells this reduced intra-kinetochore stretch correlates with decreased APC activity (Uchida et al., 2009), and it was proposed this stretching may serve to inactivate SAC signaling (Uchida et al., 2009; Maresca and Salmon, 2009). Yet, using similar techniques it was recently shown that the SAC can be silenced without full intra-kinetochore stretch when error correction was abolished (Etemad et al., 2015; Tauchman et al., 2015), although anaphase onset was delayed (Tauchman et al., 2015). Moreover, integrated light and electron microscopy revealed that super-resolution microscopy measurements of intra-kinetochore stretch are sensitive to variable shape and organizational changes in response to tension, fixation techniques and visualization methods (Magidson et al., 2016). We used a centromere marker to measure inter-centromere distance and centromere breathing dynamics as a readout of inter-kinetochore tension. This method allowed assessment of individual sister kinetochores and shows that overall tension is reduced by Taxol treatment, but

does not reveal the status of intra-kinetochore tension directly. However, contrary to silencing the SAC, we find that reducing tension in preformed spindles, in which bipolar attachments have been established and experienced tension, still delays anaphase onset. Reducing tension also induces delay in *mad* mutants, in which SAC activation, and subsequent need for silencing, is inhibited. Thus, rather than silencing the SAC, our data show that a lack of tension generates a wait-anaphase signal that postpones mitotic progression.

The mechanism that delays anaphase onset in response to reduced tension is distinct from that of unattached kinetochores. In the presence of unattached kinetochores, the SAC components Bub1, Bub3, Mad1, Mad2 and Mad3 all contribute to formation of the mitotic checkpoint complex (MCC) that sequesters Cdc20 and inhibits the anaphase promoting complex (APC) (Lara-Gonzalez et al., 2012; London and Biggins, 2014b). In complete spindles with bipolar kinetochore attachments, the delay induced by reduced tension requires Bub1, but not Mad3. In cells released from G1, the delay persists in the absence of Mad1, Mad2, or Mad3. Both Mad2 and Mad3 are part of the MCC, whereas Mad1 is needed for catalytic formation of the MCC (Lara-Gonzalez et al., 2012; London and Biggins, 2014b). Therefore, it is unlikely that the delay in cells released from G1 is due to unattached kinetochores. If so, it must involve a yet unrecognized mechanism independent of MCC formation. In budding yeast Bub1 and Bub3 normally localize to kinetochores early in mitosis, yet Mad1 and Mad2 do so only when microtubule-kinetochore attachments are absent (Gillett et al., 2004). Similarly, *Xenopus* Bub1 remains associated with kinetochores that have bound microtubules, whereas Mad1 and Mad2 do not (Sharp-Baker and Chen, 2001).

Additionally, both Bub1 and Bub3 are bound to purified yeast kinetochores, whereas Mad1 is bound only after treatment with the microtubule destabilizer benomyl (London and Biggins, 2014a). These observations indicate that Bub1 and Bub3 behave differently than Mad1 and Mad2 in the context of attached versus unattached kinetochores. This is consistent with our conclusion that a lack of microtubule-generated tension delays anaphase onset via a mechanism that differs from that induced by unattached kinetochores. The tension mediated delay involves SAC components but is independent of the canonical MCC. Intriguingly, Bub1 has been linked to the tension-dependent localization of pericentromeric shugoshin (Sgo1) (Nerusheva et al., 2014), and Sgo1 can delay anaphase onset by inhibiting separase (Clift et al., 2009). Additionally, in HeLa cells Bub1 and Polo-like kinase Plk1 function together to phosphorylate Cdc20 and inhibit APC activation, separate from MCC mediated inhibition (Jia et al., 2016). It will be important to determine whether the tension delay is mediated Sgo1, and if the phosphorylation of Cdc20 is linked to tension status.

The delay resulting from reduced tension is shorter than that produced by unattached kinetochores. Transient delays have been observed in various organisms under conditions that reduce tension (Makrantoni and Stark, 2009; Zasadil et al., 2014; Maresca and Salmon, 2009; Uchida et al., 2009; Tauchman et al., 2015; O'Connell et al., 2008; Biggins and Murray, 2001). In human RPE1 cells, Taxol treatment in late metaphase produced a modest delay in most cells, and prolonged delay was correlated with Mad2 recruitment to detached kinetochores (Magidson et al., 2016). Our data show that reduced tension transiently delays mitotic progression across the population of cells. Together these results suggest that a lack of tension generates a wait-anaphase

signal that can delay, but not prevent anaphase onset in the absence of kinetochore detachment. Consistent with this, treatment of HeLa cells with a low dose of nocodazole to suppress microtubule-generated tension during metaphase significantly inhibited, but did not abolish, APC activity leading to anaphase onset (Uchida et al., 2009). However, it remains possible that reducing tension produces a graded response, as seen with the number of unattached kinetochores (Dick and Gerlich, 2013; Collin et al., 2013; Heinrich et al., 2013). In this regard, rendering all kinetochores tensionless in yeast via unpaired chromosomes generates extended delays, albeit difficult to exclude a contribution from unattached kinetochores with this approach (Makrantoni and Stark, 2009; Biggins and Murray, 2001; Stern and Murray, 2001; Barnhart et al., 2011; King et al., 2007; Lee and Spencer, 2004; Indjeian et al., 2005). Delayed mitotic progression when tension is low may importantly provide cells time to establish a robust bipolar spindle, or to detach tensionless connections and respond to the unattached kinetochore. In HeLa cells, it requires at least 5 min for a freshly detached kinetochore to inhibit the APC (Dick and Gerlich, 2013). Thus, a detachment shortly before anaphase onset risks chromosome missegregation. Perhaps the wait-anaphase signal contributed by tensionless kinetochores helps shorten this vulnerable period. One challenge will be to separate the tension and attachment mediated signaling output. Doing so will prove valuable for understanding how cells utilize these two mechanisms to safeguard their genome.

## 2.5 Materials and methods

### *2.5.1 Strains*

Yeast strains are described in Table S1. The original Taxol sensitive yeast tubulin contains five substitutions (A19K, T23V, G26D, N227H, Y270F) (Gupta et al., 2003) and does not perturb microtubule dynamics in vivo (Entwistle et al., 2012). In this study we utilized tubulin with four substitutions (A19K, T23V, G26D, Y270F) that retains full Taxol sensitivity (Winefield et al., 2008). The drug sensitive background was created by *pdr1*Δ *pdr3*Δ *erg6*Δ. The Taxol sensitive background is *pdr1*Δ *pdr3*Δ *erg6*Δ *tub2-A19K-T23V-G26D-Y270F*. Yeast media and genetic techniques were performed as described previously (Rose et al., 1990). Genetic deletions were introduced into control cells by fragment-mediated homologous recombination or by genetic crossing. Deletions were sequence-verified, then crossed into the Taxol-sensitive background and re-verified to generate the Taxol-sensitive mutant strains. Yeast strains are of S288C background. Details of strain construction are available upon request.

### *2.5.2 Media specifications*

We found Taxol to be more effective at inhibiting cell proliferation on agar plates than in liquid media. Taxol effectiveness in liquid media was increased by adding 0.02% methylcellulose (cP15) to SC or YPD media from a sterile 2% stock. However, Taxol in liquid media containing 0.02% methylcellulose remained less effective relative to agar

plates. To ensure that drug sensitive yeast (*pdr1*Δ *pdr3*Δ *erg6*Δ) were not affected by environmental components or detergents, all glassware was cleaned by filling with glass distilled water and autoclaving, then emptied and autoclaved again to sterilize and dry. Media was also made with glass distilled water. YPD and SC drop-out media were made according to standard recipes. However, we found the growth of drug sensitive yeast in YPD can be influenced by peptone from various sources, particularly at room temperature. After comparative testing we found BD-brand Bacto™peptone to be most consistent between control and drug sensitive yeast. We found no growth variation attributable to components of SC media or other ingredients of YPD.

### *2.5.3 Spotting assays*

2X YPD (filter sterilized) was mixed with 2X agar (hot; autoclaved) and stirred. Before cooling, 35 ml was poured into a 50mL conical tube and Taxol was added from a 1 mM stock in DMSO. The tube was closed and inverted 5 times to mix before pouring the plate. All plates contained the same amount of DMSO regardless of Taxol concentration. Plates were allowed to dry under a laminar flow hood and used within one day. Serial dilutions (10x) were prepared from 2 day saturated cultures, 2.2 μl of each dilution was spotted onto the plates, and the plates were incubated at 24 °C for 5 days.

### *2.5.4 G1 release assay*

*MAT*a cells grown to mid log phase (30˚C) in SC media were spun down and resuspended in SC media containing 100 μM alpha factor. Following a 2.5 hour incubation at 30˚C, the zero minute time point was collected. The G1-synchronized culture was then split in two, washed three times with water and resuspended in 5 ml SC media containing 0.02% methylcellulose (cP15) and DMSO +/- 30 μM Taxol (final from 1 mM stock in DMSO). The cultures were then maintained on the bench and gently mixed by hand every 10 min. Samples were removed and fixed in ice cold 70% ethanol at 60, 90, 120, 150, 165, 180, 195, 210, 240, and 270 min. Fixed cells were washed twice in PBS and stained with 50 nM DAPI. To image cells, 10-12 z-plane DIC and DAPI images were collected at 0.5 μm intervals. To quantify images, cells were categorized based on DNA and cell morphology; single cells with unseparated DNA, lacking a bud were considered "unbudded"; those with a bud < ¾ the diameter of the mother were "small budded metaphase", while those with a bud ≥ ¾ the diameter of the mother were "big budded metaphase"; budded cells whose DNA had visibly separated into two distinct masses were considered "anaphase" cells; and finally in the later time points, cells with DNA morphology indicating they had undergone anaphase and had also grown a new bud, were considered "anaphase rebudded." Budding index was calculated as the number of small + large-budded cells out of the total number of cells. Percent anaphase cells was calculated as the number of anaphase + anaphase rebudded cells out of the total number of cells. Images were

coded and all G1 release assays were scored blinded to both cell genotype and Taxol status.

### *2.5.5 Preparing preformed metaphase spindles by Cdc20 depletion (Cdc20 arrest)*

*MAT*a strains were modified to place the Anaphase Promoting Complex co-activator, Cdc20, under the methionine-inducible *MET3* promoter (Uhlmann et al., 2000). Cells were maintained and grown to mid log phase (30˚C) in SC -Met media. Cells were transferred to SC -Met with 100 µM alpha factor for 2.5 hours at 30˚C to synchronize in G1. These cells were washed three times in 1 ml water and resuspended in SC -Met containing 0.02% methylcellulose and supplemented with 0.2 mg/ml methionine, to suppress Cdc20 production. After 75 min at 30˚C, >90% of cells were arrested in metaphase, and DMSO +/- 30 µM Taxol (final from 1 mM stock in DMSO) was added to the cultures. 15 min later cells were either imaged live, or fixed with 3.7% formaldehyde and imaged within 24 h.

### *2.5.6 Cdc20 release assay*

Cells were prepared as in the Cdc20 arrest (above), however, following the 15-minute incubation +/- Taxol, cells were quickly washed three times in 1 ml water (to remove methionine) and resuspended in 5 ml SC -Met containing 0.02% methylcellulose and DMSO +/- 30 µM Taxol (final from 1 mM stock in DMSO). In the

absence of methionine, cells produce Cdc20 and release from arrest. Cultures were maintained on the bench and gently mixed by hand every 10 min. Samples were removed and fixed in ice cold 70% ethanol every 10 min over 80 min. Cells were washed 2 times with PBS and nuclei were stained with 50 ng/ml DAPI. For imaging, 10-12 z-plane DIC and DAPI images were collected at 0.5 µm intervals. Images were coded and all Cdc20 release assays and missegregation assays were scored blinded to both cell genotype and Taxol status. To quantify images, cells were categorized based on DNA and cell morphology; single cells lacking a bud were considered “single cells”, cells with a small or large bud whose DNA had not yet begun to separate were considered “metaphase”, and budded cells whose DNA had visibly separated into two distinct masses were considered “anaphase” cells. To score chromosome missegregation, cells in which *CEN1* was marked by tetO/tetR-GFP were used in the Cdc20 release assay and imaged with 20 z-planes spaced 0.3 µm apart. At 50 and 70 min post Cdc20 release, cells with elongated spindles were scored for whether the two tetO/tetR-GFP foci were segregated correctly into the mother and daughter cells.

### *2.5.7 Microscopy*

Spindle poles were visualized with endogenous Spc29-mRFP, and microtubules with an exogenous copy of GFP-Tub1 integrated at the URA3 locus. Centromeres were visualized by tetO/tetR-GFP arrays; 224 tandem repeats of the tetO were integrated 228 bp 3’ of CDEIII on chromosome 1 using plasmid pPM290 (Hsu et al., 2003) and visualized with TetR-GFP (Michaelis et al., 1997) or TetR-YFP (Janke et al., 2002).

Fixed cell imaging was performed on a Carl Zeiss AxioImager M2 microscope with a piezoelectric-driven Z-stage and a cooled CCD camera (CoolSNAP $HQ^2$; Photometrics). Images were obtained with a 63× 1.4 NA Plan Apochromat objective and Semrock filters using SlideBook software (Intelligent Imaging Innovations, Inc.). Live cell imaging was performed on a Nikon ECLIPSE-Ti inverted microscope equipped with a Ti-ND6-PFS Perfect Focus Unit and a Yokogawa CSU-XI spinning disk confocal scanner. Images were captured on an Andor iXon3 897 EMCCD camera using a Nikon CFI Plan Apo VC 60X 1.2 NA water immersion objective and MetaMorph Microscopy Automation & Image Analysis Software (Molecular Devices**,** LLC**.**).

### *2.5.8 Image and analyze metaphase spindles in fixed cells*

20 z-plane images spaced 0.3 μm apart were captured in the RFP (SPB; 1200 ms) and either YFP or GFP (*CEN1*-tetO/tetR; 700 ms) channels. Images were coded and then scored in blinded fashion with respect to Taxol and nocodazole status. For analysis, only spindles fully contained within the image stacks were used. Slidebook software was used to measure distances between the outer edges of spindle pole bodies or sister centromeres in 3-dimensions across the z-stack. To determine the distance between the centroids of separated sister centromeres, the x-y-z coordinates representing the centroid of each centromere fluorescence signal was determined using Slidebook software and used to calculate the 3-dimensional distance. To score centromere/kinetochore attachment to metaphase spindles, a square was generated by extending lines from each pole at 45° angles to the spindle axis.

Centromeres/kinetochores were considered attached if both centromere foci were within this square.

### *2.5.9 Image and analyze metaphase spindles in live cells*

Cells were mounted on agarose pads as described (Luchniak et al., 2013) containing 1% agarose in SC -Met media, 0.2mg/ml methionine, 0.02% methylcellulose and DMSO +/- 30 μM Taxol. A mixture of agarose, SC -Met and methionine was solubilized in a microwave, 1 ml was placed in a microcentrifuge tube and cooled briefly before being supplemented with 0.02% methylcellulose and DMSO +/-30 μM Taxol (final from 1 mM stock in DMSO). Approximately 300 μL was rapidly pipetted onto three separate slides. After 30 s, a second slide was placed on top of each pool of agarose mixture to flatten it to ~3mm thickness. At the time of imaging, 1 ml of log phase culture was spun down in a microfuge and 10 μl of concentrated cells were pipetted onto the pad. A coverslip was placed on top of the cells, excess pad cut away with a razor blade, and the coverslip edges sealed with VALAP. Images were captured in the GFP (*CEN1*-tetO/tetR; 200 ms) and RFP (SPB; 700 ms) channels at 2-3 s intervals. Timelapse images of individual cells were cropped out and coded before centromere separation and breathing was scored blinded with regard to +/- Taxol treatment. Only images in which both spindle poles were in focus were used to score centromere separation as either a single or two separated fluorescence foci. Transitions per minute, or ‘breathing’ was calculated as the number of transitions from unseparated to separated, and vice versa, over time. To generate kymographs, at each time point the centroid of one SPB

was located using the ‘find foci’ tool and then translated (along with other channels) to the center of the image. The centroid of the second SPB was then located and the image rotated to align both SPBs on the x-axis. Kymographs were then generated using ImageJ (National Institutes of Health).

### *2.5.10 Spindle elongation in live cells*

10 ml culture dishes with Poly-D Lysine coated glass coverslips embedded in the bottom (MatTek) were primed by pipetting 300 µl of SC media containing 0.02% methylcellulose and DMSO +/- 30 µM Taxol onto the glass coverslip; the lid of the dish was sealed closed with Parafilm and incubated at 37˚C for 15 min. Next, 1 ml of culture was spun down and resuspended in ~400 µl of identical media, of which 300 µl was then applied to the primed coverslip. The cells were allowed to settle for 15 min at room temperature, after which 5 ml of identical media was gently added to the dish. Parafilm was used to seal the dish and cells were imaged at room temperature over the next few hours. At 1 min intervals, 10 z-plane images spaced 0.5µm apart were captured in the DIC, RFP (700 ms) and GFP (200 ms) channels.

### *2.5.11 Generating best-fit sigmoidal curves for G1 release data*

The program used to fit my G1 release data to sigmoidal curves was written with the help of Dr. Allan Drummond (University of Chicago) using R software based off the following description of a curve:

$$b * \left( \frac{1}{(1^{e(-a*(time.min - d)})} \right)$$

Where: a = coefficient of e; b = maximum percentage of anaphase cells; and d = the time to half-maximum anaphase. It is designed to iterate these values until it generates best-fit curves for any given strain's experimental data, with the first iteration testing values of a=0.1. b=60, and d=175. In italics are sections that are subject to change based on the data. To generate files that this program can read, all replications of a strain's release data were converted to tab-delimited files with four categories of information organized in columns: time (minutes), variable treatment, replicate, and percent anaphase, in the script below, this tab-delimited file was named *'proudfoot/mad1-delta-anaphase-melted.txt'*.

```
x <- read.delim(paste(dropbox.dir,'proudfoot/mad1-delta-anaphase-melted.txt',sep='/'),
comment.char='#')

fit.fxn <- function(a,b,d,time.min) {
        b*(1/(1+exp(-a*(time.min-d))))
}

start.values <- list(a=0.1, b=60, d=175)
time.test <- 0:300

test.data <- data.frame(time.min=time.test, pct.anaphase=fit.fxn(start.values[['a']], start.values[['b']],
start.values[['d']], time.test), treatment=NA)

fit.control <- nls(pct.anaphase~fit.fxn(a,b,d,time.min), data=subset(x, treatment=='control'),
        start=start.values)
fit.taxol <- nls(pct.anaphase~fit.fxn(a,b,d,time.min), data=subset(x, treatment=='taxol'),
        start=start.values)

fit.control.df <- data.frame(time.min=time.test,
        pct.anaphase=fit.fxn(coef(fit.control)[['a']], coef(fit.control)[['b']], coef(fit.control)[['d']],
time.test),
        treatment='control', rep=NA)
fit.taxol.df <- data.frame(time.min=time.test,
```

```
        pct.anaphase=fit.fxn(coef(fit.taxol)[['a']], coef(fit.taxol)[['b']], coef(fit.taxol)[['d']], time.test),
        treatment='taxol', rep=NA)
fit.data <- rbind(fit.control.df, fit.taxol.df)

g <- ggplot(x, aes(x=time.min, y=pct.anaphase, colour=treatment)) + geom_point() +
        geom_line(data=fit.data)
print(g)
```

### *2.5.12 analyze microtubule dynamics in live cells*

The parameters of microtubule dynamic instability we determined essentially as described in Entwistle et al. (ChemMedChem, 2012 vol 7(9) pp. 1580-1586). The only difference was that in addition to polymerization and depolymerization events being defined as a line through at least four data points (24 s) that spanned a range of > 0.4 μm with an $R^2$ value of ≥ 0.84, because length changes were minor and velocities lower in the presence of Taxol, events that spanned < 0.4 μm but persisted for more than 10 data points (60 s) with an $R^2$ value of ≥ 0.9 we also included. As described in Entwistle et al, the three-dimensional length of astral microtubules was determined at each time point by using SlideBook software. Polymerization and depolymerization events were defined as a line through at least four data points (24 s) that spanned a range of > 0.4 mm with an $R^2$ value of ≥ 0.84. Periods of attenuation were defined as persisting at least four data points with net length changes of < ±0.2 μm. Data points that did not fit these criteria were discarded. The percentage of time spent in each phase was determined by dividing the sum of the time in each phase by the total classified time for all microtubules analyzed. Catastrophes were defined as a transition into depolymerization following polymerization or attenuation. Rescues were defined as transition out of depolymerization into polymerization or attenuation. Only the time spent

polymerizing or attenuated was considered to determine the catastrophe frequency. Similarly, only time spent depolymerizing was considered to calculate rescue frequency. Cells were imaged ±Taxol on two separate days. Cells were grown and maintained at 23 °C during imaging; p values were determined by Student's t-test.

### *2.5.13 Statistical analysis*

*p* values were determined by unpaired 2-tailed student's *t*-test (*$p \leqslant 0.05$, **$p \leqslant 0.01$, ***$p \leqslant 0.001$, ****$p \leqslant 0.0001$, ns = not statistically significant). S.D. and S.E.M. refer to standard deviation and standard error of the mean, respectively.

# Chapter 3:

# Discussion

During metaphase, a group of proteins works in concert to ensure that genetic material is equally partitioned between mother and daughter cell via several evolutionarily conserved signaling pathways, referred to as the mitotic checkpoint. These signaling cascades respond to both the tension and attachment status of kinetochores; however, they are so deeply interconnected by shared protein components, similar timing within the cell cycle, and the common goal to promote accurate spindle assembly that, historically, these signaling pathways have been mechanistically difficult to classify. Specifically, it remained unclear whether or not the tension status at kinetochores could delay a cell in metaphase, regardless of the microtubule attachment status. Here I will review the tension-mediated delay that we have identified and discuss broadly how it may function in cells. I will hypothesize how tension-specific signaling fits within the context of known mitotic signaling pathways that promote genome stability, and will propose possible reasons why this signaling was overlooked in the past. Importantly, a mechanistic understanding of tension mediated signaling, beyond error correction, is essentially unknown, and here I will propose several lines of research which may potentially reveal a more complete picture of the tension mediated signaling pathway.

Our data describe a novel signaling pathway in budding yeast, mediated by a subset of canonical SAC proteins, that transiently delays cells in metaphase in response

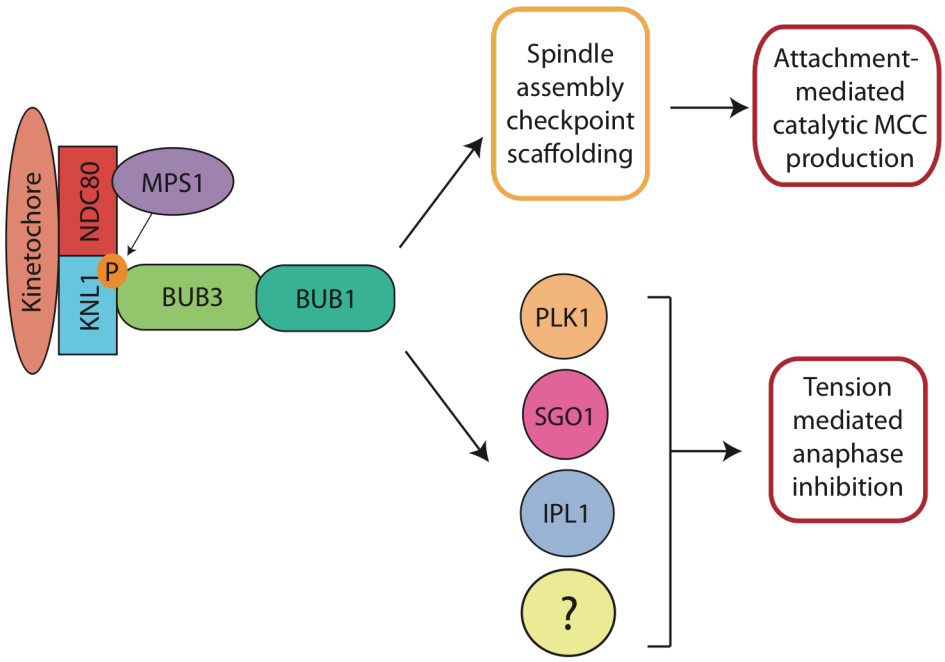


**Figure 23. Recruitment of the Bub1-Bub3 complex to the kinetochore represents a potential branch point for attachment-mediated and tension-mediated signaling.** Once recruited to the kinetochore and activated by Mps1 phosphorylation the Bub1-Bub3 complex can form the core of SAC scaffolding, promoting the catalytic production of the MCC in response to a detached kinetochore. Additionally, before SAC scaffolding is initiated (if drawing from the same pool of Bub1-Bub3) or regardless of SAC activation (if drawing from a separate pool of Bub1-Bub3), the Bub1-Bub3 complex interacts with several partners to promote tension-mediated inhibition of anaphase. These proteins include but are not limited to Plk1, Sgo1, Ipl1, and potentially yet unknown proteins partners that coordinate to promote biorientation.

to reduced kinetochore tension. One major aspect that remains to be determined is how the tension mediated signaling is functionally and mechanistically integrated with other signaling pathways at metaphase (Figure 23). In particular, it will be important to determine whether the kinetochore recruitment of the Bub1/Bub3 complex functions as a branch point leading to both activation of the SAC and/or tension-mediated anaphase inhibition, or whether separate pools of these proteins allow the tension-mediated delay to function as an independent mechanism in parallel with the SAC (Figure 23). To answer these questions, it will be instrumental to determine the complete set of proteins

that participate in the tension mediated signaling pathway, and how the tension mediated signaling culminates in the inhibition of anaphase onset.

When determining the protein components necessary for the tension mediated delay, additional insight may be provided by the original screens that discovered the *BUB* and the *MAD* genes. Once again, these screens uncovered the majority of central SAC proteins known today, but intriguingly they uncovered two, non-overlapping sets of proteins: the Mads (Mitotic Arrest Deficient) and the Bubs (Budding Uninhibited by Benzimidazole) (Li and Murray, 1991; Hoyt et al., 1991). That these two screens uncovered two separate sets of mutants has thus far been credited to circumstance; but the true reason may lie in the related, yet fundamentally different screening strategies that I will discuss below. Because our own research identifies a functional difference between these two groups of proteins, I will summarize the differences between these two screens to conceptualize how they may have selected for different functional deficits.

In brief, the setup of the two screens was as follows. In the screen that discovered *BUB1, BUB2,* and *BUB3* (Hoyt et al., 1991), cells were mutagenized, and colonies were selected that recovered poorly from 20 hours of growth on 70µg/mL benomyl (a microtubule destabilizing drug concentration sufficiently high to transiently ablate all microtubule structure within the cell). Colonies of interest were analyzed further by microscopy to reveal mutants that continued to rebud (*bub* mutants) under microtubule destabilizing conditions that caused mitotic arrest in metaphase and prevented rebudding in control cells. Benomyl sensitive strains that were found to re-bud in the presence of benomyl were complemented with a genomic library to identify

the mutated genes *bub1* and *bub2*, while *bub3* was found in the same study because increased expression also complemented *bub1* mutants.

In retrospect, during the initial selection of mutants in this study, strains were challenged to arrest for 20 hours in the absence of a spindle; checkpoint mutants would have biochemically proceeded into anaphase without assembling a spindle, likely producing daughter cells that have no nucleus, and mother cells with double the DNA content in a single nucleus. Although abnormal ploidy is not ideal for any cell type, it is not necessarily a death sentence in budding yeast (Storchová et al., 2011), and so it is possible that this whole-genome missegregation was not lethal to all checkpoint mutants. Upon transfer to recovery media, a checkpoint mutant would have to build its spindle without the aid of positional cues that predispose sister chromatids to biorient (Indjeian and Murray, 2007). Without these cues, all cells would rely more heavily on both tension and attachment mediated signaling to achieve proper spindle assembly. Checkpoint mutants, unable to sense tension and/or kinetochore detachment, would be at a disadvantage and would be more likely to missegregate chromosomes at a high frequency, leading to cell death. In contrast, cells with an intact checkpoint would have remained arrested for 20 hours but then upon recovery would have rebuilt their spindle and successfully executed anaphase. Because of the second recovery step in this screen, one could imagine how it may have inadvertently emphasized selection for SAC proteins that have additional roles in biorientation. It is not entirely clear why the *MAD* genes were not also discovered in this screen, but one possibility is that, if Mad proteins are not required for biorientation, they might still be able to produce a short, tension-mediated delay when their kinetochores did not initially biorient on the spindle. If the

short delay provided *mad* mutants sufficient time to repair any spindle damage, those mutant strains would survive and would not be readily detected in this assay.

The screen responsible for uncovering the *MAD* genes (Li and Murray, 1991) demonstrated that *mad* mutants are also sensitive to benomyl and die as a result of premature mitotic exit in the spindle poison; however, in this screen strains were mutagenized and selected by the inability to grow on 15 μg/mL benomyl for an extended period of time (a typically nonlethal concentration, much lower than the concentration used for the screen conducted by Hoyt et al.. Analysis of the growth of individual microcolonies on benomyl revealed select "mitotic-arrest deficient" mutants which proceeded into anaphase with misassembled spindles roughly as fast as wild type cells with healthy bipolar spindles would in the absence of the drug. Challenging cells to build spindles in the presence of a spindle poison should have selected for all SAC mutants, including the *BUB* genes. It's possible that the *BUB*s were not discovered in this screen due to the general sickliness of the mutants; *bub* mutants are more sickly than *mad* mutants, and may have been overlooked or may not have survived this step of the screen.

In practice, beyond these screens, further experimental interrogation of the tension mediated signaling that delays anaphase is complicated by the presence of additional tension mediated signaling occurring at metaphase. This signaling includes error correction and SAC silencing, (Figure 24A) as well as less-characterized, non-canonical mechanisms that promote biorientation (Figure 24B). Experimental testing of tension mediated signaling is difficult in part because error correction can influence the status of microtubule-kinetochore attachments, and associated signaling. Moreover, it

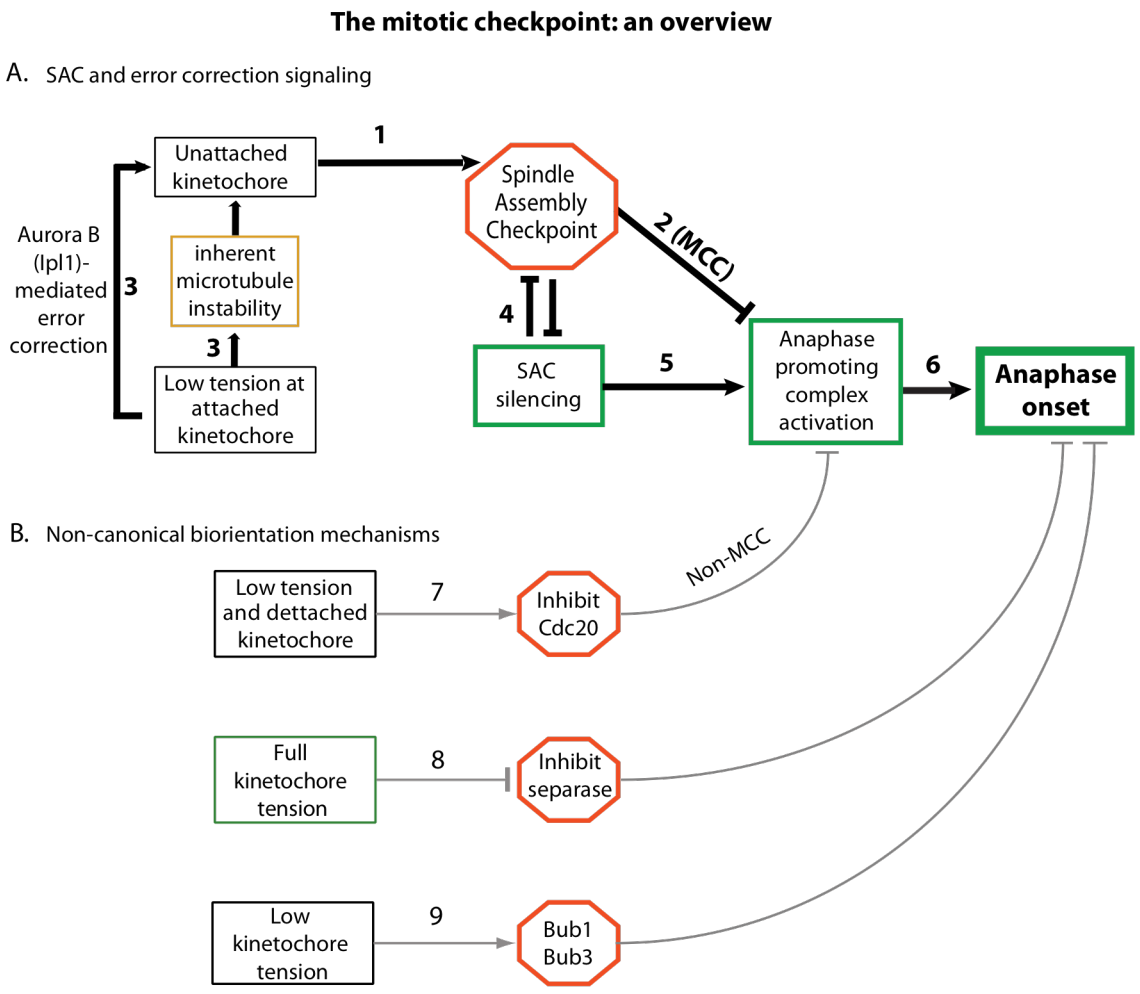


**Figure 24. Revisiting the many mechanisms that make up the mitotic checkpoint.** (A) Bold arrows represent canonical mechanisms that activate in response to detached/tensionless kinetochores. (1) A detached kinetochore activates the spindle assembly checkpoint, which assembles (2) the mitotic checkpoint complex (MCC) to inhibit activation of the anaphase promoting complex. (3) Kinetochore attachments with insufficient tension are inherently unstable, and either come detached on their own or are actively destabilized via the Aurora B-mediated error correction pathway to activate the SAC as unattached kinetochores. (4) Signaling promoting SAC silencing and the spindle assembly checkpoint are in direct competition; however, when conditions favor SAC deactivation, i.e. when attachments come under tension, (5) SAC silencing rapidly promotes anaphase promoting complex activation and subsequent (6) anaphase onset. (B) Non-canonical mechanisms whose timing and purpose have not yet been fully incorporated into the traditional picture of the mitotic checkpoint further promote kinetochore biorientation. (7) low tension and kinetochore detachment both promote inhibitory phosphorylation of Cdc20 to inhibit the APC in a MCC-independent manner in HeLa cells. (8) Full tension at kinetochores signifies bipolar attachment and reversibly opposes an APC-independent mechanism that inhibits Separase and consequentially anaphase onset. Notably, the relative contributions kinetochore tension status vs. attachment status in both of these pathways remains unclear. (9) In contrast, we have shown that reduced kinetochore tension, independent of kinetochore detachment causes a delay in anaphase onset mediated by the core SAC proteins Bub1 and Bub3. Currently, however, it is unclear if these three non-canonical pathways function separately or if they are part of a single, larger mechanism.

remains unclear if these pathways and the tension mediated delay that we report act independently of one another or not. One strategy to navigate these potentially redundant signaling pathways will be to conduct experiments in cells that have these additional pathways specifically inactivated. It is possible that conducting experiments using cells which have, for instance, the error correction mechanism inactivated might reveal that error correction and the tension delay are part of a single signaling pathway. On the other hand, such an experiment could reveal that the error correction mechanism obscures the tension delay under certain experimental conditions. In fact, it is not surprising that a tension-specific signaling mechanism has remained uncertain in the field – its delay is brief and obscured by several other signaling pathways, some of which are much more apparent than the 20-minute delay that we observe. Most drastically, while attachment mediated SAC activation produces a long delay that lasts >3 hours in yeast, tension mediated signaling is transient, lasting only about 20 minutes. This observation suggests an important point, however: that because the tension delay and the SAC operate on significantly different time scales, the tension delay may serve an inherently different purpose than SAC signaling at metaphase, one which its transient nature is tailored to. Further, if the tension delay and the SAC serve distinct purposes during spindle assembly, both may be equally important in promoting accurate chromosome segregation and ultimately proper cellular function. Finally, transient delays associated with reduced tension have been observed in a number of organisms (Makrantoni and Stark, 2009; Zasadil et al., 2014; Maresca and Salmon, 2009; Uchida et al., 2009; Tauchman et al., 2015; O'Connell et al., 2008; Biggins and Murray, 2001), further suggesting that the tension mediated delay serves a highly-conserved function.

Activating a short delay at metaphase in response to reduced tension at kinetochores would give cells time to determine whether or not a kinetochore-microtubule attachment is truly aberrant and in need of repair without mounting a strong inhibitory signal that would further delay cell division. This strategy would be particularly advantageous during development or in competitive niches. As the cell enters prometaphase and begins to build its spindle, Bub1 and Bub3 are at kinetochores constitutively, while Mad proteins are only recruited to a kinetochore if it later becomes detached (London and Biggins, 2014a). It is possible that during the early stages of spindle assembly, tension mediated signaling plays a key role, acting as the primary inhibitor of the APC. Later on in the cell cycle, kinetochore breathing means that even properly attached kinetochores experience varying degrees of tension during metaphase. Thus, the tension mediated delay might act together with the error correction mechanism: if a kinetochore lags below a certain threshold of tension during prometaphase through metaphase, the sensitive but short-lived tension mediated delay may stall the cell in metaphase briefly to provide a window of time, during which the error correction mechanism may be mounted only if tension remains low or drops below some additional threshold. Also, how long the error correction machinery requires to detach a tensionless attachment is unknown. Perhaps the tension mediated delay serves to ensure that error correction has time to occur when needed. Finally, the brief tension delay may supplement the attachment mediated SAC in response to kinetochores that become detached as the spindle nears full assembly, either by delaying anaphase onset before the attachment mediated SAC signal has fully activated

in response to newly detached kinetochores, or by signaling in unison with the SAC while it is active.

Beyond the potential role of inhibiting APC activity to inhibit anaphase onset before the SAC has activated, there are multiple, additional ways in which the tension mediated delay might supplement SAC signaling. First, it is possible that tension mediated signaling intensifies the inhibition of anaphase onset while the SAC is active, either by directly inhibiting the APC, or by targeting another key step required for anaphase onset, such as Separase activation. Second, it is possible that tension mediated signaling acts sequentially with SAC signalling, lengthening the amount of time an inhibitory signal persists in response to spindle damage. In this case, the tension delay could be important to prevent anaphase onset during the ~ 5-minute time period (in HeLa cells) before the attachment mediated SAC signal is activated in response to kinetochore detachment (Dick and Gerlich, 2013), or perhaps the tension delay serves to prolong the length of time that an inhibitory signal persists after the attachment mediated SAC alone would have stopped inhibiting the APC. Because the two proteins which we have shown to operate in tension mediated signaling, Bub1 and Bub3, are also essential SAC proteins, it will be vital to discover protein components that are unique to tension mediated signaling. Such knowledge will allow the design of experiments to clearly separate the functions and timing of these two pathways.

Defining additional components of the tension mediated delay mechanism described here will likely implicate the biochemical process by which tension mediated signaling inhibits anaphase onset independent of the canonical SAC. Because Mad1, Mad2, and Mad3 are not required for tension mediated signaling, it follows that the

tension mediated signaling we describe here does not involve the conventional mitotic checkpoint complex (MCC), which requires these proteins to form. Here I consider two broad strategies that cells may use to delay anaphase onset in response to reduced tension; namely, that tension mediated signaling could directly inhibit the APC (similar to canonical SAC signaling) or that tension mediated signaling could inhibit anaphase onset independent of the APC, for instance, by protecting chromosome cohesion (independent of canonical SAC signaling).

It was recently shown in HeLa cells that Bub1 and the Polo-like kinase Plk1 function together to phosphorylate Cdc20 and inhibit APC activation (Figure 24B), separate from the conventional MCC mediated inhibition (Jia. et al., 2016). Several experiments can be envisioned that would determine if the tension mediated delay is the result of Bub1 and/or Plk1 phosphosignaling in budding yeast. Initially, observing the delay profile of a *cdc5*Δ (Plk1) mutant in our Cdc20 release assay would indicate whether this protein is required for the tension delay based on whether or not the delay in Taxol is abolished in this mutant. To test this possibility further, collecting a protein lysate from Cdc20-arrested cells +/- 30 μM Taxol and Western blotting for Cdc20 may reveal a Taxol-dependent, tension-specific phospho-shift. If this shift disappeared upon the deletion of either *CDC5* or the kinase domain of *BUB1*, it would provide further evidence that the tension mediated delay is dependent on Bub1 or Plk1 directly inhibiting the APC, independent of the MCC. Additionally, co-immunopurification of Cdc20 may reveal other proteins that bind to, and possibly inhibit Cdc20 analogous to the MCC. Finally, Bub3's role in tension mediated signaling must be defined. For

instance, its main role may be to properly localize Bub1. Alternatively, Bub3 may perform some other as yet unknown function.

Another possibility is that the tension delay is the result of APC-independent signaling mediated by Shugoshin (Sgo1) and Cdc55, as described by Clift, Bizzari, and Marston in budding yeast (Clift et al., 2009). These authors showed that Sgo1 activates Cdc55 to inhibit Separase (Figure 24B). Separase is therefore prevented from cleaving sister chromatid Cohesin and sisters remain bound together, prolonging metaphase. Because Bub1 and Bub3 have been linked to the tension-dependent, pericentromeric localization of Sgo1 (Nerusheva et al., 2014), it will be important to determine if they are upstream players in this APC/Securin-independent inhibition of anaphase. If so, such tension mediated signaling could act in parallel with the SAC, producing centromere-localized inhibition of anaphase in addition to the SAC signaling that permeates the cell's cytoplasm.

To distinguish between these possible pathways, the protein components that produce the tension mediated delay must be defined. This could be accomplished both by targeted molecular genetics and by forward genetic screening. In addition to Sgo1, Cdc55, and Cdc5 (Plk1), it will be important to conduct targeted experiments to determine if inactivation of additional proteins including Bub2, Mps1 and Aurora B, which have been implicated as potential tension sensors in the past (Biggins and Murray, 2001; Dorer et al., 2005; Santaguida et al., 2010; Storchová et al., 2011), are required for the tension delay. Aurora B in particular plays a pivotal role in the error correction pathway (Tanaka et al., 2002; Biggins and Murray, 2001; Pinsky et al., 2006; Krenn and Musacchio, 2015), and so it will be intriguing to determine if it also plays a

separate role in the tension mediated delay. In contrast to reverse genetics, on the -other hand, two screening strategies may prove useful to discover new proteins involved in the tension specific delay.

Pathways and checkpoints involved in promoting accurate spindle assembly rely heavily on phosphosignaling. Therefore, a screen which detects changes in the phosphoproteome when chromosomes are under reduced tension may reveal new proteins and or phosphorylation events involved in this mechanism. Such a screen could be accomplished using SILAC (stable-isotope labeling by amino acids in cell culture) (Mann, 2006; Reiter et al., 2012), a mass spectrometry-based procedure which uses heavy isotopes to quantitatively distinguish between phosphorylation events under different culture conditions. For our purposes, Taxol sensitive yeast could be arrested in metaphase and split into three cultures, one treated with DMSO, one with Taxol to reduce tension at kinetochores, and one with nocodazole to reduce both attachment and tension at kinetochores. Comparing the differences between the phosphoproteome profiles of the three cultures would reveal proteins and amino acids which are phosphorylated specifically in response to reduced tension.

An alternative screen, designed to uncover proteins essential to tension mediated signaling, e.g. phosphosignaling or any vehicle or scaffold proteins, could employ a Tn7-derived transposon library (Kumar et al., 2004). This library has been designed to produce budding yeast colonies which have a single, nonessential gene inactivated at random. Replica plating transformant colonies onto Taxol plates would reveal mutant strains that display increased sensitivity to the drug. Such strains could then be isolated and the gene mutation responsible for increased Taxol sensitivity

determined. Subjecting mutants to the battery of release assays in the presence of Taxol could determine if the mutated protein is required to produce the tension mediated delay.

Using screens to identify additional proteins involved in the tension delay will likely also shed light on the nature of the signal that cells sense in response to reduced kinetochore tension. Broadly, there are two camps of thought: originally it was though that tension signaling is sensitive to inter-kinetochore stretch, or the distance between two sister centromeres (Waters et al., 1996), whereas the idea favored currently suggests that tension mediated signaling responds to intra-kinetochore stretch, or the mechanical deformation within an individual kinetochore (Maresca and Salmon, 2009; Uchida et al. 2009; Wan et al. 2009). However, recent evidence obtained using similar sub-diffractional image processing techniques of the kinetochore together with mutant kinetochore proteins that inhibit detachment of tensionless microtubule attachments argues against intra-kinetochore stretch being the source of the signal (Etemad et al., 2015; Tauchman et al., 2015). Yet, it remains possible that a tension-sensitive change in the nature of the kinetochore-microtubule binding interaction may activate the tension delay, largely independent of detectable stretching across the kinetochore structure.

Identifying the components required for the tension mediated delay will progressively reveal the source of the initial signal, i.e. if the flexibility of the structural kinetochore protein Ndc80 is required for the tension delay, it will suggest that individual kinetochore deformation initiates the signal (Nannas and Murray, 2014), whereas if Aurora B, which is located between pairs of sister centromeres during metaphase (Carmena et al., 2012) is required for the tension delay, it will support an alternative

model: that inter-kinetochore stretch is involved in the signaling. Interestingly, our data indicate that even modest decreases in inter-kinetochore distance are sufficient to produce the tension mediated delay in our system (Figure 2.2 D-F, figure 2.2 supplemental), which speaks to the sensitivity of the signaling response and suggests that even minor decreases in microtubule-generated tension can produce a signal to delay anaphase onset. It is important to note that in our measurements, a decrease in inter-kinetochore tension would also be accompanied by a corresponding reduction in intra-kinetochore tension. Thus, our results do not discriminate between the two as potential sources of tension mediated signaling. To distinguish between these possibilities, it will be necessary to measures changes in intra-kinetochore stretch concurrently with changes in inter-kinetochore distance in the presence and absence of Taxol.

In conclusion, we have developed a system in budding yeast which, for the first time, uses Taxol to reduce tension at otherwise attached kinetochores in normal, bipolar spindles. This reduction in tension causes changes in spindle architecture that produce a signal to transiently delay anaphase onset. We show that this tension mediated signaling requires the proteins Bub1 and Bub3, but additional protein components have yet to be determined. Obtaining a more detailed mechanistic understanding of the tension delay will elucidate how tension mediated signaling is coordinated with additional signaling mechanisms during metaphase, such as SAC activation, error correction, and SAC silencing, to faithfully segregate genetic material during each cell division. Such mechanistic insight is prerequisite to understanding how tension mediated signaling functions in the cell, and how it may participate in crosstalk with

signaling processes beyond metaphase and spindle assembly, such as cortical strain and apoptosis. By obtaining a holistic view of how multiple signaling cascades interact with one another, we will be better equipped to comprehend their function in healthy tissue, to understand the pathology of diseases associated with these signaling pathways, and to generate more specific and effective therapies to combat such diseases.

# Bibliography

Akache, B., & B. Turcotte. 2002. New regulators of drug sensitivity in the family of yeast zinc cluster proteins. *Journal of Biological Chemistry*, *277*(24), 21254–21260. http://doi.org/10.1074/jbc.M202566200.

Akiyoshi, B., K.K. Sarangapani, A.F. Powers, C.R. Nelson, S.L. Reichow, Arellano-H. Santoyo, S., T. Gonen, J.A. Ranish, C.L. Asbury, Biggins, S. 2010. Tension directly stabilizes reconstituted kinetochore-microtubule attachments. *Nature*, *468*(7323), 576–9. http://doi.org/10.1038/nature09594

Alexandru, G., W. Zachariae, A. Schleiffer, and K. Nasmyth. 1999. Sister chromatid separation and chromosome re-duplication are regulated by different mechanisms in response to spindle damage. *The EMBO Journal*. 18:2707–2721. doi:10.1093/emboj/18.10.2707.

Araujo, A. R., L. Gelens, R. S., M. Sheriff, & S. D. M. Santos. 2016. Positive Feedback Keeps Duration of Mitosis Temporally Insulated from Upstream Cell-Cycle Events. *Molecular Cell*, *64*(2), 362–375. http://doi.org/10.1016/j.molcel.2016.09.018.

Aravamudhan, P.; A.A. Goldfarb, A.P. Joglekar. 2015. The kinetochore encodes a mechanical switch to disrupt spindle assembly checkpoint signaling. *Nat. Cell Biol*. 17, 868–879.

Barnes, G., K.A. Louie, and D. Botstein. 1992. Yeast proteins associated with microtubules in vitro and in vivo. *Mol Biol Cell*. 3:29–47.

Barnhart, E.L., R.K. Dorer, A.W. Murray, and S.C. Schuyler. 2011. Reduced Mad2 expression keeps relaxed kinetochores from arresting budding yeast in mitosis. *Mol Biol Cell*. 22:2448–2457. doi:10.1091/mbc.E09P01P0029.

Baro, B., J. A. Rodriguez-Rodriguez, I. Calabria, M. L. Hernáez, C. Gil, & E. Queralt. 2013. Dual Regulation of the Mitotic Exit Network (MEN) by PP2A-Cdc55 Phosphatase. *PLoS Genetics*, *9*(12). http://doi.org/10.1371/journal.pgen.1003966.

Biggins, S., F.F. Severin, N. Bhalla, I. Sassoon, A.A. Hyman, and A.W. Murray. 1999. The conserved protein kinase Ipl1 regulates microtubule binding to kinetochores in budding yeast. *Genes Dev.* 13, 532–544.

Biggins, S., and A.W. Murray. 2001. The budding yeast protein kinase Ipl1/Aurora allows the absence of tension to activate the spindle checkpoint. *Genes Dev*. 15:3118–3129. doi:10.1101/gad.934801.

Bajer, A. and J. Molè-Bajer. 1955. Cine-micrographic studies on mitosis in endosperm. *Chromosoma.,* 7, 558–607.

Bode, C.J., M.L. Gupta, E.A. Reiff, K.A. Suprenant, G.I. Georg, and R.H. Himes. 2002. Epothilone and paclitaxel: unexpected differences in promoting the assembly and stabilization of yeast microtubules. *Biochemistry*. 41:3870–3874. doi:10.1021/bi0121611.

Botchkarev, V. V., M. V. Garabedian, B. Lemos, E. Paulissen, and J. E. Haber. 2017. The budding yeast Polo-like kinase localizes to distinct populations at centrosomes during mitosis. *Molecular Biology of the Cell*. E16-05-0324. http://doi.org/10.1091/mbc.E16-05-0324.

Burgess, A., M. Rasouli, and S. Rogers. 2014. Stressing Mitosis to Death. *Frontiers in Oncology*, *4*(June), 140. http://doi.org/10.3389/fonc.2014.00140.

Callan, H.G. and P.A. Jacobs. 1957. The meiotic process in Mantis religiosa L. males. J. *Genet.* 55, 200–217.

Campbell, C. S. and A. Desai. 2013. Tension sensing by Aurora B kinase is independent of survivin-based centromere localization. *Nature*, *497*(7447), 118–21. http://doi.org/10.1038/nature12057.

Carmena, M., X. Pinson, M. Platani, Z. Salloum, Z. Xu, A. Clark, and W.C. Earnshaw. 2012. The chromosomal passenger complex activates Polo kinase at centromeres. *PLoS Biology*, *10*(1), e1001250. http://doi.org/10.1371/journal.pbio.1001250.

Chan, C. S., and D. Botstein. 1993. Isolation and characterization of chromosome-gain and increase-in-ploidy mutants in yeast. *Genetics*, *135*(3), 677–91.

Cheeseman, I. M., S. Anderson, M. Jwa, E. M. Green, J. S. Kang, J. R. Yates, G. Barnes. 2002. Phospho-regulation of kinetochore-microtubule attachments by the Aurora kinase Ipl1p. *Cell*, *111*(2), 163–72.

Cheeseman I.M., J.S. Chappie, E.M. Wilson-Kubalek, A. Desai. 2006. The conserved KMN network constitutes the core microtubule-binding site of the kinetochore. *Cell.* 127: 983–997.

Ciosk, R., W. Zachariae, C. Michaelis, A. Shevchenko, M. Mann, K. Nasmyth. 1998. An ESP1/PDS1 complex regulates loss of sister chromatid cohesion at the metaphase to anaphase transition in yeast. *Cell.* 93, 1067–1076.

Clift, D., F. Bizzari, and A.L. Marston. 2009. Shugoshin prevents cohesin cleavage by PP2A(Cdc55)-dependent inhibition of Separase. *Genes Dev*. 23:766–780. doi:10.1101/gad.507509.

Collin, P., O. Nashchekina, R. Walker, and J. Pines. 2013. The spindle assembly checkpoint works like a rheostat rather than a toggle switch. *Nat Cell Biol*. doi:10.1038/ncb2855.

De Antoni, A., C.G. Pearson, D. Cimini, J.C. Canman, V. Sala, L. Nezi, M. Mapelli, L. Sironi, M. Faretta, E.D. Salmon, A. Musacchio. 2005. The Mad1/Mad2 complex as a template for Mad2 activation in the spindle assembly checkpoint. *Curr. Biol.* 15, 214–225.

De Brabander, M., G. Geuens, R. Nuydens, R. Willebrords, and J. De Mey. 1981. Taxol induces the assembly of free microtubules in living cells and blocks the organizing capacity of the centrosomes and kinetochores. *Proc Natl Acad Sci USA*. 78:5608–5612.

DeLuca, J.G., B. Moree, J.M Hickey, J.V. Kilmartin, E.D. Salmon. 2002. hNuf2 inhibition blocks stable kinetochore-microtubule attachment and induces mitotic cell death in HeLa cells. *J. Cell Biol.* 159, 549–555.

DeLuca, J.G., B.J Howell, J.C. Canman, J.M. Hickey, G. Fang, E.D. Salmon, E.D. 2003 Nuf2 and Hec1 are required for retention of the checkpoint proteins Mad1 and Mad2 to kinetochores. *Curr. Biol.* 13, 2103–2109.

DeLuca K.F., S.M. Lens, J.G. DeLuca. 2011. Temporal changes in Hec1 phosphorylation control kinetochore-microtubule attachment stability during mitosis. *J Cell Sci*. 124:622–634.

Dick, A.E., and D.W. Gerlich. 2013. Kinetic framework of spindle assembly checkpoint signalling. *Nat Cell Biol*. 15:1370–1377. doi:10.1038/ncb2842.

Di Fiore, B.; N.E. Davey, A. Hagting, D. Izawa, J. Mansfeld, T.J. Gibson, J. Pines. 2015. The ABBA Motif Binds APC/C Activators and Is Shared by APC/C Substrates and Regulators. *Dev. Cell.* 32, 358–372.

Ditchfield, C., V.L. Johnson, A. Tighe, R. Ellston, C. Haworth, T. Johnson, S.S. Taylor. 2003. Aurora B couples chromosome alignment with anaphase by targeting BubR1, Mad2, and Cenp-E to kinetochores. *The Journal of Cell Biology*, *161*(2), 267–80.

Dorer, R. K., Zhong, S., Tallarico, J. a, Wong, W. H., Mitchison, T. J., & Murray, A. W. (2005). A small-molecule inhibitor of Mps1 blocks the spindle-checkpoint response to a lack of tension on mitotic chromosomes. *Current Biology: CB*, *15*(11), 1070–6. http://doi.org/10.1016/j.cub.2005.05.020.

Emter, R., A. Heese-Peck, A. Kralli. 2002. ERG6 and PDR5 Regulate Small Lipophilic Drug Accumulation in Yeast Cells via Distinct Mechanisms. *FEBS Lett.*, *521*, 57–61.

Entwistle, R.A., R.S. Rizk, D.M. Cheng, G.H. Lushington, R.H. Himes, and M.L. Gupta. 2012. Differentiating between models of epothilone binding to microtubules using tubulin mutagenesis, cytotoxicity, and molecular modeling. *ChemMedChem*. 7:1580–1586. doi:10.1002/cmdc.201200286.

Espert, A., P. Uluocak, R.N. Bastos, D. Mangat, P. Graab, U. Gruneberg. 2014. PP2A-B56 opposes Mps1 phosphorylation of Knl1 and thereby promotes spindle assembly checkpoint silencing. *J. Cell Biol.* 206, 833–842.

Etemad, B., T.E.F. Kuijt, and G.J.P.L. Kops. 2015. Kinetochore-microtubule attachment is sufficient to satisfy the human spindle assembly checkpoint. *Nat Commun*. 6:8987. doi:10.1038/ncomms9987.

Etemad, B., and G.J.P.L. Kops. 2016. Attachment issues: Kinetochore transformations and spindle checkpoint silencing. *Current Opinion in Cell Biology*, *39*(Mcc), 101–108. http://doi.org/10.1016/j.ceb.2016.02.016.

Evans, T., E.T. Rosenthal, J. Youngblom, D. Distel, T. Hunt. 1983. Cyclin: A protein specified by maternal mRNA in sea urchin eggs that is destroyed at each cleavage division. *Cell.* 33, 389–396.

Foland, T.B., W.L. Dentler, K.A. Suprenant, M.L. Gupta, and R.H. Himes. 2005. Paclitaxel-induced microtubule stabilization causes mitotic block and apoptotic-like cell death in a paclitaxel-sensitive strain of Saccharomyces cerevisiae. *Yeast*. 22:971–978. doi:10.1002/yea.1284.

Foltman, M., I. Molist, I. Arcones, C. Sacristan, Y. Filali-Mouncef, C. Roncero, and A. Sanchez-Diaz. 2016. Ingression Progression Complexes Control Extracellular Matrix Remodeling during Cytokinesis in Budding Yeast. *PLoS Genetics*, *12*(2). http://doi.org/10.1371/journal.pgen.1005864.

Foster, S. A., and D. O. Morgan. 2012. The APC/C Subunit Mnd2/Apc15 Promotes Cdc20 Autoubiquitination and Spindle Assembly Checkpoint Inactivation. *Molecular Cell*, *47*(6), 921–932. http://doi.org/10.1016/j.molcel.2012.07.031

Fraschini, R., E. Formenti, G. Lucchini, and S. Piatti. 1999. Budding yeast Bub2 is localized at spindle pole bodies and activates the mitotic checkpoint via a different pathway from Mad2. *Journal of Cell Biology*, *145*(5), 979–991. http://doi.org/10.1083/jcb.145.5.979.

Fuchs, D.A., and R.K. Johnson. 1978. Cytologic evidence that Taxol, an antineoplastic agent from Taxus brevifolia, acts as a mitotic spindle poison. *Cancer Treat Rep*. 62:1219–1222.

Gillett, E.S., C.W. Espelin, and P.K. Sorger. 2004. Spindle checkpoint proteins and chromosome microtubule attachment in budding yeast. *J Cell Biol*. 164:535–546. doi:10.1083/jcb.200308100.

Glotzer, M., A.W. Murray, M.W. Kirschner. 1991. Cyclin is degraded by the ubiquitin pathway. *Nature.* 349, 132–138.

Gordon, D.J., B. Resio, and D. Pellman. 2012. Causes and consequences of aneuploidy in cancer. *Nat. Rev. Genet.* 13:189–203. doi:10.1038/nrg3123.

Goshima, G., and M. Yanagida. 2000. Establishing biorientation occurs with precocious separation of the sister kinetochores, but not the arms, in the early spindle of budding yeast. *Cell*. 100:619–633.

Grallert, A., E. Boke, A. Hagting, B. Hodgson, Y. Connolly, J.R. Griffiths, D.L. Smith, J. Pines, and I.M. Hagan. 2015. A PP1-PP2A phosphatase relay controls mitotic progression*. Nature.* 517, 94–98.

Gupta, M.L., C.J. Bode, G.I. Georg, and R.H. Himes. 2003. Understanding tubulin Taxol interactions: mutations that impart Taxol binding to yeast tubulin. *Proc Natl Acad Sci USA*. 100:6394–6397. doi:10.1073/pnas.1131967100.

Haase, J., A. Stephens, J. Verdaasdonk, E. Yeh, and K. Bloom. 2012. Bub1 Kinase and Sgo1 Modulate Pericentric Chromatin in Response to Altered Microtubule Dynamics. *Current Biology*. 22:471–481. doi:10.1016/j.cub.2012.02.006.

Hardwick, K.G., R.C. Johnston, D.L. Smith, and A.W. Murray. 2000. MAD3 encodes a novel component of the spindle checkpoint which interacts with Bub3p, Cdc20p, and Mad2p. *J Cell Biol*. 148:871–882.

Hassold, T., and P. Hunt. 2001. To err (meiotically) is human: the genesis of human aneuploidy. *Nat. Rev. Genet.* 2:280–291. doi:10.1038/35066065.

He, X., S. Asthana, and P.K. Sorger. 2000. Transient sister chromatid separation and elastic deformation of chromosomes during mitosis in budding yeast. *Cell*. 101:763–775.

Heinrich, S., E.PM. Geissen, J. Kamenz, S. Trautmann, C. Widmer, P. Drewe, M. Knop, N. Radde, J. Hasenauer, and S. Hauf. 2013. Determinants of robustness in spindle assembly checkpoint signalling. *Nat Cell Biol*. 15:1328–1339. doi:10.1038/ncb2864.

Hewitt, L., A. Tighe, S. Santaguida, A.M. White, C.D. Jones, A. Musacchio, S. Green, S.S. Taylor. 2010. Sustained Mps1 activity is required in mitosis to recruit O-Mad2 to the Mad1-C-Mad2 core complex. *J. Cell Biol.,* 190, 25–34.

Hiruma, Y., C. Sacristan, S.T. Pachis, A. Adamopoulos, T. Kuijt, M. Ubbink, E. von Castelmur, A. Perrakis, and G.J. Kops. 2015. Competition between MPS1 and microtubules at kinetochores regulates spindle checkpoint signaling. *Science* 348, 1264–1267.

Holloway, S.L.; M. Glotzer, R.W. King, A.W. Murray. 1993. Anaphase is initiated by proteolysis rather than by the inactivation of maturation-promoting factor. *Cell.* 73, 1393–1402.

Howell, B.J.; D.B. Hoffman, G. Fang, A.W. Murray, E.D. Salmon. 2000. Visualization of Mad2 dynamics at kinetochores, along spindle fibers, and at spindle poles in living cells. *J. Cell Biol.*150, 1233–1250.

Howell, B.J., B. Moree, E.M. Farrar, S. Stewart, G. Fang, E.D. Salmon. 2004. Spindle checkpoint protein dynamics at kinetochores in living cells. *Curr. Biol.* 14, 953–964.

Hoyt, M.A., L. Totis, and B.T. Roberts. 1991. S. cerevisiae genes required for cell cycle arrest in response to loss of microtubule function. *Cell*. 66:507–517.

Hsu, J.PM., J. Huang, P.B. Meluh, and B.C. Laurent. 2003. The yeast RSC chromatin-remodeling complex is required for kinetochore function in chromosome segregation. *Mol Cell Biol*. 23:3202–3215.

Hwang, L.H. and Murray, A.W. 1997. A novel yeast screen for mitotic arrest mutants identifies DOC1, a new gene involved in cyclin proteolysis. Mol. Biol. Cell 8: 1877–1887.

Hwang, L.H., L.F. Lau, D.L. Smith, C.A. Mistrot, K.G. Hardwick, E.S. Hwang, A. Amon, and A.W. Murray. 1998. Budding yeast Cdc20: a target of the spindle checkpoint. *Science*. 279:1041–1044.

Ikeda, M., and K. Tanaka. 2017. Plk1 bound to Bub1 contributes to spindle assembly checkpoint activity during mitosis. *Scientific Reports*, *7*(1), 8794. http://doi.org/10.1038/s41598-017-09114-3.

Indjeian, V.B., and A.W. Murray. 2007. Budding yeast mitotic chromosomes have an intrinsic bias to biorient on the spindle. *Curr Biol*. 17:1837–1846. doi:10.1016/j.cub.2007.09.056.

Indjeian, V.B., B.M. Stern, and A.W. Murray. 2005. The centromeric protein Sgo1 is required to sense lack of tension on mitotic chromosomes. *Science*. 307:130–133. doi:10.1126/science.1101366.

Izawa, D., and J. Pines. 2014. The mitotic checkpoint complex binds a second CDC20 to inhibit active APC/C. *Nature*. http://doi.org/10.1038/nature13911.

Jacobs, C.W., A.E. Adams, P.J. Szaniszlo, and J.R. Pringle. 1988. Functions of microtubules in the Saccharomyces cerevisiae cell cycle. *J Cell Biol*. 107:1409– 1426.

Jang, Y.J., J.H. Ji, Y.C. Choi, C.J. Ryu, S.Y. Ko. 2007 Regulation of Polo-like kinase 1 by DNA damage in mitosis. Inhibition of mitotic PLK-1 by protein phosphatase 2A. J *Biol. Chem*.

Janke, C., J. Ortiz, T.U. Tanaka, J. Lechner, and E. Schiebel. 2002. Four new subunits of the Dam1-Duo1 complex reveal novel functions in sister kinetochore biorientation. *The EMBO Journal*. 21:181–193. doi:10.1093/emboj/21.1.181.

Ji, Z. J., H. S. Gao, and H.T. Yu. 2015. Kinetochore attachment sensed by competitive Mps1 and microtubule binding to Ndc80C. *Science* 348, 1260–1264.

Jia, L., B. Li, and H. Yu. 2016. The Bub1-Plk1 kinase complex promotes spindle checkpoint signalling through Cdc20 phosphorylation. *Nat Commun*. 7:10818. doi:10.1038/ncomms10818.

Jordan, M.A., R.J. Toso, D. Thrower, and L. Wilson. 1993. Mechanism of mitotic block and inhibition of cell proliferation by Taxol at low concentrations. *Proc Natl Acad Sci USA*. 90:9552–9556.

Kaji, N., A. Muramoto, and K. Mizuno. 2008. LIM kinase-mediated cofilin phosphorylation during mitosis is required for precise spindle positioning. *Journal of Biological Chemistry*, *283*(8), 4983–4992. http://doi.org/10.1074/jbc.M708644200.

Kamenz, J., S. Hauf, S. 2016. Time To Split Up: Dynamics of Chromosome Separation. *Trends in Cell Biology*, *0*(0), 473–485. http://doi.org/10.1016/j.tcb.2016.07.008

Kapoor, T. M., Mayer, T. U., Coughlin, M. L. & Mitchison, T. J. Probing spindle assembly mechanisms with monastrol, a small molecule inhibitor of the mitotic kinesin, Eg5. J. Cell Biol. 150, 975–988 (2000).

Kawashima, S., Y. Yamagishi, T. Honda, K. Ishiguro, and Y. Watanabe. 2010. Phosphorylation of H2A by Bub1 prevents chromosomal instability through localizing shugoshin. *Science. 327*(5962), 172–7. http://doi.org/10.1126/science.1180189.

Kelling, J., K. Sullivan, L. Wilson, and M.A. Jordan. 2003. Suppression of centromere dynamics by Taxol in living osteosarcoma cells. *Cancer Res*. 63:2794–2801.

Khodjakov, A., and J. Pines. 2010. Centromere tension: a divisive issue. *Nat Cell Biol*. 12:919–923. doi:10.1038/ncb1010P919.

Kim T., M.W. Moyle, P. Lara-Gonzalez, C. De Groot, K. Oegema, A. Desai. 2015. Kinetochore-localized BUB-1/BUB-3 complex promotes anaphase onset in C. elegans. *J Cell Biol* 209: 507–517.

Kim, T., P. Lara-Gonzalez, B. Prevo, F. Meitinger, D.K. Cheerambathur, K. Oegema, and A. Desai. 2017. Kinetochores accelerate or delay APC/C activation by directing Cdc20 to opposing fates. *Genes and Development*, *31*(11), 1089–1094. http://doi.org/10.1101/gad.302067.117.

King, E.M.J., N. Rachidi, N. Morrice, K.G. Hardwick, and M.J.R. Stark. 2007. Ipl1pP dependent phosphorylation of Mad3p is required for the spindle checkpoint response to lack of tension at kinetochores. *Genes Dev*. 21:1163–1168. doi:10.1101/gad.431507.

King, J.M., and R.B. Nicklas. 2000. Tension on chromosomes increases the number of kinetochore microtubules but only within limits. *J Cell Sci*. 113 Pt 21:3815–3823.

Kodedová, M. and H. Sychrová. 2015. Changes in the sterol composition of the plasma membrane affect membrane potential, salt tolerance and the activity of multidrug resistance pumps in Saccharomyces cerevisiae. *PLoS ONE*, *10*(9), 1–19. http://doi.org/10.1371/journal.pone.0139306.

Kovalchuk, A. and A.J.M. Driessen. 2010. Phylogenetic analysis of fungal ABC transporters. *BMC Genomics*, *11*(1), 177. http://doi.org/10.1186/1471-2164-11-177.

Krenn, V., and A. Musacchio. 2015. The Aurora B Kinase in Chromosome BiP Orientation and Spindle Checkpoint Signaling. *Front Oncol*. 5:225. doi:10.3389/fonc.2015.00225.

Krishnan, R., F. Pangilinan, C. Lee, and F. Spencer. 2000. Saccharomyces cerevisiae BUB2 prevents mitotic exit in response to both spindle and kinetochore damage. *Genetics*, *156*(2), 489–500.

Kuhn, J. and S. Dumont. 2017. Spindle assembly checkpoint satisfaction occurs via end-on but not lateral attachments under tension. *J Cell Biology.* 5;216(6):1533-1542. doi: 10.1083/jcb.201611104.

Kumar, A., M. Seringhaus, M.C. Biery, R.J. Sarnovsky, L. Umansky, S. Piccirillo, M. Snyder. 2004. Large-Scale Mutagenesis of the Yeast Genome Using a Tn7-Derived Multipurpose Transposon, *Genome Res.*1975–1986. http://doi.org/10.1101/gr.2875304.

Kunda, P., A.E. Pelling, T. Liu, and B. Baum. 2008. Moesin Controls Cortical Rigidity, Cell Rounding, and Spindle Morphogenesis during Mitosis. *Current Biology*, *18*(2), 91–101. http://doi.org/10.1016/j.cub.2007.12.051.

Lampson, M., K. Renduchitala, A. Khodjakov, and T.M. Kapoor. 2004. Correcting improper chromosome-spindle attachments during cell division. *Nature Cell Biology*, *6*(3), 232–7. http://doi.org/10.1038/ncb1102.

Lampson, M.A. and T.M. Kapoor. 2005. Microtubule attachment and spindle assembly checkpoint signaling at the kinetochore. *Nat. Cell Biol.* 7, 93–98.

Lampson, M., and E. Grishchuk. 2017. Mechanisms to Avoid and Correct Erroneous Kinetochore-Microtubule Attachments. *Biology*, *6*(1), 1. http://doi.org/10.3390/biology6010001.

Lara-Gonzalez, P., F.G. Westhorpe, and S.S. Taylor. 2012. The spindle assembly checkpoint. *Curr Biol*. 22:R966–80. doi:10.1016/j.cub.2012.10.006.

Lee, M.S., and F.A. Spencer. 2004. Bipolar orientation of chromosomes in Saccharomyces cerevisiae is monitored by Mad1 and Mad2, but not by Mad3. *Proc Natl Acad Sci USA*. 101:10655–10660. doi:10.1073/pnas.0404102101.

Li, R., and A.W. Murray. 1991. Feedback control of mitosis in budding yeast. *Cell*. 66:519–531.

Li, X., and R.B. Nicklas. 1995. Mitotic forces control a cell-cycle checkpoint. *Nature*. 373:630–632. doi:10.1038/373630a0.

Lim, H.H., P.Y. Goh, and U. Surana. 1998. Cdc20 is essential for the cyclosome-mediated proteolysis of both Pds1 and Clb2 during M phase in budding yeast. *Curr. Biol*. 8:231–234.

Liu, D., G. Vader, M.J. Vromans, M.A. Lampson, S.M. Lens. 2009. Sensing chromosome bi-orientation by spatial separation of Aurora B kinase from kinetochore substrates. *Science.* 323:1350–3. doi:10.1126/science.1167000.

Liu, D., M. Vleugel, C.B. Backer, T. Hori, T. Fukagawa, I.M. Cheeseman, M.A. Lampson. 2010. Regulated targeting of protein phosphatase 1 to the outer kinetochore by KNL1 opposes Aurora B kinase. *J. Cell Biol.* 188, 809–820.

Liu H, L. Jia, H. Yu. 2013. Phospho-H2A and cohesin specify distinct tension-regulated Sgo1 pools at kinetochores and inner centromeres. *Curr Biol.* 23:1927–33. doi:10.1016/j.cub.2013.07.078.

Liu, H., Q. Qu , R. Warrington , A. Rice , N. Cheng, H. Yu. 2015. Mitotic transcription installs Sgo1 at centromeres to coordinate chromosome segregation. *Mol. Cell*. 59:426–36. doi:10.1016/j.molcel.2015.06.018.

London, N., S. Ceto, J.A. Ranish, and S. Biggins. 2012. Phosphoregulation of Spc105 by Mps1 and PP1 regulates Bub1 localization to kinetochores. *Current Biology*, *22*(10), 900–906. http://doi.org/10.1016/j.cub.2012.03.052.

London, N., and S. Biggins. 2014a. Mad1 kinetochore recruitment by Mps1-mediated phosphorylation of Bub1 signals the spindle checkpoint. *Genes Dev*. 28:140–152. doi:10.1101/gad.233700.113.

London, N., and S. Biggins. 2014b. Signalling dynamics in the spindle checkpoint response. *Nat Rev Mol Cell Biol*. 15:736–747. doi:10.1038/nrm3888.

Long, B.H., and C.R. Fairchild. 1994. Paclitaxel inhibits progression of mitotic cells to G1 phase by interference with spindle formation without affecting other microtubule functions during anaphase and telephase. *Cancer Res*. 54:4355–4361.

Louage, B., O. De Wever, W.E. Hennink, and B.G. De Geest. 2017. Developments and future clinical outlook of taxane nanomedicines. *Journal of Controlled Release*, *253*, 137–152.

Luchniak, A., Y. Fukuda, and M.L. Gupta. 2013. Structure-function analysis of yeast tubulin. *Methods Cell Biol*. 115:355–374. doi:10.1016/B978P0P12P407757P7.00022P0.

Magidson, V., J. He, J.G. Ault, C.B. O'Connell, N. Yang, I. Tikhonenko, B.F. McEwen, H. Sui, and A. Khodjakov. 2016. Unattached kinetochores rather than intrakinetochore tension arrest mitosis in Taxol-treated cells. *J Cell Biol*. 212:307– 319. doi:10.1083/jcb.201412139.

Makrantoni, V., and M.J.R. Stark. 2009. Efficient chromosome biorientation and the tension checkpoint in Saccharomyces cerevisiae both require Bir1. *Mol Cell Biol*. 29:4552–4562. doi:10.1128/MCB.01911P08.

Malumbres, M. 2014. Cyclin-dependent kinases. *Genome Biology*, *15*(6), 122. http://doi.org/10.1186/gb4184.

Manic, G., F. Corradi, A. Sistigu, S. Siteni, and I. Vitale. 2017. Molecular Regulation of the Spindle Assembly Checkpoint by Kinases and Phosphatases. *Int Rev Cell Mol Biol*. 328:105–161. doi:10.1016/bs.ircmb.2016.08.004.

Mann, M. 2006. Functional and quantitative proteomics using SILAC. *Nature Reviews. Molecular Cell Biology*, *7*(12), 952–8. http://doi.org/10.1038/nrm2067.

Maresca, T.J., and E.D. Salmon. 2009. Intrakinetochore stretch is associated with changes in kinetochore phosphorylation and spindle assembly checkpoint activity. *J Cell Biol*. 184:373–381. doi:10.1083/jcb.200808130.

Maresca, T.J., and E.D. Salmon. 2010. Welcome to a new kind of tension: translating kinetochore mechanics into a wait-anaphase signal. *J Cell Sci*. 123:825–835. doi:10.1242/jcs.064790.

Martin-Lluesma, S., V.M. Stucke, E.A. Nigg. 2002. Role of Hec1 in spindle checkpoint signaling and kinetochore recruitment of Mad1/Mad2. *Science*. 297: 2267–2270.

McCleland, M.L., R.D. Gardner, M.J. Kallio, J.R. Daum, G.J. Gorbsky, D.J. Burke, P.T. Stukenberg. 2003. The highly conserved Ndc80 complex is required for kinetochore assembly, chromosome congression, and spindle checkpoint activity. *Genes Dev* 17: 101–114.

McEwen, B.F., A.B. Heagle, G.O. Cassels, K.F. Buttle, and C.L. Rieder. 1997. Kinetochore fiber maturation in PtK1 cells and its implications for the mechanisms of chromosome congression and anaphase onset. *J Cell Biol*. 137:1567–1580.

Michaelis, C., R. Ciosk, and K. Nasmyth. 1997. Cohesins: chromosomal proteins that prevent premature separation of sister chromatids. *Cell*. 91:35–45.

Morin, V., Prieto, S., Melines, S., Hem, S., Rossignol, M., Lorca, T. Abrieu, A. 2012. CDK-dependent potentiation of MPS1 kinase activity is essential to the mitotic checkpoint. *Current Biology: CB*, *22*(4), 289–95. http://doi.org/10.1016/j.cub.2011.12.048.

Murray, A.W. 2011. A brief history of error. *Nat Cell Biol*. 13:1178–1182. doi:10.1038/ncb2348.

Nannas, N. J., & A.W. Murray. 2014. Tethering Sister Centromeres to Each Other Suggests the Spindle Checkpoint Detects Stretch within the Kinetochore. *PLoS Genetics*, *10*(8). http://doi.org/10.1371/journal.pgen.1004492

Nerusheva, O.O., S. Galander, J. Fernius, D. Kelly, and A.L. Marston. 2014. Tension dependent removal of pericentromeric shugoshin is an indicator of sister chromosome biorientation. *Genes Dev*. 28:1291–1309. doi:10.1101/gad.240291.114.

Nezi, L. and A. Musacchio. 2009. Sister chromatid tension and the spindle assembly checkpoint. *Curr. Opin. Cell Biol*. 21:785–795. doi:10.1016/j.ceb.2009.09.007.

Nicklas, R.B., C.A. Staehly. Chromosome micromanipulation. I. The mechanics of chromosome attachment to the spindle. 1967. *Chromosoma.* 21:1–16.

Nicklas, R.B. Chromosome micromanipulation. 2. Induced reorientation and the experimental control of segregation in meiosis. *Chromosoma*. 1967, 21, 17–50.

Nicklas, R. B., and C.A. Koch. 1969. Chromosome micromanipulation. 3. Spindle fiber tension and the reorientation of mal-oriented chromosomes. *Journal of Cell Biology*, *43*(1), 40–50. http://doi.org/10.1083/jcb.43.1.40

Nicklas, R.B., and S.C. Ward. 1994. Elements of error correction in mitosis: microtubule capture, release, and tension. *J Cell Biol*. 126:1241–1253.

Nicklas, R.B., J.C. Waters, E.D. Salmon, and S.C. Ward. 2001. Checkpoint signals in grasshopper meiosis are sensitive to microtubule attachment, but tension is still essential. *J Cell Sci*. 114:4173–4183.

Nicklas, R. B. and S.C. Ward. 1994. Elements of error correction in mitosis: Microtubule capture, release, and tension. *Journal of Cell Biology*, *126*(5), 1241–1253. http://doi.org/10.1083/jcb.126.5.1241.

Nicklas, R.B., S.C. Ward, and G.J. Gorbsky. 1995. Kinetochore chemistry is sensitive to tension and may link mitotic forces to a cell cycle checkpoint. *J Cell Biol*. 130:929– 939.

Nilsson, J.; Yekezare, M.; Minshull, J.; Pines, J. The APC/C maintains the spindle assembly checkpoint by targeting Cdc20 for destruction. *Nat. Cell Biol.* 2008, 10, 1411–1420.

O'Connell, C.B., J. Loncarek, P. Hergert, A. Kourtidis, D.S. Conklin, and A. Khodjakov. 2008. The spindle assembly checkpoint is satisfied in the absence of interkinetochore tension during mitosis with unreplicated genomes. *J Cell Biol*. 183:29–36. doi:10.1083/jcb.200801038.

Pagliuca, C., V.M. Draviam, E. Marco, P.K. Sorger, P. De Wulf. 2009. Roles for the conserved Spc105p/Kre28p complex in kinetochore-microtubule binding and the spindle assembly checkpoint. *PLoS ONE*. 4: e7640.

Palframan, W.J., J.B. Meehl, S.L. Jaspersen, M. Winey, A.W. Murray. 2006. Anaphase inactivation of the spindle checkpoint. *Science*. 313, 680–684.

Piatti, S., C. Lengauer, and K. Nasmyth. 1995. Cdc6 is an unstable protein whose de novo synthesis in G1 is important for the onset of S phase and for preventing a "reductional" anaphase in the budding yeast Saccharomyces cerevisiae. *The EMBO Journal*. 14:3788–3799.

Pinsky, B.A., C. Kung, K.M. Shokat, and S. Biggins. 2006. The Ipl1P-Aurora protein kinase activates the spindle checkpoint by creating unattached kinetochores. *Nat Cell Biol*. 8:78–83. doi:10.1038/ncb1341.

Pringle, J.R. The use of conditional lethal cell cycle mutants for temporal and functional sequence mapping of cell cycle events. *J. Cell. Physiol.* 1978, 95, 393–405.

Primorac, I.; J.R. Weir, E. Chiroli, F. Gross, I. Hoffmann, S. van Gerwen, A. Ciliberto, A. Musacchio, A. 2013. Bub3 reads phosphorylated MELT repeats to promote spindle assembly checkpoint signaling. *Elife*. 2.

Qi, W., H. Yu. 2007. KEN-box-dependent degradation of the Bub1 spindle checkpoint kinase by the anaphase-promoting complex/cyclosome. *J. Biol. Chem.* 282, 3672–3679.

Reiter, W., D. Anrather, I. Dohnal, P. Pichler, J. Veis, M. Grøtli, G. Ammerer. 2012. Validation of regulated protein phosphorylation events in yeast by quantitative mass spectrometry analysis of purified proteins. *Proteomics*, *12*(19–20), 3030–43. http://doi.org/10.1002/pmic.201200185.

Richheimer, S.L., T.M. Tinnermeier, and D.W. Timmons. 1992. High-performance liquid chromatographic assay of Taxol. *Anal. Chem.,* 64, 2323,

Rieder, C.L., A. Schultz, R. Cole, and G. Sluder. 1994. Anaphase onset in vertebrate somatic cells is controlled by a checkpoint that monitors sister kinetochore attachment to the spindle. *J Cell Biol*. 127:1301–1310.

Rieder, C.L., R.W. Cole, A. Khodjakov, and G. Sluder. 1995. The checkpoint delaying anaphase in response to chromosome monoorientation is mediated by an inhibitory signal produced by unattached kinetochores. *J Cell Biol*. 130:941–948.

Rose, M.D., F. Winston, and P. Hieter. 1990. *Methods in Yeast Genetics*. Cold Spring Harbor Laboratory Press, Cold Spring Harbor, NY.

Rosenberg, J.S., F.R. Cross, H. Funabiki. 2011. KNL1/Spc105 recruits PP1 to silence the spindle assembly checkpoint. *Curr. Biol.* 21, 942–947.

Rudner, D., K.G. Hardwick, and A.W. Murray. 2000. Cdc28 activates exit from mitosis in budding yeast. *The Journal of Cell Biology*, *149*(7), 1361–76.

Sandquist, j., A. Kita, W. Bement. 2011. And the dead shall rise: Actin and myosin return to the spindle. *Dev Cell*, 21(3), 410-419.

Santaguida, S., A. Tighe, A.M. D'Alise, S.S. Taylor, and A. Musacchio. 2010. Dissecting the role of MPS1 in chromosome biorientation and the spindle checkpoint through the small molecule inhibitor reversine. *The Journal of Cell Biology*, *190*(1), 73–87. http://doi.org/10.1083/jcb.201001036.

Sarangapani, K. K.& Asbury, C. L. (2012). Catch and release: How do kinetochores hook the right microtubules during mitosis. *Trends Genet.*, *37*(1), 62–70. http://doi.org/10.1007/s12020-009-9266-z.

Saurin, A. T., M. S. van der Waal, R.H. Medema, S.M.A. Lens, and G.J.P.L. Kops. 2011. Aurora B potentiates Mps1 activation to ensure rapid checkpoint establishment at the onset of mitosis. *Nature Communications*, *2*(May), 316. http://doi.org/10.1038/ncomms1319.

Schiff, P.B., and S.B. Horwitz. 1980. Taxol stabilizes microtubules in mouse fibroblast cells. *Proc Natl Acad Sci USA*. 77:1561–1565.

Shah, J.V. and D.W. Cleveland. 2000. Waiting for anaphase: Mad2 and the spindle assembly checkpoint. *Cell.* 103, 997–1000.

Shannon, K.B., J.C. Canman, and E.D. Salmon. 2002. Mad2 and BubR1 function in a single checkpoint pathway that responds to a loss of tension. *Mol Biol Cell*. 13:3706–3719. doi:10.1091/mbc.E02P03P0137.

Sharp-Baker, H., and R.H. Chen. 2001. Spindle checkpoint protein Bub1 is required for kinetochore localization of Mad1, Mad2, Bub3, and CENP-E, independently of its kinase activity. *J Cell Biol*. 153:1239–1250.

Shepperd, L., J.C. Meadows, A.M. Sochaj, T.C. Lancaster, J. Zou, G.J. Buttrick, J.B. Millar. 2012. Phosphodependent recruitment of Bub1 and Bub3 to Spc7/KNL1 by Mph1

kinase maintains the spindle checkpoint. *Current Biology: CB*, *22*(10), 891–9. http://doi.org/10.1016/j.cub.2012.03.051.

Shonn, M.A., R. McCarroll, and A.W. Murray. 2000. Requirement of the spindle checkpoint for proper chromosome segregation in budding yeast meiosis. *Science*. 289:300–303.

Siegel, J.J., and A. Amon. 2012. New insights into the troubles of aneuploidy. *Annu Rev Cell Dev Biol*. 28:189–214. doi:10.1146/annurevPcellbioP101011P155807.

Skoufias, D.A., P.R. Andreassen, F.B. Lacroix, L. Wilson, and R.L. Margolis. 2001. Mammalian mad2 and bub1/bubR1 recognize distinct spindle-attachment and kinetochore-tension checkpoints. *Proc Natl Acad Sci USA*. 98:4492–4497. doi:10.1073/pnas.081076898.

Sparreboom, A., C.D. Scripture, V. Trieu, P.J. Williams, T. De, A. Yang, B. Beals, W.D. Figg , Hawkins , M. Desai. 2005. Comparative Preclinical and Clinical Pharmacokinetics of a Cremophor-Free, Nanoparticle Albumin-Bound Paclitaxel (ABI-007) and Paclitaxel Formulated in Cremophor (Taxol)., *Clin. Cancer Res.* 11, 4136–4143.

Spencer, F., P. Hieter. 1992. Centromere DNA mutations induce a mitotic delay in Saccharomyces cerevisiae. *Proc. Natl. Acad. Sci. USA*. 89, 8908–8912.

Stern, B.M., and A.W. Murray. 2001. Lack of tension at kinetochores activates the spindle checkpoint in budding yeast. *Curr Biol*. 11:1462–1467.

Storchová, Z., J.S. Becker, N. Talarek, S. Kögelsberger, and D. Pellman. 2011. Bub1, Sgo1, and Mps1 mediate a distinct pathway for chromosome biorientation in budding yeast. *Molecular Biology of the Cell*, *22*(9), 1473–85. http://doi.org/10.1091/mbc.E10-08-0673.

Straight, A.F., W.F. Marshall, J.W. Sedat, and A.W. Murray. 1997. Mitosis in living budding yeast: anaphase A but no metaphase plate. *Science*. 277:574–578.

Sudakin, V., D. Ganoth, A. Dahan, H. Heller, J. Hershko, F.C. Luca, J.V. Ruderman, A. Hershko. 1995. The cyclosome, a large complex containing cyclin-selective ubiquitin ligase activity, targets cyclins for destruction at the end of mitosis. *Mol. Biol. Cell.* 6, 185–197.

Suzuki, Y., R.P. St Onge, R. Mani, O.D. King, A. Heilbut, V.M. Labunskyy, F.P. Roth. 2011. Knocking out multigene redundancies via cycles of sexual assortment and fluorescence selection. *Nature Methods*, *8*(2), 159–64. http://doi.org/10.1038/nmeth.1550.

Tanaka, T., J. Fuchs, J. Loidl, and K. Nasmyth. 2000. Cohesin ensures bipolar attachment of microtubules to sister centromeres and resists their precocious separation. *Nat Cell Biol*. 2:492–499. doi:10.1038/35019529.

Tanaka, T.U., N. Rachidi, C. Janke, G. Pereira, M. Galova, E. Schiebel, M.J.R. Stark, and K. Nasmyth. 2002. Evidence that the Ipl1-Sli15 (Aurora kinase-INCENP) complex promotes chromosome bi-orientation by altering kinetochore-spindle pole connections. *Cell*. 108:317–329.

Tang Z., H. Shu, W. Qi, N.A. Mahmood, M.C. Mumby, H. Yu. 2006. PP2A is required for centromeric localization of Sgo1 and proper chromosome segregation. *Dev Cell* 2006; 10:575-85.

Tauchman, E.C., F.J. Boehm, and J.G. DeLuca. 2015. Stable kinetochore-microtubule attachment is sufficient to silence the spindle assembly checkpoint in human cells. *Nat Commun*. 6:10036. doi:10.1038/ncomms10036.

Théry, M., and M. Bornens. 2008. Get round and stiff for mitosis. *HFSP Journal*, *2*(2), 65–71. http://doi.org/10.2976/1.2895661.

Tipton, A.R., W. Ji, B. Sturt-Gillespie, M.E. Bekier, K. Wang, W.R. Taylor, S.T. Liu, 2013. Monopolar spindle 1 (MPS1) kinase promotes production of closed MAD2 (C-MAD2) conformer and assembly of the mitotic checkpoint complex. *J. Biol. Chem.* 288, 35149–35158.

Uchida, K.S.K., K. Takagaki, K. Kumada, Y. Hirayama, T. Noda, and T. Hirota. 2009. Kinetochore stretching inactivates the spindle assembly checkpoint. *J Cell Biol*. 184:383–390. doi:10.1083/jcb.200811028.

Uhlmann, F., D. Wernic, M.A. Poupart, E.V. Koonin, and K. Nasmyth. 2000. Cleavage of cohesin by the CD clan protease separin triggers anaphase in yeast. *Cell*. 103:375–386.

Wan, X., R.P. O'Quinn, H.L. Pierce, A.P. Joglekar, W.E. Gall, J.G. DeLuca, C.W. Carroll, S.PT. Liu, T.J. Yen, B.F. McEwen, P.T. Stukenberg, A. Desai, and E.D. Salmon. 2009. Protein architecture of the human kinetochore microtubule attachment site. *Cell*. 137:672–684. doi:10.1016/j.cell.2009.03.035.

Wang, F., J. Dai, J.R. Daum, E. Niedzialkowska, B. Banerjee, P.T. Stukenberg, G.J. Gorbsky, J.M. Higgins. 2010. Histone H3 Thr-3 phosphorylation by Haspin positions Aurora B at centromeres in mitosis. Science (2010) 330:231–5. doi:10.1126/ science.1189435.

Waters, J.C., R.V. Skibbens, and E.D. Salmon . 1996. Oscillating mitotic newt lung cell kinetochores are, on average, under tension and rarely push. J. Cell Sci. 109: 2823 – 2831.

Waters, J.C., R.H. Chen, A.W. Murray, and E.D. Salmon. 1998. Localization of Mad2 to kinetochores depends on microtubule attachment, not tension. *J Cell Biol*. 141:1181–1191.

Weinert, T.A., L.H. Hartwell. 1988. The RAD9 gene controls the cell cycle response to DNA damage in Saccharomyces cerevisiae. *Science.* 241, 317–322.

Winefield, R.D., R.A. Entwistle, T.B. Foland, G.H. Lushington, and R.H. Himes. 2008. Differences in paclitaxel and docetaxel interactions with tubulin detected by mutagenesis of yeast tubulin. *ChemMedChem*. 3:1844–1847. doi:10.1002/cmdc.200800288.

Winey, M., C.L. Mamay, E.T. O'Toole, D.N. Mastronarde, T.H. Giddings, K.L. McDonald, and J.R. McIntosh. 1995. Three-dimensional ultrastructural analysis of the Saccharomyces cerevisiae mitotic spindle. *J Cell Biol.* 129:1601–1615.

Wloka, C., and E. Bi. 2012. Mechanisms of cytokinesis in budding yeast. *Cytoskeleton*, 69(10), 710–726. http://doi.org/10.1002/cm.21046.

Xu, Q., L.A. Trissel, J.F. Martinez. 1994. Stability of paclitaxel in 5% dextrose injection or 0.9% sodium chloride injection at 4, 22, or 32 degrees C. Am. *J. Hosp. Pharm.,* 51, 3058.

Yamagishi, Y., C. Yang, Y. Tanno, and Y. Watanabe. 2012. MPS1/Mph1 phosphorylates the kinetochore protein KNL1/Spc7 to recruit SAC components. *Nature Cell Biology*, 14(7), 746–752. http://doi.org/10.1038/ncb2515.

Yang, Z., A.E. Kenny, D. Brito, and C.L. Rieder. 2009. Cells satisfy the mitotic checkpoint in Taxol, and do so faster in concentrations that stabilize syntelic attachments. *Journal of Cell Biology,* 186(5), 675–684. http://doi.org/10.1083/jcb.200906150.

Yang, Y., D. Tsuchiya, S. Lacefield. 2015. Bub3 promotes Cdc20-dependent activation of the APC/C in S. cerevisiae*. J Cell Biol.* 209: 519–527.

Zasadil, L.M., K.A. Andersen, D. Yeum, G.B. Rocque, L.G. Wilke, A.J. Tevaarwerk, R.T. Raines, M.E. Burkard, and B.A. Weaver. 2014. Cytotoxicity of paclitaxel in breast cancer is due to chromosome missegregation on multipolar spindles. Sci Transl Med. 6:229ra43–229ra43. doi:10.1126/scitranslmed.3007965.

Zirkle, R.E. 1970. Ultraviolet-microbeam irradiation of newt-cell cytoplasm: Spindle destruction, false anaphase, and delay of true anaphase. *Radiat. Res.* 41, 516–537.

# Appendix 1:

# Technical developments in working with drug sensitive yeast

## A1.1 Abstract

Drug sensitive cells, deficient for ABC transporter proteins or lacking proteins required for lipid metabolism, are popular tools for scientific research. Drug sensitive yeast lack the ability to prevent toxins from entering the cell or facilitate toxin removal, enabling studies that use drugs that yeast are not naturally sensitive to, such as Taxol. Nonetheless, drug sensitive yeast can have unique experimental requirements. The original work reported in Foland et al., 2005 demonstrated microtubule stabilization in live yeast cells, strain AD1-8-tax; however, numerous mutations in this strain left little opportunity for further genetic manipulation. Determining a simpler combination of mutations necessary to render yeast Taxol sensitive enabled us, for the first time, to leverage Taxol-mediated microtubule stabilization for cell biological assays in live yeast cells. Here we determined optimal conditions, both to manage Taxol sensitive yeast's increased sensitivity to environmental perturbations, and to work with Taxol in aqueous yeast media. Experiments reported here may inform future work with drug sensitive yeast, including the unanticipated technical requirements and potential pitfalls of working with drug sensitive strains.

## A1.2 Introduction

The cell employs both passive and active strategies to regulate drug transport across the cell membrane. ATP binding cassette proteins and their regulators make up the superfamily of ABC proteins, and the function of many of these proteins is to actively export compounds out of the cell (Kovalchuk and Driessen, 2010). On the other hand, changes in lipid biosynthesis and composition of the plasma membrane affect membrane permeability and the degree of passive diffusion of small molecules across the plasma membrane (Kodedová and Sychrová, 2015; Emter et al., 2002). Moreover, changes in lipid composition of the plasma membrane can indirectly affect the function of ACB proteins (Kodedová and Sychrová, 2015).

Sterol composition in the yeast plasma membrane dictates important qualities, such as membrane fluidity, vesicle formation, protein sorting, cytoskeleton organization, endocytosis, and mating (Kodedová and Sychrová, 2015). Yeast produce their primary sterol, ergosterol, via a series of 20 distinct reactions. The enzymes responsible for the first 14 steps of ergosterol production are essential, whereas deletion of enzymes that regulate the last 6 steps, in particular Erg6, produce viable mutants with membranes of altered lipid composition (Kodedová and Sychrová, 2015). Mutations in *ERG* genes alter the plasma membrane's permeability and fluidity, rendering cells drug sensitive (Kodedová and Sychrová, 2015; Emter et al., 2002). Importantly, Erg6 mutants also display reduced Pdr5 activity (Kodedová and Sychrová, 2015) which renders these cells less capable of exporting small molecules actively via the Pdr5 ABC transporter pump.

ABC proteins form a massive family of proteins, with members present in bacteria, archaea, and eukaryotes (Kovalchuk and Driessen, 2010). Abnormal expression of many of these proteins leads to both pathogenic and non-pathogenic drug resistance, while their deletion renders organisms supersensitive to drugs. Additionally, mutation of these genes has been linked to several human diseases such as cystic fibrosis, adrenoleukodystrophy, and disorders of cholesterol metabolism (Kovalchuk and Driessen, 2010). Thus, the controlled study of these proteins holds potential for a wide range of practical applications to counter human disease.

Additionally, controlled mutagenesis of ABC transporter proteins in yeast, and to a lesser extent proteins involved in ergosterol biosynthesis, has proven a powerful research tool; labs across the world use drug sensitive, ABC transporter-deficient, yeast to search for new antibiotics and pesticides, develop treatments for drug resistant pathogens and cancers, and study general cell dynamics and function (Kovalchuk and Driessen, 2010). To sensitize yeast, any combination of up to 16 ABC transporter genes (Suzuki et al., 2011) are deleted, which prevents cells from exporting toxins from their cytoplasm. Although these studies have important implications for human health, they may be hindered by the fact that rendering budding yeast drug-sensitive can also render it sensitive to a range of environmental perturbations that do not noticeably affect wild type yeast. For example, in our experiments, drug sensitive yeast became sensitive to particular growth media, ingredients of standard experimental protocols, and physiological aggravations. Because drug sensitive yeast carrying mutations in the ergosterol biosynthesis pathways or ABC transporter deletions have become a relatively popular model organism, it will be necessary to compile protocols made specifically for

these classes of mutants, record known effects that drug-sensitization has on yeast, and perform careful controls with wild type yeast at every step of experimentation to account for unpredicted sensitivities which might arise in drug-sensitized strains. Documenting this information will help ensure that experimental results gained using drug sensitive yeast are relevant and have not been produced by avoidable confounding factors.

In previous studies, (Figure 8A) mutations in beta-tubulin rendered yeast tubulin sensitive to Taxol (Gupta et al., 2003), and when this mutated beta-tubulin was expressed in ABC transporter deficient yeast, (Figure 8B and C) Taxol became toxic to the cells and caused a mitotic delay (Foland et al., 2005). However, this original Taxol sensitive strain expressed a different, and more extensive, set of ABC-related mutations than our newer strain; *(Δyor1, Δsnq2, Δpdr5, Δpdr10, Δpdr11, Δycf1, Δpdr3, Δpdr15* in the old strain versus *Δpdr1, Δpdr3, and Δerg6* in the new strain*)* and contained 5 amino acid substitutions in yeast beta tubulin (A19K, T23V, G26D, N227H, Y270F) (Gupta et al., 2003), in contrast to four substitutions (A19K, T23V, G26D, Y270F) in our current strain that still retains robust Taxol sensitivity. Fewer ABC-related mutations in the new strain left more genetic markers available to use for introducing additional genetic alterations; however, we could not predict the behavior of our new strain under certain environmental conditions based on the behavior wild type yeast or the previous drug-sensitized strain. Despite having fewer ABC transporter mutations, the deletion of the ergosterol biosynthesis enzyme, Erg6, in our new strain ultimately appeared to render it more sensitive to environmental perturbations and required us to revise a number of our basic protocols in order to maintain optimal growing conditions during experiments. As

we encountered these sensitivities, we developed a number of new protocols and specifications which may serve those working with drug sensitive yeast better than standard protocols. In turn, some phenotypes we encountered in our ABC transport-deficient background may hint at unexpected interplay between broader areas of cell physiology. Although some results are observational or preliminary in nature, I record them here as a potential benefit to future researchers.

## A1.3 Results

### *A1.3.1 Media conditions which alter Taxol potency*

Taxol and other related Taxanes have proven invaluable both as chemotherapy drugs and as tools to further basic research. Taxol is a hydrophobic molecule, and exploration of methods to improve solubilization in aqueous solutions and therapeutic half-life are ongoing (Louage et al., 2017; Sparreboom et al., 2005). Taxol is typically administered in solutions favorable to the growth of animal cells (which are naturally sensitive to the drug) and, particularly in chemotherapy, is diluted into an aqueous solution immediately prior to intravenous infusion, with a half-life on the order of up to ~3 days (Richheimer et al., 1992; Xu et al., 1994). Thus, knowledge is limited for how Taxol behaves in aqueous solutions over longer periods of time, particularly in yeast media.

In this study, experiments treating drug sensitive yeast with Taxol were conducted both on solid agar and in liquid media, and each media type required strict

protocols to maintain the consistency of Taxol's effectiveness. Taxol is effective at inhibiting growth on agar plates. However, it does not inhibit growth in conventional liquid media. A major obstacle overcome just prior to, and in the early stages of the research reported in this thesis was the discovery that liquid media supplemented with 0.02% methylcellulose was effective for Taxol to inhibit growth of the sensitized yeast. Further, methylcellulose stocks may only be kept ~2 weeks above -20˚C before their ability to promote Taxol's toxicity rapidly declines.

Based on our own estimations of Taxol's solubility in aqueous media, and because Taxol does not completely block mitosis in our yeast, we typically used the maximum possible dose in liquid media, 30 μM Taxol. We considered the possibility that we had underestimated the maximum solubility and that a higher dose of Taxol may be more effect in our experiments; or, in contrast, that we had overestimated the limit of solubility, and that the excess Taxol was causing Taxol precipitation in solution and lowering the effective dose. To address these possibilities, we performed the Cdc20 arrest and release assay in media containing 0, 30, or 100 μM Taxol (Figure 25). Cells delayed in metaphase approximately the same amount of time in 30 and 100 μM Taxol, indicating that 1) 30μM is likely a good estimation for the limit of solubility of Taxol in YPD because adding more Taxol does not enhance the delay, and thus, does not appear to make more Taxol available in the media, and 2) precipitation of Taxol in excess of the solubility limit does not appear to promote precipitation of that below the limit, and maintains the maximum effective concentration. Therefore, the 30μM Taxol added in experiments likely reflects the highest effective concentration available to cells.

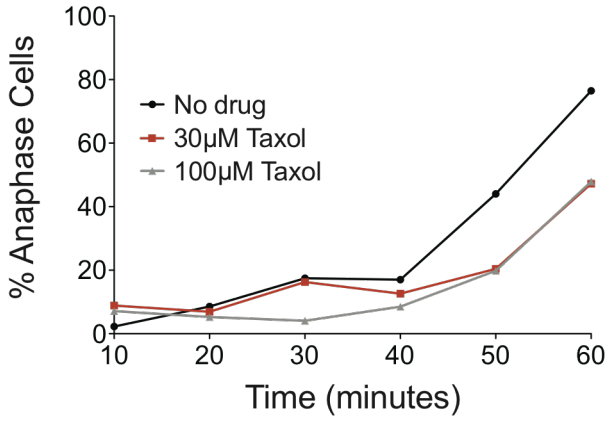


**Figure 25. 30 μM Taxol causes the maximal possible delay in anaphase onset without signs of Taxol precipitation.** The Cdc20 release assay was performed as in 14A. This graph represents a single experiment measuring the timing of anaphase onset in Taxol sensitive control cells released into 0μM, 30μM, and 100μM Taxol. 100-200 cells scored per time point per drug condition.

In contrast to liquid media, Taxol is toxic to yeast when mixed into hot YPD-agar just before pouring solid plates without the need of solubilizing agents like methylcellulose. Additionally, and potentially due to increased solubility, Taxol is more potent in YPD plates than in liquid media. Specifically, significant Taxol growth inhibition can be achieved on plates using ~1/4$^{th}$ the concentration of Taxol needed for liquid media, with massive growth inhibition by 8μM Taxol on plates vs. 30μM Taxol in liquid media. In contrast, while Taxol is effective in liquid SC or YPD media as long as the media is supplemented with methylcellulose, Taxol is utterly impotent on SC plates regardless of the presence of various additives known to increase the solubility of Taxol or other compounds, such as methylcellulose, cyclodextrin, and sodium succinate (data not shown). It is likely that the abundance of peptides in YPD, but not SC media, help to solubilize Taxol on YPD plates.

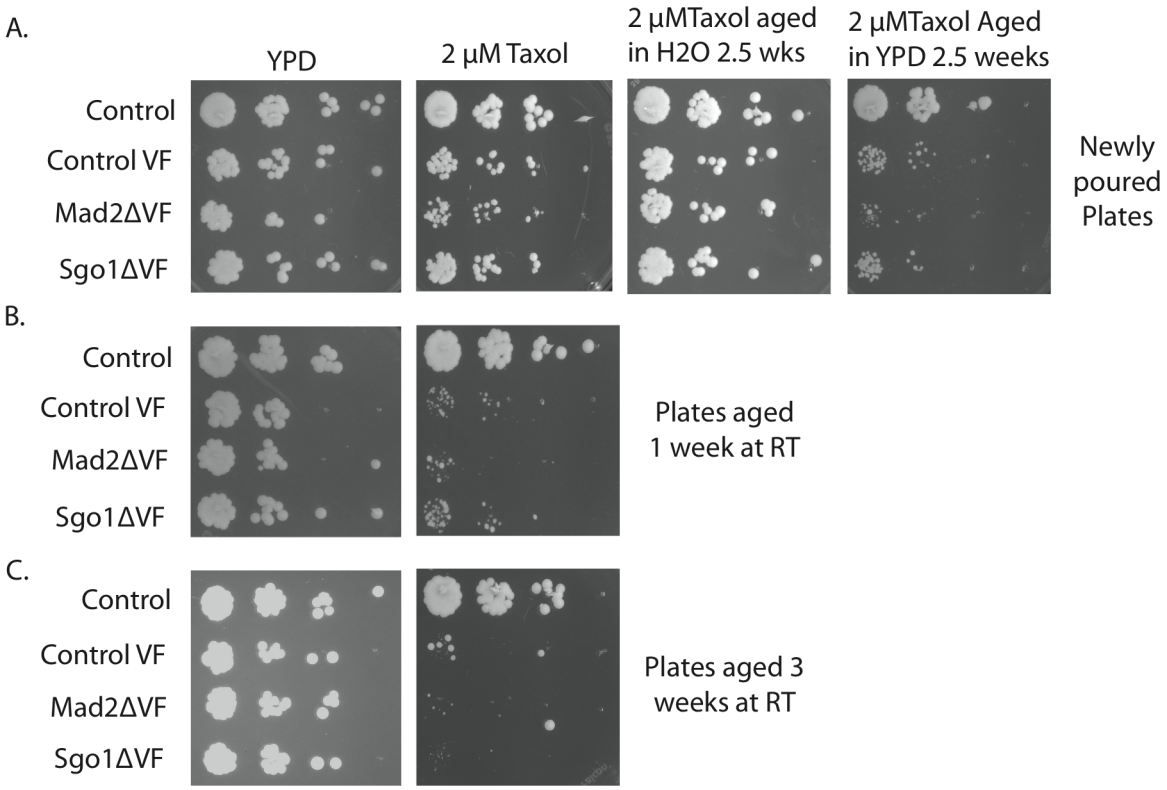


**Figure 26. Taxol's potency increases over time in YPD media.** Serial dilutions and equal volumes of respective strains (Taxol sensitive control and Taxol sensitive strains harboring the Cdc28 VF allele) were spotted on three sets of YPD plates containing either 0µM and 2µM Taxol and grown for two days at 30˚C. (A) Newly poured plates: the first set of plates had been made according to standard protocol 24 hours prior to the experiment; one contained no Taxol, the second contained Taxol from a fresh, frozen stock in DMSO, the third contained Taxol that had incubated at room temperature in water for 2.5 weeks, and the fourth Taxol that had been incubated in liquid 2XYPD at room temperature for 2.5 weeks. (B) A second and (C) third set of plates had been made alongside the first set, and at the time of pouring were made with DMSO ± 2 µM Taxol from a fresh, frozen stock. These plates aged at room temperature 1 week (B) and 3 weeks (C) respectively before the growth assay was performed.

Remarkably, we noticed that Taxol's potency increases over time in YPD plates and may increase over time in YPD in general. To demonstrate this, we grew serial dilutions of several strains of WT, drug sensitive and Taxol sensitive yeast on three sets of YPD and 2µM Taxol plates (Figure 26). The first set of plates were prepared 24 hours

prior to the experiment; one contained no Taxol, the second contained Taxol from a fresh, frozen stock in DMSO, the third contained Taxol that had been aged at room temperature in water for 2.5 weeks, and the fourth Taxol that had been aged in liquid 2xYPD for 2.5 weeks (Figure 26A). A second and third set of plates were prepared alongside the first set, and at the time of pouring were made with DMSO+/- 2 μM Taxol from a fresh, frozen stock. These plates were aged at room temperature 1 week and 3 weeks, respectively, before the growth assay was performed (Figures 26B and C). Importantly, aside from the variations noted here, all plates were otherwise made according to the same protocol, and when growth assays were performed, all yeast were grown to the same optical density before being serially diluted 1:10, and all plates were all incubated at 30˚C for two days.

Surprisingly, in the aged plates, 2 μM Taxol became increasingly potent the longer it was incubated in the plate (Figure 26, left two columns). This increased toxicity was related specifically to YPD, because in newly poured plates containing Taxol that had been aged in water for 2.5 weeks were less toxic to cells, whereas Taxol aged 2.5 weeks in liquid 2X YPD were more toxic to cells, even compared to the plate containing 2 μM Taxol fresh from the frozen DMSO stock (Figure 26A). It is intriguing that Taxol becomes more potent over time in the presence of YPD media. Taxol is a hydrophobic molecule (Richheimer et al., 1992); therefore, in aqueous YPD, we would predict its activity to also decrease over time. In reality, when we perform growth assays on identical plates, Taxol becomes increasingly potent over the course of 2.5 weeks. We hypothesize that the contents of YPD may create an environment in which Taxol degrades into a more potent compound, and if true, the discovery of a more potent, or

more soluble, microtubule stabilizing agent could be highly relevant in the realm of chemotherapy. Alternatively, it's possible that prolonged incubation in YPD increases the fraction of solubilized Taxol. Notably, it remains to be determined whether the increased potency will translate to mammalian cells, or if it acts on microtubules in the same manner that freshly diluted Taxol does.

Several preliminary experiments may determine whether or not characterizing this compound is a worthwhile endeavor. First, the initial experiment must be repeated with several slight variations: Taxol aged different lengths of time in liquid and solid YPD could be incorporated into YPD plates made with peptone that has been sterile filtered rather than autoclaved (to be sure the peptone is treated exactly the same in each experiment). On these plates growth of WT, drug sensitive, and Taxol sensitive yeast would reveal whether or not the compound in aged Taxol acts on WT yeast tubulin in addition to tubulin harboring the Taxol mutations, and whether or not the compound is more effective on strains that are ABC transporter deficient.

If Taxol does appear to increase in potency in yeast assays, it will be important to determine if the same holds true for human cells too. Comparing growth inhibition/apoptosis in HeLa cells by new and old Taxol would reveal whether or not aged Taxol is also a more potent growth inhibitor of human cells. Finally, if aging Taxol does cause it to degrade into a more potent chemical derivative, it would be important to determine the molecular structure of this new derivative, and mass spectrometry will be one strategy.

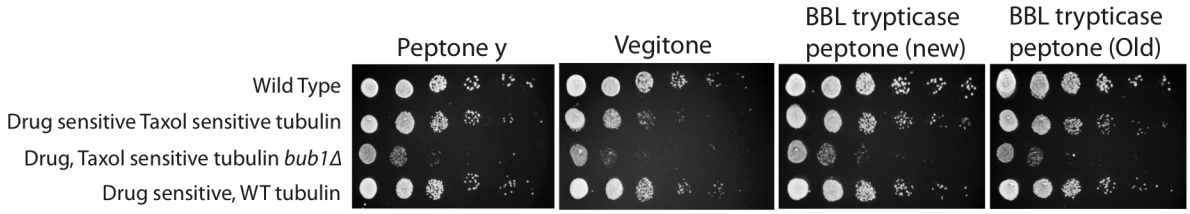


**Figure 27. Drug sensitive yeast growth varies on different brands of peptone.** YPD plates were prepared using identical ingredients according to standard protocol, but each contained a different brand of peptone. Two containers of BBL trypticase peptone, one bought immediately prior to this experiment (New) and the second bought several years prior (Old) were tested. Serial dilutions and equal volumes of respective strains were spotted on these plates and grown for two days at 30˚C.

### *A1.3.2 Media Specifications*

When growing drug sensitive yeast on our lab's standard media, we noticed growth inconsistencies on agar plates made according to the same protocol with seemingly identical ingredients; when this effect was most severe, growth of drug sensitive yeast was totally inhibited on basic YPD plates. We hypothesized that an ingredient of the media contained variable contaminants that do not affect wild type yeast with its full complement of ABC transporters, but poisoned drug sensitive yeast. Thus, we tested each different component of yeast media in an attempt to determine which ingredient was the source of the toxicity.

The components of yeast media that we considered as possible sources of the growth inconsistency were as follows: peptone (YPD), SC powder (SC media), yeast nitrogen base, dextrose, and water. We further considered the manner by which our containers were cleaned, brand of plastic petri dish (solid media), cleanliness of glass culture tubes (liquid media), pH, conductivity, concentration of agar, and variations in time of autoclaving and volume of media. We concluded that the following were not the

source of variation in yeast growth: pH (range 4.4 – 7.0), conductivity, concentration of agar, yeast nitrogen base brand, dextrose brand, and brand of petri dish. To account for potential variability in water quality, we used double glass-distilled water unless otherwise noted in all of our solutions. To be certain that no contaminants were present on any of our bottles, beakers, or culture tubes, we cleaned them by filling them with double glass-distilled water, autoclaving to remove any potential residue, and then emptying the water and autoclaving again to dry.

After ruling out the possibilities listed above, we concluded that yeast peptone was the source of the observed growth inconsistencies. We initially tested alternative sources of peptone to the lab's standard peptone (BD-brand Bacto™Peptone); we made plates each containing one of 4 different brands of peptone according to an identical protocol. We spotted serial dilutions of wild type and drug sensitive yeast on these agar plates and grew them for two days at 30˚C and room temperature to determine if the chemical makeup of peptone was the source of the variable growth (Figure 27). Although drug sensitive yeast grew slightly slower on Vegitone™, there were no major differences in growth on other varieties of peptone. On the other hand, when comparing similar serial dilutions of yeast grown on our lab's standard BD-brand Bacto™peptone or Peptone Y plates ± Taxol, Taxol appeared less effective on Peptone Y than on BD-brand Bacto™Peptone (data not shown). Thus, BD-brand Bacto™peptone remained our preferred brand and we continued to use it as our peptone source for all subsequent experiments.

To complicate matters further, however, we observed that drug sensitive yeast growth and Taxol's effectiveness also varied based on different lot numbers of BD-

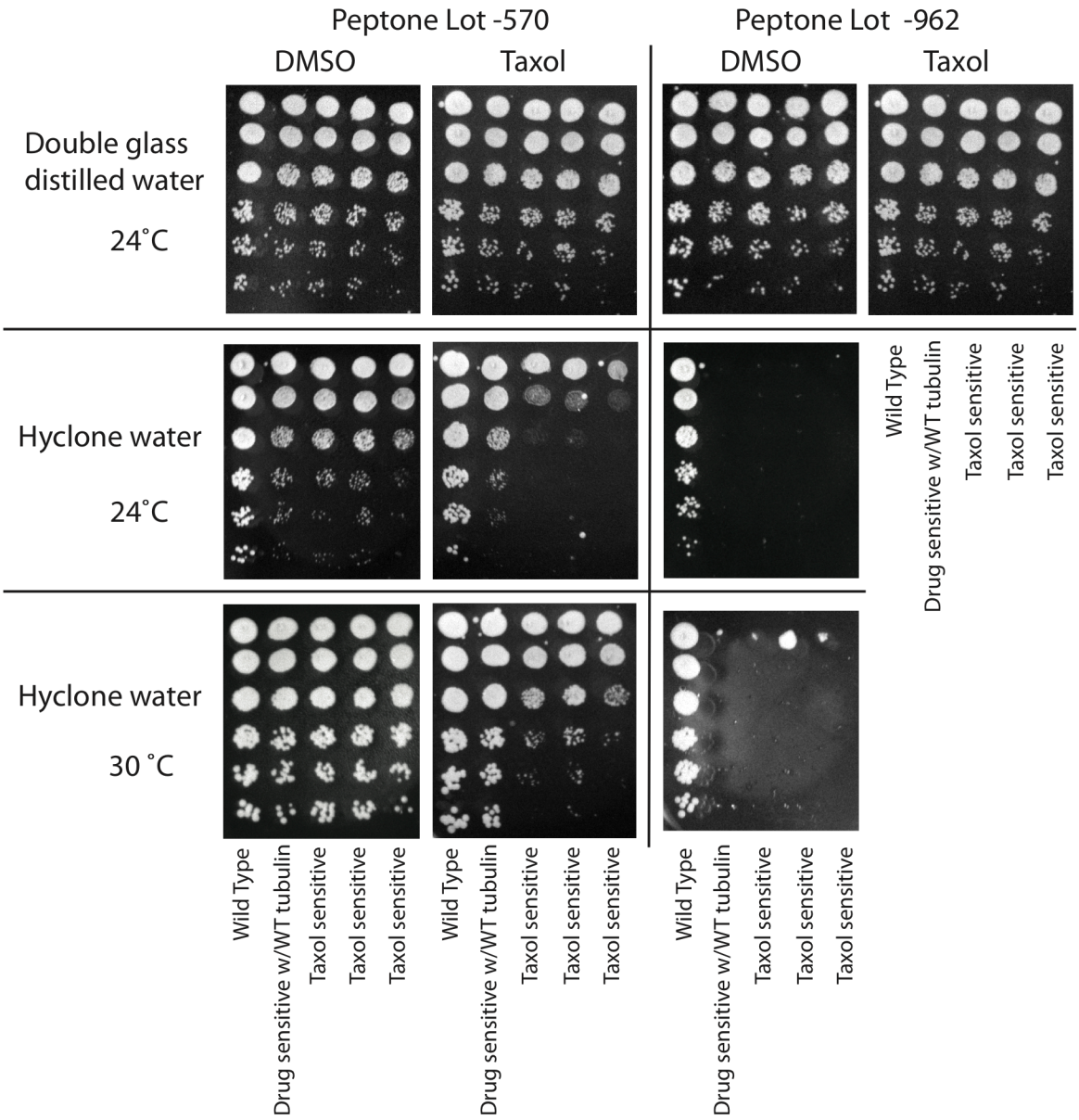


**Figure 28. Incubation temperature, water source, and Peptone source have conflicting effects on drug sensitive yeast's growth and Taxol's toxicity.** An array of YPD plates were prepared according to standard protocol with varying ultrapure water sources (either Hyclone water (GE Life Sciences) or double glass distilled water) and varying Bacto™Peptone lots (Either lot -570 or lot -962). The same 5 strains of yeast were serially diluted and spotted on each plate in the same order; from left to right wild type, drug sensitive with WT yeast peptone, and three independent strains of Taxol sensitive yeast (drug sensitive with Taxol sensitive yeast tubulin). Plates were incubated for two days as indicated, either at 24˚C or at 30˚C.

brand Bacto™peptone, the source of highly-pure water used to mix the plates, and the temperature that the plates were incubated at (Figure 28). While plates made with peptone lot -570 could support growth under all conditions (Figure 28, left two columns), drug sensitive yeast could not grow at all on plates made with peptone lot -962 mixed with highly pure, Hyclone water (Figure 28, right two columns). We hypothesize that trace impurities in different water sources solubilize the peptone to different extents, and that different peptone lots may be more readily solubilized. Broadly speaking, the growth of drug sensitive yeast appears to be more drastically inhibited under conditions where peptone is not maximally solubilized, whereas wild type yeast grows robustly in general and seems minimally affected by these variations. On the other hand, (Figure 28, left two columns) although drug sensitive yeast grow most robustly on plates made with peptone lot -507 and double glass-distilled water, Taxol's toxicity was not apparent on these plates. Further, Taxol's toxicity was more apparent when plates were incubated at room temperature, where the drug sensitive yeast's growth is generally less robust on all control plates. Thus, control conditions must be carefully assessed for growth when working with drug sensitive yeast.

All subsequent experiments were conducted at room temperature with careful attention to peptone lot number; however, we subsequently discovered that the length of time our media was autoclaved had the greatest effect on the functionality of our Taxol-containing plates. All further experiments were then conducted using double glass distilled water, and for liquid media, media that had been autoclaved 20 minutes (as cells appeared to produce a more robust mitotic arrest in this media (Figure 29)). For

spotting assays on agar plates, filter sterilized 2xYPD was mixed with autoclaved 2x agar before cooling.

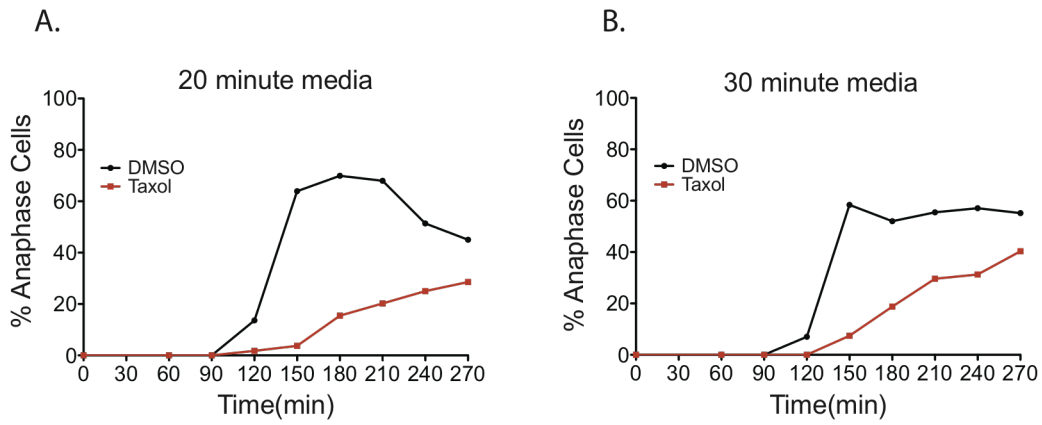


**Figure 29. Autoclaving duration moderately affects Taxol potency.** Timing of anaphase onset in Taxol sensitive cells monitored by the G1 release assay (± 30μM Taxol). During a single experiment, cells underwent the G1 release assay as described in Figure 9B growing in media mixture that had been made according to standard protocol, but had been autoclaved either (A) 20 minutes (20-minute media) or (B) 30 minutes (30-minute media). 100-200 cells scored per time point per drug treatment per media type. Control cells delay in anaphase onset for approximately one hour during Taxol treatment, which produces both unattached and low tension kinetochores, however the delay is more robust in when the experiment is conducted in 20-minute media.

### *A1.3.3 Transformation specifications*

Deletion of Erg6 rendered our drug sensitive yeast highly sensitive to certain mechanical and chemical perturbations and forced us to change several standard protocols, including the methods we used to manipulate genes for our experiments. We used two standard methods to transform our drug sensitive yeast: a standard lithium acetate protocol and electroporation. While drug sensitive yeast could be transformed

by either method, lithium acetate transformation was only possible when cells carried a plasmid harboring an extra copy of the ERG6 gene with a selectable *URA3* marker, which could then be removed by growing positive transformants in the presence of 5-FOA. However, at times when both methods were problematic, we most commonly transformed the desired genetic alteration into a wild type strain, which we then crossed with a Taxol sensitive strain to recover the desired mutant spores.

### *A1.3.4 Taxol sensitivity may be reduced when drug sensitive yeast experience cortical strain*

Several of our assays contain steps during which the cell population must arrest or progress synchronously to a particular stage of the cell cycle. During these periods cells must remain in suspension; however, we learned that drug sensitive cells' ability to delay in metaphase in response to spindle damage is inhibited when cultures are incubated on a rotator during experiments (Figures 30B and C), whereas when they were incubated with minimal, periodic resuspension by hand, cells delayed robustly (Figures 30A and C).

Although it is unclear why the timing of anaphase onset responds to mechanical rotation in our yeast system, and we do not have enough data to suggest a mechanism, this phenomenon potentially indicates a link between cortical strain and mitotic progression in budding yeast. Related to the phenomenon we observe in budding yeast, when animal cells enter mitosis their cortex becomes more ridged, a process

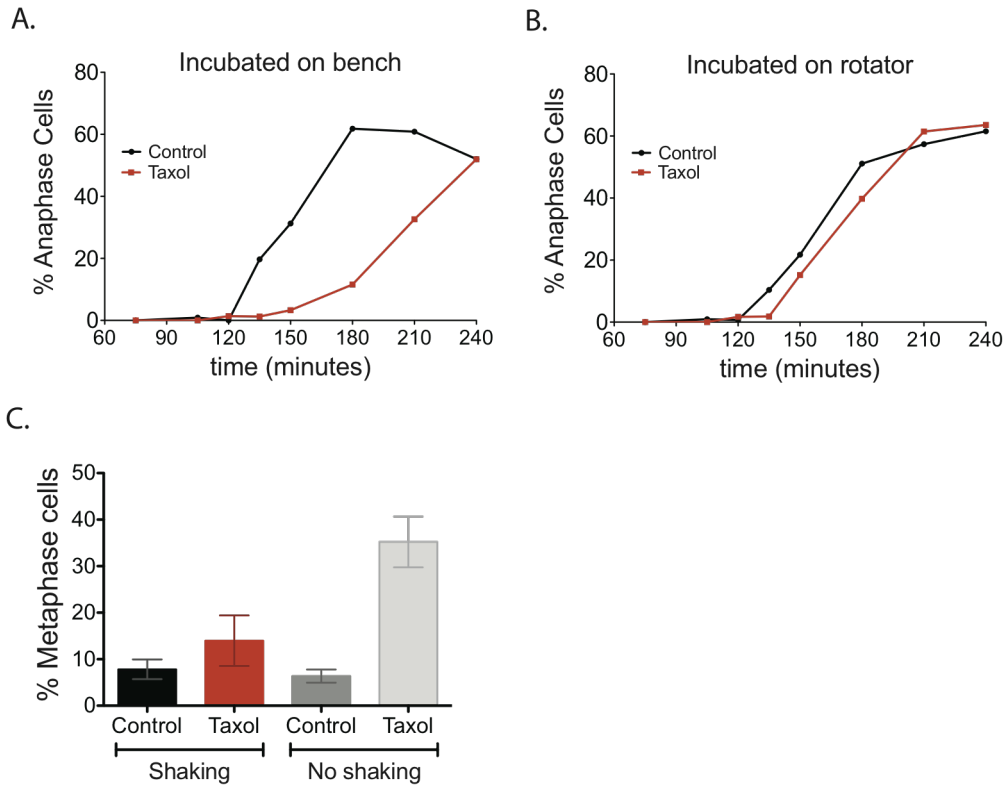


**Figure 30. Rotating cells do not delay anaphase onset in response to Taxol treatment, whereas cells experiencing little agitation readily exhibit a Taxol-mediated delay**. Timing of anaphase onset in Taxol sensitive cells monitored by the G1 release assay (± 30μM Taxol) as described in Figure 9B. (A and B) A single culture was grown up overnight, arrested in G1 (alpha-factor), and divided in two. These two cultures were released from the arrest in the presence and absence of Taxol and to maintain cellular suspension during were either (A) incubated at room temperature with only gentle pipetting every ~15 minutes, or (B) incubated on a mechanical rotator at room temperature. (C). The G1 release assay performed in A and B was repeated, but to quantify metaphase arrest, cells were instead fixed and imaged at 240 minutes post-G1 release. Metaphase arrest was quantified as percentage of cells whose DAPI-stained DNA fit a metaphase phenotype (cells in which both copies of DNA appeared as one unseparated spot that also displayed a bud greater than 3/4 the size of the mother bud). In all cases 100-200 cells were quantified per time point, per drug treatment, per experiment.

mediated by a number of membrane-associated proteins, in particular Myosin II and phosphorylated Moesin (Théry and Bornens, 2008). During the initial stages of mitosis this increased cortical rigidity is essential for proper spindle integrity and positioning in

animal cells (Carreno et al., 2008; Kunda et al., 2008; Kaji et al., 2008). Subsequently, prior to anaphase, Myosin II and Moesin concentrate at the cell midzone to promote cortical contractions at the future site of cytokinesis, a process during which the cell experiences mechanical strain (Kunda et al., 2008). Notably, several studies have implicated changes in cortical rigidity in changes in the timing of anaphase onset (Carreno et al., 2008; Kunda et al., 2008; Kaji et al., 2008). Cytokinesis in budding yeast differs from cytokinesis in animal cells because budding yeast have a ridged cell wall; however, in coordination with septum formation, the budding yeast plasma membrane is also constricted by an actomyosin ring (Wloka and Bi, 2012; Foltman et al., 2016) and similar to animal cells should experience mechanical strain on the plasma membrane. Therefore, although the two processes are not identical, it is possible that signaling in response to cortical changes is conserved amongst eukaryotes.

Although the molecular mechanism behind how the cell cortex communicates with the SAC remains unclear (Sandquist et al., 2011), conceptually such crosstalk could prevent chromosome missegregation. For example, it would be devastating if the cell stalled at a prior step of mitosis while the cell cortex physically divided the cytoplasm. Thus, based on our results, one possibility, although speculative, is that cortical strain can activate fail-safe biochemical changes that commit the cell to undergoing anaphase: spindle elongation would thus be completed and genetic material positioned to be partitioned into each new daughter cell by the time the cytokinesis occurs. However, one drawback of this scenario is that, if the cell's response to cortical strain overrode the mitotic checkpoint before chromosomes were bioriented on the

spindle, as it could have in my experiments, this might increase the chance of chromosome missegregation and cell death.

In our drug sensitive strains, deletion of Erg6 alters plasma membrane composition, (Kodedová and Sychrová, 2015; Emter et al., 2002) and may weaken overall cortical structure, rendering it less ridged. In the plasma membrane's slightly weakened state, extensive agitation in spite of a protective cell wall may mimic the cortical strain produced during cytokinesis, altering cell signaling and forcing cells to proceed without delay through mitosis. It will be critical to understand whether cortical strain prevents metaphase arrest in wild type yeast and perhaps higher eukaryotes in the future. If altered cortical rigidity in mammalian cells prevents them from arresting in metaphase in response to Taxol treatment, then this may indicate possible steps to take to make the drug more therapeutically effective in a medical practice.

### *A1.3.5 Tactics used to increase Taxol potency*

Although our experiments using Taxol were highly reproducible, we were concerned that 1) our experiments may be significantly affected by subtle changes in experimental procedure, and 2) that Taxol only has a moderate effect on cells, reducing but not eliminating microtubule dynamics and delaying anaphase onset for a brief time compared to canonical SAC activation. Thus, we tested a number of strategies aimed at increasing Taxol's effect on cells, both by mutating the genotype of our cells and by altering media additives in our experiments. However, despite testing numerous

strategies, no method we used successfully and reliably made Taxol's effect on the cells any more drastic than it was currently.

We first introduced the *cdc28-VF* allele into our Taxol sensitive background, which we hypothesized would amplify any delay in anaphase onset in response to reduced tension at kinetochores. The mutation *cdc28-VF* (budding yeast Cdk1) lacks inhibitory phosphorylation sites, displays reduced APC activity, and is hypersensitive to spindle perturbations (Rudner et al*.,* 2000). Therefore, we predicted that if Taxol activated signaling to inhibit the APC, this signaling would have a proportionally larger effect on the limited APC activity in *cdc28-VF* cells, ultimately inhibiting APC activation to a greater degree and causing the cells to delay in metaphase longer in response to reduced tension at kinetochores. All of this may be true, however in practice, Taxol sensitive, *cdc28-VF* mutants, particularly in combination with deletion of the panel of SAC proteins necessary for our experiments, rendered yeast so sickly and slow-growing that they became experimentally intractable (Figure 26).

Aware of the fact that Taxol experiments in liquid media require 0.02% methylcellulose in order to promote microtubule stabilization, we hypothesized that methylcellulose promotes Taxol's solubility. However, we were concerned that the effective concentration of Taxol in our experiments was still fluctuating in spite of the presence of methylcellulose, and that it may be sometimes much lower than 30μM. We tested a number of additives to further promote Taxol solubility, cyclodextrin, horse serum, fetal bovine serum, streptomycin, additional methylcellulose, and extra yeast nitrogen base; however, none of these additives reliably increased Taxol's potency in our liquid assays. Although these results don't exclude the possibility that additives may

increase Taxol's effectiveness under more ideal conditions, we conclude that under standard conditions 30μM Taxol has a moderate effect on yeast metaphase spindles.

We next compared the original Taxol-sensitive strain from (Gupta et al., 2003, Foland et al., 2005) to our own and observed that the major difference was that our current Taxol sensitive strain lacks the ergosterol biosynthesis enzyme gene *ERG6* whereas the original strain did not. We therefore suspected that the Erg6 deletion was the main reason why our strain displayed increased sensitivity to environmental perturbations and reacted drastically to slight differences in experimental procedure. We hypothesized that we could delete alternative proteins instead of Erg6 in the Taxol sensitive beta tubulin, Δ*pdr1,* Δpdr3 background and still retain Taxol sensitivity in live budding yeast. To this end we deleted Snq2, a multidrug ABC transporter (Akache and Turcotte, 2002), but found that Taxol had no appreciable effect on the growth of this new drug sensitive strain in our standard assays in both liquid and solid media (data not shown). We interpret this to mean that, although Snq2 was deleted in the original Taxol sensitive strain in combination with several other ABC pumps, deleting it does not sufficiently reduce the cells' ability to pump Taxol out of their cytoplasm to render them sensitive to Taxol *in vivo*. We recognized that, although it may be possible to delete an alternative protein(s) instead of Erg6 to render cells Taxol sensitive, without having a strong sense of which pumps are more important than others in specifically removing Taxol from within cells, pursuing that approach could not guarantee a quick or easy improvement of our experimental setup.

We next considered the possibility that, by expressing the APC activator Cdc20 from the pMET3::Cdc20 promoter, we may inadvertently be causing overexpression of

Cdc20 and subsequent premature activation of anaphase. The signaling that causes cells to transition from metaphase to anaphase is in precarious balance, highly sensitive to the relative levels of different proteins whose production and degradation is tightly regulated. Overexpression of Cdc20 might tip that balance and artificially shorten the delay we observed following a Cdc20 release. To address this possibility, we designed experiments similar to the Cdc20 arrest that used alternative methods to release cells from a metaphase arrest (Figure 31). First, we arrested a log phase culture in metaphase using the proteasome inhibitor MG132 which prevented the degradation of metaphase-specific proteins. MG132 is not typically used in experiments with budding yeast because WT yeast are not sensitive to the drug, but because our strain is drug sensitive, we predicted that it may be sensitive to MG132. Indeed, our Taxol sensitive yeast strain's progression through the cell cycle is effected by MG132, but not in a manner which allowed us to use it in our experiments. Cells released slowly and asynchronously from the metaphase arrest by MG132 with or without prior synchronization in $\alpha$-factor, and a delay in Taxol was not conclusively detectable (Figure 31A).

Our next alternative method of metaphase release involved deleting a component of the APC, Cdc26, which renders the process of anaphase onset temperature sensitive. Thus, when *cdc26*$\Delta$ mutants are grown at 37˚C, they arrest in metaphase (Hwang and Murray, 1997; Biggins and Murray, 2001). However, when we

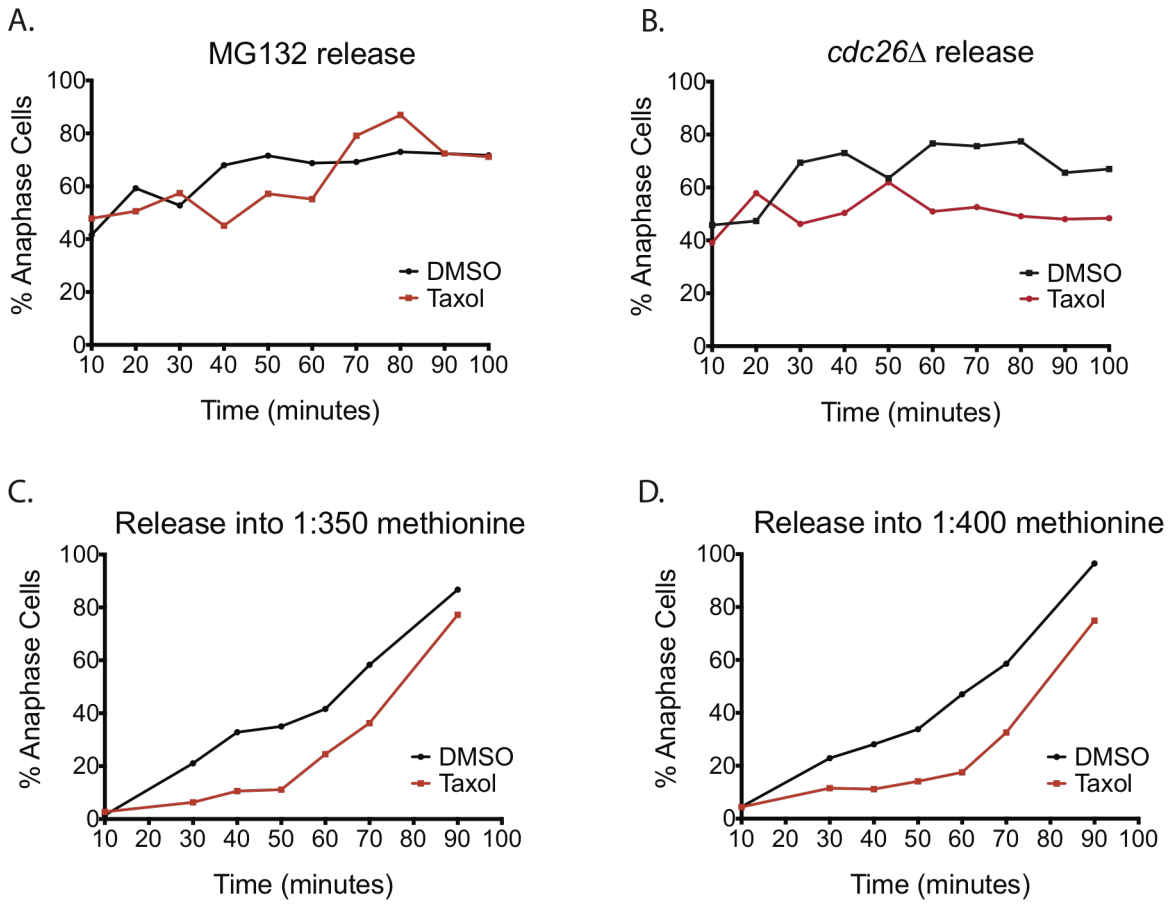


**Figure 31. Altering the Cdc20 release assay does not amplify the tension delay.** (A and B) alternate methods were used to arrest cells in metaphase prior to release. (A) Taxol sensitive control cells were released from a G1 arrest into media containing MG132 and incubated until ≥70% of cells appeared arrested in metaphase. To release, cells were washed 3 times in water and then resuspended ± 30 μM Taxol. (B) Taxol sensitive cdc26Δ mutants were released from a G1 arrest and incubated at 37˚C for 1.25 hours until ≥70% of cells appeared arrested in metaphase. Cells were released from arrest ± 30 μM Taxol by shifting their incubation temperature down to 24˚C. (C and D) Standard Cdc20 release assays were performed as described in Figure 14A, but cells were released ± 30 μM Taxol into media supplemented with a (A)1:350 or (B) 1:400 dilution of 2g/L methionine. In all cases 100-200 cells were quantified per time point, per drug treatment, per experiment.

released *cdc26*Δ mutants from a G1 arrest into media at 37˚C, arrest in metaphase was not sufficiently complete, and release was again slow and asynchronous (Figure 31B).

We finally hypothesized that if releasing cells expressing pMET3::Cdc20 in media lacking methionine turned Cdc20 expression on to a maximal level, perhaps releasing

these pMET3::Cdc20 cells into media containing minute amounts of methionine would reduce Cdc20 expression to lower-than-endogenous levels. Lower levels of Cdc20 might reduce APC activation, making it easier for weak SAC activation to inhibit anaphase. We determined that adding 1:350 and 1:400 dilutions of 2g/L methionine to our experiments slowed down the cell cycle but still allowed cells to enter anaphase, suggesting reduced but still biologically sufficient Cdc20 production. When we released cells into anaphase in media containing 1:350 and 1:400 methionine, in the presence and absence of Taxol, anaphase onset was slower. However, cells did not delay in Taxol sufficiently longer to merit pursing an experimental setup where we further manipulated protein levels in a manner which may potentially cause unpredictable side effects (Figures 31C and D).

We finally attempted to increase the tension-mediated delay by replacing Taxol in our experiments with Epothilone B, a powerful microtubule stabilizing drug similar to Taxol that can stabilize wild type and Taxol sensitive yeast microtubules (Bode *et al.* 2002). At the start of this project, access to Epothilone B was proprietary and extremely limited, but over the course of several years it had become commercially available. We performed several of our standard experiments (Figure 32), observing metaphase arrested spindles, measuring the distance between centromere pairs, and quantifying percentages that were separated or off-axis (Figures 32A-32D). We also performed a Cdc20 arrest and release into media containing Epothilone B and tracked anaphase onset over time (Figure 32A). Although in preliminary experiments Epothilone B did not appear to reduce kinetochore attachment at metaphase, (Figure 32A) it did not reliably

reduce distance between sister centromeres, and in some cases even appeared to increase the frequency of separated pairs, suggesting increased tension (Figures 32B and D). In contrast to Taxol treatment, treatment with Epothilone B also increased metaphase spindle length, indicating that the microtubule stabilization by these two drugs may have fundamentally different effects on spindle architecture (Figure 32C). Further, when cells were released from a metaphase arrest into Epothilone B, the drug did cause a delay in anaphase onset; however, during our experiment over 95% of control cells reached anaphase, while only 55% of Epothilone B-treated cells entered anaphase (Figure 32E). Because a large portion of the population remained arrested in metaphase for the duration of our experiment, we hypothesize that cells with sufficient kinetochore attachments entered anaphase in 1μM Epothilone B after a short tension-mediated delay, but that Epothilone B treatment caused many cells to detach kinetochores, causing half the population to activate the attachment-mediated SAC and undergo a prolonged arrest.

### *A1.3.6 Alternative methods to observe cell cycle progression*

In our experiments, we use a method to observe a tension mediated delay in anaphase onset in a manner that was not possible in yeast until now; namely, we release cells from a metaphase arrest in the presence and absence of Taxol, and then

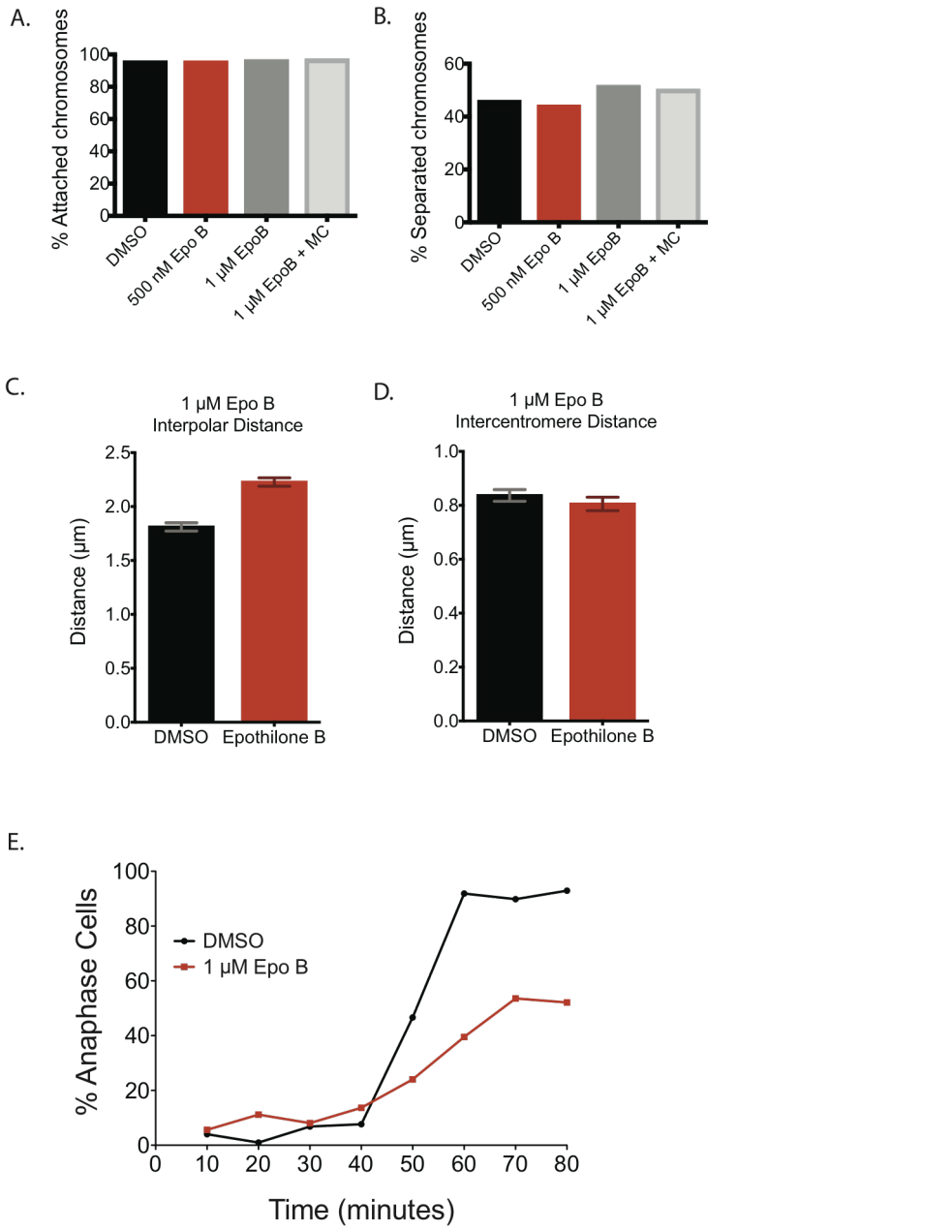


**Figure 32. Microtubule stabilizer Epothilone B (Epo B) affects metaphase spindle architecture and the timing of anaphase onset differently than Taxol.** (A-D) Cells were arrested in metaphase with preformed spindles as in Figure 11A. (A and B) in a single experiment, cell cultures were divided into 4 and treated with 0, 500nM, 1μM Epo B, or 1μM Epo B + 0.02% Methylcellulose (Although not typically required for Epo B toxicity, this concentration of methylcellulose is required for Taxol-mediated microtubule stabilization in liquid yeast cultures) and were then fixed and imaged. (A) Chromosome attachment and (B) centromere separation were quantified as in Figures 10A and 13B respectively. (C and D) The experiment described in A and B was replicated, but changes in spindle architecture were instead assessed by quantifying (A) Interpolar distance or (B) intercentromere distance ± 1μM Epo B as described in Figures 11B and 13C respectively. (E) The Cdc20 release assay was performed as in Figure 14A; cells were released from metaphase arrest into ± 1μM Epo B. Data points represent a single experiment with n = 100-200 cells scored per time point per drug treatment.

visually observed images of the population to determine on a cell-by-cell basis the percentage of cells that have elongated their spindles and entered anaphase. In contrast, standard experimental methods in the field use microtubule destabilizing drugs or mutant yeast that ultimately disrupt spindle morphology, making it impossible to quantify anaphase onset visually. Thus, past studies tracked anaphase onset using biochemical markers for APC activation, primarily using Western blotting to track the degradation of two APC targets, Pds1 or Clb2. In these assays, when the attachment mediated SAC is active, cells arrest in metaphase and Pds1 and Clb2 levels remain high for up to 3 hours. On the other hand, results using this method to track tension mediated signaling have been conflicted, and it was unclear how the tension mediated delay would manifest, if at all, in our assay. We predicted that previous assays may have missed the 15-minute tension delay because their samples were often taken at widely spaced time intervals more optimal for observing the longer, attachment mediated delay. Therefore, we last sought to confirm the tension mediated delay using these time-tested, protein degradation-based methods (tracking both Clb2 and Pds1 levels) by taking samples at much smaller time intervals.

We began by tracking degradation of Pds1. We performed our Cdc20 release assay in a strain harboring Pds1-18myc, which revealed a slight delay in Pds1 degradation in Taxol compared to control cells (Figures 33A and B). We concluded that this assay, although informative of the overall culture's bulk biochemical transition into anaphase, was less sensitive than our microscopy based assay. Further, tracking anaphase onset during our Cdc20 release assay using commercial primary antibodies for Pds1 or Clb2 was unsuccessful in our hands. Neither of these antibodies was

specific enough to conclusively track the degradation of either protein, particularly with the degree of temporal sensitivity needed to visualize the tension delay. In sum, we concluded that these assays, which assess populations of cells rather than on a cell-by-cell basis, are less sensitive than our microscopy based assays. Although these assays revealed that cells clearly enter anaphase after a slight delay during Taxol treatment in the Cdc20 release assay (Figure 33C), tracking anaphase onset via protein degradation was not sensitive enough to reliably measure the tension mediated delay.

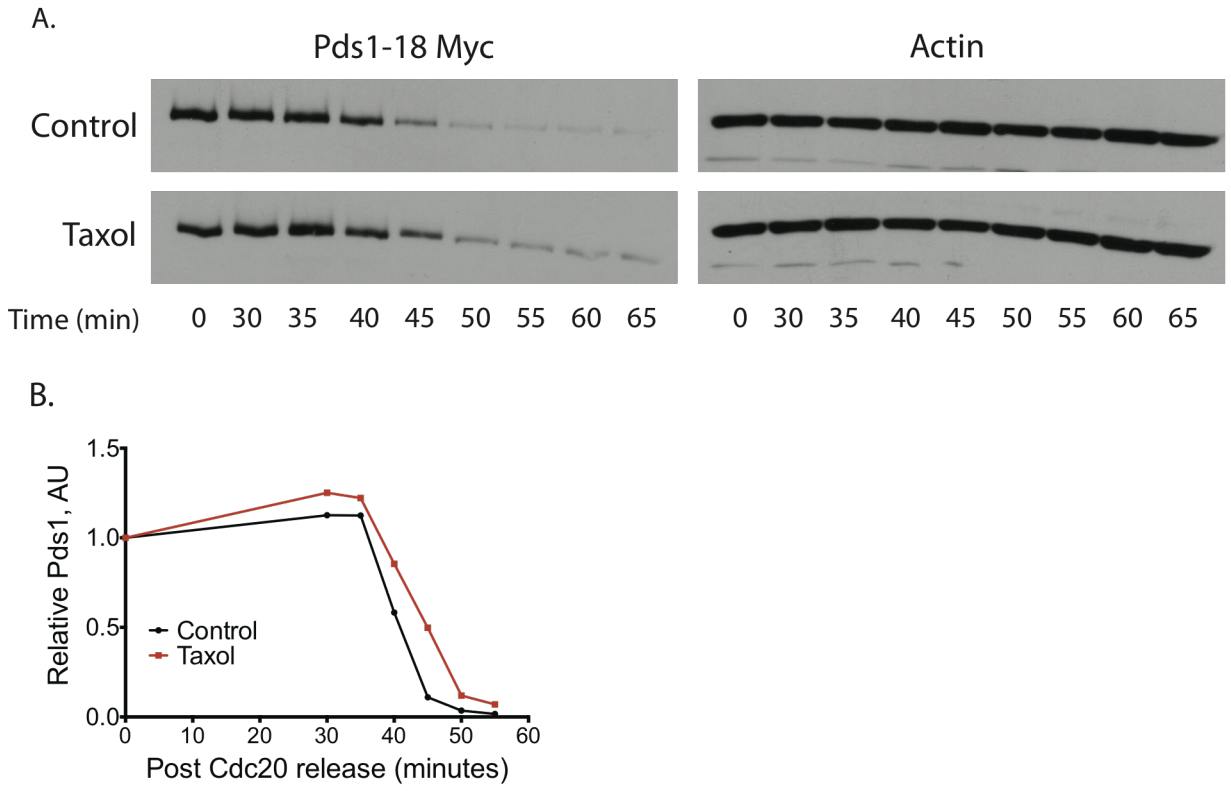


**Figure 33. Western blotting for Pds1 degradation is marginally sensitive enough to reveal that Taxol causes a delay in anaphase onset.** Cells carrying an MYC epitope-tagged allele for Pds1 underwent a Cdc20 release assay as described in Figure 14A (A) at the indicated times following release from the metaphase arrest, aliquots of each culture were removed and processed for Western blotting. Samples were blotted with an anti-MYC antibody to visualize Pds1; Actin, loading control. (B) Quantification of the intensity of the bands in (A) relative to the loading control.

## A1.4 Discussion

It is essential to know the strengths, weaknesses, and potential pitfalls when working with any model organism. Beyond the two initial studies which together generated a Taxol sensitive yeast strain (Gupta et al., 2003, Foland et al., 2005), this is the first body of work implementing Taxol sensitive yeast as a model organism, and the first body of work to explore its strengths and weaknesses in practice. Further, because no one had ever stabilized yeast microtubules with Taxol for cell-based experiments, the conditions required optimization in order to maximize Taxol's effectiveness in the context of our experiments.

Our results demonstrate that working with both Taxol and drug sensitive yeast requires caution. Both the drug and the strain of yeast are highly sensitive to seemingly minor changes in experimental setup, an observation most clearly demonstrated by their conflicting YPD/peptone and temperature requirements. Additionally, the fact that we do not fully understand why Taxol sensitive yeast become insensitive to Taxol when incubated on a rotator should inspire a sense of caution when working with drug sensitive yeast. Changes in experimental procedure, that cause no obvious phenotype in wild type yeast, can cause drastic changes in phenotypes and experimental outcomes in drug sensitive yeast. However, as long as all reagents are prepared and experiments conducted in a very precise, consistent manner, we have shown that it is possible to perform reliable experiments with reproducible results using Taxol sensitive yeast.

Experiments recorded here to optimize our Taxol sensitive yeast system often yielded negative or unclear results. Still, performing and comparing methods popularly used in the field to our primary methods allowed us to determine which function most robustly for our purposes. Most importantly, these comparisons showed us that the assays we developed specifically for this study were better suited for our purposes, and that alternative assays, that are the gold standard in other contexts, are not sensitive enough to reliably measure the tension delay.

In the future, our lab and other labs performing studies with drug sensitive yeast can benefit from the groundwork detailed here. As the technical details of our Taxol sensitive yeast system develop, more applications will be discovered to interrogate the effects of microtubule stabilization on cell signaling and dynamics in this single-celled, genetically tractable model organism. The tension mediated metaphase delay is still poorly understood, and substantial work must still be done to understand how it functions in coordination with the SAC and other signaling pathways in metaphase. And beyond metaphase, it will additionally be important to explore how cortical strain may affect mitotic signaling and if this is related to cytokinesis. In sum, signaling pathways that govern one cellular function are often closely linked to pathways that govern others. Our Taxol sensitive yeast system may prove valuable to develop a mechanistic understanding of these links, thereby increasing understanding of integrated cellular dynamics. Such advancements will be important for improving Taxol-based chemotherapy and other medical treatments.

## A1.5 Supplementary methods

Many of the methods in this appendix were performed as described in Chapter 2 Section 2.5 with slight variations as indicated in the text. However, I will record supplemental methods unique to this appendix here.

### *A1.5.1 Alternative methods of metaphase release*

**Mg132 release:** *MAT*a cells were maintained and grown to mid log phase (30˚C) in SC media. Cells were transferred to SC with 100 μM alpha factor for 2.5 hours at 30˚C to synchronize in G1. These cells were washed three times in 1 ml water and resuspended in SC containing 0.02% methylcellulose and supplemented with 50μM MG132 to suppress protein degradation and arrest cells in metaphase. After 75 min at 30˚C, >70% of cells were arrested in metaphase, and, following a 15-minute incubation +/- Taxol, cells were quickly washed three times in 1 ml water (to remove MG132) and resuspended in 5 ml SC containing 0.02% methylcellulose and DMSO +/- 30 μM Taxol (final from 1 mM stock in DMSO). In the absence of MG132, cells degrade metaphase-specific proteins and release from arrest. Cultures were maintained on the bench and gently mixed by hand every 10 min. Samples were removed and fixed in ice cold 70% ethanol every 10 min over 80 min.

***Cdc26*Δ *ts* release:** *MAT*a *cdc26*Δ cells were maintained and grown to mid log phase (24˚C) in SC media. Cells were transferred to SC with 100 μM alpha factor for 2.5 hours at 24˚C to synchronize in G1. These cultures were supplemented with 0.02%

methylcellulose and were shifted to a 37˚C water bath to suppress Cdc26 activity and arrest cells in metaphase. After 75 min at 37˚C, >70% of cells were arrested in metaphase, and, following a 15-minute incubation +/- Taxol, cells were quickly washed three times in room temperature 1 ml and resuspended in 5 ml room temperature SC containing 0.02% methylcellulose and DMSO +/- 30 μM Taxol (final from 1 mM stock in DMSO). Cdc26 functionality returns at room temperature, and cells release from arrest. Cultures were maintained on the bench and gently mixed by hand every 10 min. Samples were removed and fixed in ice cold 70% ethanol every 10 min over 80 min.

For both the MG132 release and the *cdc26*Δ release, cells were stained, imaged and quantified as in Chapter 2: Cells were washed 2 times with PBS and nuclei were stained with 50 ng/ml DAPI. For imaging, 10-12 z-plane DIC and DAPI images were collected at 0.5 μm intervals. Images were coded and all Cdc20 release assays and missegregation assays were scored blinded to both cell genotype and Taxol status. To quantify images, cells were categorized based on DNA and cell morphology; single cells lacking a bud were considered “single cells”, cells with a small or large bud whose DNA had not yet begun to separate were considered “metaphase”, and budded cells whose DNA had visibly separated into two distinct masses were considered “anaphase” cells. To score chromosome missegregation, cells in which *CEN1* was marked by tetO/tetR-GFP were used in the Cdc20 release assay and imaged with 20 z-planes spaced 0.3 μm apart. At 50 and 70 min post Cdc20 release, cells with elongated spindles were scored for whether the two tetO/tetR-GFP foci were segregated correctly into the mother and daughter cells.

### *A1.5.2 Western blotting*

Cells were treated an in the Cdc20 release assay but instead of fixing, aliquots of cells were placed on ice at each time point. After the last time point, the cell lysates were prepared from the samples. Cells were pelleted, resuspended in ice cold 0.1M NaOH and incubated on ice for 10 min. Next, they were pelleted and resuspended in 100 µL SDS-PAGE cold sample buffer. Samples were heated for 10 min at 99˚C, and then incubated on ice for 10 min. Finally, samples were spun for 10 min at 14,000 rpm in a microfuge at 4˚C. The supernatant was transferred to a new tube and used for western blotting and the pellet was discarded. SDS-PAGE was conducted with 7.5% gels and membranes were probed with primary antibodies for three hours at room temperature or 4˚C overnight, and secondary antibody for three hours at room temperature. Primary antibodies: mouse anti-myc clone 9e10, 1:5000, University of Chicago core facility, 1:1000; mouse anti-alpha actin, Abcam ab8224, 1:1000, secondary antibody: sheep HRP-anti-mouse, GE Healthcare Life Sciences NA931, 1:20,000.

# Appendix 2

## List of Strains

| YEAST STRAIN | MATING TYPE | GENOTYPE | SOURCE |
|---|---|---|---|
| **MGY 50** | *MATα* | | This study |
| | | *Control strain used for spotting assay* | |
| **MGY 980** | *MATα* | *tub2-A19K-T23V-G26D-Y270F (no marker), erg6::trp1::HIS3, pdr1::hygB, pdr3::NAT, his3Δ200, leu2Δ1, LYS2, MET15, ura3-52, trp1Δ63, cen1::URA3-CEN3-TetOP, pURA3:TetR:YFP:ADHterm:LEU2, spc29-mRFP-KanR, pMet3-3xHA-Cdc20::TRP1* | This study |
| | | *Control strain used to measure spindle length, CEN distance, CEN attachment, and 1-dot/2-dot, and some early missegregation experiments* | |
| **MGY 1293** | *MATα* | *tub2-A19K-T23V-G26D-Y270F (no marker), erg6::trp1::HIS3, pdr1::hygB, pdr3::NAT, his3Δ200, leu2Δ1, LYS2, MET15, ura3-52, trp1Δ63, pMet-Cdc20::TRP1* | This study |
| | | *Control strain used in Cdc20 release assays* | |
| **MGY 1315** | *MATα* | *tub2-A19K-T23V-G26D-Y270F (no marker ), erg6::trp1::HIS3, pdr1::hygB, pdr3::NAT, his3Δ200, leu2Δ1, LYS2, MET15, ura3-52, trp1Δ63, pMet-Cdc20::TRP1, bub1Δ::KanR* | This study |
| | | *bub1Δ strain used in Cdc20 release assays* | |
| **MGY 1428** | *MATα* | *erg6::trp1::HIS3, pdr1::hygB, pdr3::NAT, his3Δ200, leu2Δ1, LYS2, MET15, ura3-52, trp1Δ63, pMet-Cdc20::TRP1* | This study |
| | | *Drug sensitive used in Cdc20 release assay* | |
| **MGY 1508** | *MATα* | *tub2-A19K-T23V-G26D-Y270F (no marker), erg6::trp1::HIS3, pdr1::hygB, pdr3::NAT, his3Δ200, leu2Δ1, LYS2, MET15, ura3-52, trp1Δ63, pMet-Cdc20::TRP1, mad3Δ:: KanR* | This study |
| | | *mad3Δ strain used in Cdc20 release assay* | |
| **MGY 1749** | *MATα* | *tub2-A19K-T23V-G26D-Y270F (no marker), erg6::trp1::HIS3, pdr1::hygB, pdr3::NAT, his3Δ200, leu2Δ1, LYS2, MET15, ura3-52, trp1Δ63, cen1::URA3-CEN3-TetOP, 5'NLS-TetR::GFP:ADHterm:LEU2, spc29-mRFP-KanR, pMet3-3XHA-Cdc20::TRP1* | This study |
| | | *Control strain used to make kymographs, measure % time separated, CEN breathing frequency, live cell spindle elongation, and the later control/mad3 missegregation experiments* | |
| **MGY 1872** | *MATα* | *erg6::TRP1, pdr1::hygB, pdr3::NAT, his3Δ200, leu2Δ1, LYS2, MET15, ura3-52, trp1Δ63* | This study |
| | | *Drug sensitive strain used in spotting assays – do not send, counterpart to 1874* | |
| **MGY 1874** | *MATα* | *tub2-A19K-T23V-G26D-Y270F (no marker), erg6::TRP1, pdr1::hygB, pdr3::NAT, his3Δ200, leu2Δ1, LYS2, MET15, ura3-52, trp1Δ63* | This study |
| | | *Control strain used in spotting assays – do not send, background mutation makes this strain extra-sensitive to benomyl* | |
| **MGY 2103** | *MATα* | *tub2-A19K-T23V-G26D-Y270F (no marker), erg6::TRP1, pdr1::hygB, pdr3::NAT, his3Δ200, leu2Δ1, LYS2, MET15, ura3-52, trp1Δ63, bub3Δ:: KanR* | This study |
| | | *bub3Δ strain used in spotting assays* | |
| **MGY 2134** | *MATα* | *tub2-A19K-T23V-G26D-Y270F (no marker), erg6::TRP1, pdr1::hygB, pdr3::NAT, his3Δ200, leu2Δ1, LYS2, MET15, ura3-52, trp1Δ63, mad2Δ:: KanR* | This study |
| | | *mad2Δ strain used in spotting assays* | |

| | | | |
|---|---|---|---|
| **MGY 2136** | *MATα* | *tub2-A19K-T23V-G26D-Y270F (no marker), erg6::TRP1, pdr1::hygB, pdr3::NAT, his3Δ200, leu2Δ1, LYS2, MET15, ura3-52, trp1Δ63, mad3Δ:: KanR* | This study |
| | | *mad3Δ strain used in spotting assays* | |
| **MGY 2127** | *MATα* | *tub2-A19K-T23V-G26D-Y270F (no marker), erg6::trp1::HIS3, pdr1::hygB, pdr3::NAT, his3Δ200, leu2Δ1, LYS2, MET15, ura3-52, trp1Δ63, cen1::URA3-CEN3-TetOP, 5'NLS-TetR::GFP:ADHterm:LEU2, pMet3-3XHA-Cdc20::TRP1, mad3Δ:: KanR* | This study |
| | | *mad3Δ strain used to measure centromere missegregation* | |
| **MGY 2128** | *MATα* | *tub2-A19K-T23V-G26D-Y270F (no marker), erg6::TRP1, pdr1::hygB, pdr3::NAT, his3Δ200, leu2Δ1, LYS2, MET15, ura3-52, trp1Δ63, bub1Δ:: KanR* | This study |
| | | *bub1Δ strain used in spotting assays* | |
| **MGY 2131** | *MATα* | *tub2-A19K-T23V-G26D-Y270F (no marker), erg6::TRP1, pdr1::hygB, pdr3::NAT, his3Δ200, leu2Δ1, LYS2, MET15, ura3-52, trp1Δ63, bub2Δ:: KanR* | This study |
| | | *bub2Δ strain used in spotting assays* | |
| **MGY 2133** | *MATα* | *tub2-A19K-T23V-G26D-Y270F (no marker), erg6::TRP1, pdr1::hygB, pdr3::NAT, his3Δ200, leu2Δ1, LYS2, MET15, ura3-52, trp1Δ63, mad1Δ:: KanR* | This study |
| | | *mad1Δ strain used in spotting assays* | |
| **MGY 2139** | *MATα* | *tub2-A19K-T23V-G26D-Y270F (no marker), erg6::TRP1, pdr1::hygB, pdr3::NAT, his3Δ200, leu2Δ1, LYS2, MET15, ura3-52, trp1Δ63, mad3::G418, bub1Δ:: KanR* | This study |
| | | *bub1Δ/mad3Δ strain used in spotting assays* | |
| **MGY 2150** | *MATα* | *tub2-A19K-T23V-G26D-Y270F (no marker), erg6::TRP1, pdr1::hygB, pdr3::NAT, his3Δ200, leu2Δ1, LYS2, MET15, ura3-52, trp1Δ63* | This study |
| | | *Control strain used in spotting assays – send this strain* | |
| **MGY 1399** | *MATα* | *tub2-A19K-T23V-G26D-Y270F (no marker), erg6::TRP1, pdr1::hygB, pdr3::NAT, his3Δ200, leu2Δ1, LYS2, MET15, ura3-52, GFP-TUB1::URA3, trp1Δ63* | This study |
| | | *Control strain used to measure microtubule dynamics* | |
| **MGY 887** | | *tub2-A19K-T23V-G26D-Y270F (no marker), erg6::TRP1, pdr1::hygB, pdr3::NAT, his3Δ200, leu2Δ1, LYS2, MET15, ura3-52, trp1Δ63* | This study |
| | | *Control strain used in release and spotting experiments in Appendix 1* | |
| **MGY 928** | | *tub2-A19K-T23V-G26D-Y270F (no marker), erg6::TRP1, pdr1::hygB, pdr3::NAT, his3Δ200, leu2Δ1, LYS2, MET15, ura3-52, trp1Δ63, bub1Δ::KanR* | This study |
| | | *Bub1Δ strain used in spotting assays in Appendix 1* | |
| **MGY 1039** | | *tub2-A19K-T23V-G26D-Y270F (no marker), erg6::trp1::HIS3, pdr1::hygB, pdr3::NAT, his3Δ200, leu2Δ1, LYS2, MET15, ura3-52, trp1Δ63, Cdc28-VF-TRP1* | This study |
| | | *Control Cdc28-VF strain used in Taxol-aging spotting assay in Appendix 1* | |
| **MGY 1040** | | *tub2-A19K-T23V-G26D-Y270F (no marker), erg6::trp1::HIS3, pdr1::hygB, pdr3::NAT, his3Δ200, leu2Δ1, LYS2, MET15, ura3-52, trp1Δ63, Cdc28-VF-TRP1, mad2Δ::KanR* | This study |
| | | *mad2Δ, Cdc28-VF strain used in Taxol-aging spotting assays in Appendix 1* | |

| | | |
|---|---|---|
| **MGY 1041** | *tub2-A19K-T23V-G26D-Y270F (no marker), erg6::trp1::HIS3, pdr1::hygB, pdr3::NAT, his3Δ200, leu2Δ1, LYS2, MET15, ura3-52, trp1Δ63, Cdc28-VF-TRP1, sgo1Δ::KanR* | This study |
| | *sgo1Δ, Cdc28-VF strain used in Taxol-aging spotting assays in Appendix 1* | |
| **MGY 1229** | *erg6::TRP1, pdr1::hygB, pdr3::NAT, his3Δ200, leu2Δ1, LYS2, MET15* | This study |
| | *Drug sensitive strain used spotting assays in Appendix 1* | |
| **MGY 1871** | *tub2-A19K-T23V-G26D-Y270F (no marker), erg6::TRP1, pdr1::hygB, pdr3::NAT, his3Δ200, leu2Δ1, LYS2, MET15, ura3-52, trp1Δ63* | This study |
| | *Control strain used to measure the effect of cortical strain and media autoclave timing on anaphase onset* | |
| **MGY 1392** | *tub2-A19K-T23V-G26D-Y270F (no marker), erg6::trp1::HIS3, pdr1::hygB, pdr3::NAT, his3Δ200, leu2Δ1, LYS2, MET15, ura3-52, trp1Δ63, pMet-Cdc20::TRP1, Pds1-18MYC::LEU2* | This study |
| | *Control strain used to monitor anaphase onset by Western blot* | |

| **PLASMID NAME** | ***DESCRIPTION AND MARKERS*** | **SOURCE** |
|---|---|---|
| **PMG 208** | *GFP-TUB1-URA3, ampR* | Marie Guillet |
| **PMG 235** | *Cen1::CEN3-tetO(224)-URA3, ampR* | Pam Meluh |
| **PMG 250** | *Trp1::HIS3, kanR, CapR* | Fred Cross |
| **PMG 263** | *MET3-3xHA-CDC20::TRP1, ampR* | Frank Uhlmann |
| **PMG 272** | *pURA3-5'NLS-tetR-GFP-ADH(term)-LEU2, ori, LEU2, ampR* | John Pellman |
| **PMG 275** | *pURA3::TetR::YFP::ADHterm, LEU2, ampR* | Tomo Tanaka |
| **PMG 366** | *GFP (s65T)-kanR(G418), ampR* | John Pringle |
| **PMG 374** | *ARS-CEN, URA3, ERG6-n266S, ampR* | |
| **PMG 541** | *Pds1-18MYC, LEU2, ARS, Ori, AmpR* | John Pellman |